Snow mechanics: from snow microstructure to avalanche formation

Pascal Hagenmuller

UNIVERSITÉ DE GRENOBLE

MÉMOIRE D'HABILITATION À DIRIGER DES RECHERCHES

Spécialité : **Ingénierie, Matériaux, Mécanique, Environnement, Energétique, Procédés, Production**

Présenté par

Dr. Pascal HAGENMULLER

Univ. Grenoble Alpes, Université de Toulouse, Météo-France, CNRS, CNRM, Centre d'Études de la Neige, Grenoble, France

Snow mechanics: from snow microstructure to avalanche formation

Soutenu publiquement le **6 Septembre 2022**,
devant le jury composé de :

Prof. Dr. Ilka WEIKUSAT
Professeur, Alfred Wegener Institute - Helmholtz Centre for Polar and Marine Research, Bremerhaven, Allemagne, Rapporteur

Prof. Dr. Christophe MARTIN
Directeur de recherche CNRS, Univ. Grenoble Alpes, Grenoble INP, SIMaP, Grenoble, France, Rapporteur

Prof. Dr. Jürg SCHWEIZER
Professeur, WSL - Institute for Snow and Avalanche Research SLF, Davos, Suisse, Rapporteur

Prof. Dr. Ian BAKER
Professeur, Thayer School of Engineering, Dartmouth College, Hanover, NH, USA, Examinateur

Prof. Dr. Christian GEINDREAU
Professeur, Univ. Grenoble Alpes, CNRS, Grenoble INP, 3SR, Grenoble, France, Président

Dr. Guillaume CHAMBON
Directeur de recherche, Univ. Grenoble Alpes, Inrae, UR ETNA, Grenoble, France, Invité

Abstract

Snow is a fascinating material. Its composition is relatively simple, mainly air and ice, but the arrangement of these components in three dimensions is extremely diverse. This diversity of microstructure, often reduced to discrete snow types, originates from different snowflake growth mechanisms in the atmosphere and the continuous evolution of snow on the ground. Indeed, snow is a hot material with a temperature close to its melting point. This thermal state, combined with high porosity, promotes fast structural changes under gravitational compaction, local phase changes, and mass transport through vapor diffusion or liquid water percolation. The geometrical arrangement of ice and air is not only a source of fascination but also fully controls the effective material properties of snow, such as its mechanical strength, thermal conductivity, and electromagnetic reflectance. However, this control remains poorly understood because of yet-incomplete microstructural characterization and natural snow variability. The snowpack structure is even more complex: stratified into numerous layers with contrasted microstructural patterns. The snowpack behavior under given boundary conditions will depend on the complex interactions between its different layers, e.g., avalanche formation is related to the combination of a weak layer and a slab with specific mechanical properties. Better understanding and characterizing snow as material and the snowpack as an essential medium between atmosphere and ground would benefit various applications such as avalanche forecasting or estimating our planet's surface energy and mass budget.

This document synthesizes my contribution to snow science and, in particular, to snow mechanics at different scales. This uneasy paragraph reduces eight years of research to a few lines. Understanding snow mechanics is intimately related to a detailed characterization of the snow microstructure, which is now possible at a micron resolution and in three dimensions thanks to tomography. I contributed to setting up an X-ray tomograph in a cold room and developing dedicated image processing tools. Computational models can exploit the wealth of tomographic data and reproduce snow properties based on the idea that snow is just a porous ice structure. Amongst others, I worked on implementing this approach into discrete and finite element models, which led to a better understanding and quantification of snow brittle failure. The combination of tomography and computational models seems key to deciphering the link between snow microstructure and its effective properties. However, this strategy is not suited to characterize, in practice, the entire snowpack. To bridge the gap between microstructure and field tests, I worked on understanding the cone penetration test in snow and its interpretation into microstructure proxies. Given the spatial variability of the snow cover, characterizing the snowpack profiles in detail may sound like looking for a needle in a haystack. However, I developed a matching algorithm between snow profiles that can effectively track tiny snow layers across mountain slopes. Besides, this snow stratigraphy controls whether an avalanche is likely to release on a slope. Fundamental knowledge in avalanche formation and this control increased considerably over the past decades, but its implementation into tools for avalanche forecasting needs to catch up. I contributed to modeling snow conditions in the French Alps and assessing the snowpack stability and associated avalanche danger based on snow physics and machine learning.

Future work will focus on finalizing ongoing projects and exploring new but related scientific questions in snow science. Some of the work is already ongoing, and some might remain utopic. In my work and in general, tomography characterizes snow in lab experiments. One of my objectives is to bring tomography to the field and monitor seasonal snowpack evolution at a resolution never reached before, which would constitute the basis for developing a new generation of snowpack models. In parallel, I plan to use the developed computational models

and the extensive collected tomographic data to build a library of effective properties of snow as a function of snow microstructure. The goal is to go beyond a qualitative understanding of snow physics and mechanics and provide quantitative relations to be used by the community in large-scale models. My focus on snow mechanics was on the brittle deformation regime, which is limited to high strain rates and does not apply to many applications such as snow settlement. I aim to explore snow mechanics at low strain rates where other mechanisms, such as sintering, ice visco-plasticity, and concomitant metamorphism, play a role. This project will require new dedicated computational models and the tomographic measurement of time series of snow evolution under controlled temperature and stress conditions. Last, mountains and, in particular, their cryospheric components are strongly affected by climate change. I will use the developed modeling tools to evaluate the evolution of avalanche hazards with global warming and provide some guidelines for risk mitigation in mountain territories.

Résumé

La neige est un matériau fascinant. Sa composition est assez simple, principalement de l'air et de la glace, mais l'agencement de ces composants en trois dimensions est extrêmement varié. Cette diversité de microstructure, souvent réduite à des types de neige discrets, provient des différents mécanismes de croissance des flocons dans l'atmosphère et de l'évolution continue de la neige au sol. En effet, la neige est un matériau chaud avec une température proche de son point de fusion. Cet état thermique, combiné à une porosité élevée, favorise des changements structurels rapides sous l'effet de la compaction sous gravité, des changements de phase localisés et du transport de masse par diffusion de vapeur ou percolation d'eau liquide. L'arrangement géométrique de la glace et de l'air n'est pas seulement source de fascination mais il contrôle aussi les propriétés matérielles effectives de la neige, telles que sa résistance mécanique, sa conductivité thermique ou encore sa réflectance électromagnétique. Cependant, ce contrôle reste mal compris en raison d'une caractérisation microstructurale encore incomplète et de la variabilité naturelle de la neige. La structure du manteau neigeux est encore plus complexe : stratifiée en de nombreuses couches aux motifs microstructuraux distincts. Le comportement du manteau neigeux dépend des interactions complexes entre ses différentes couches. Par exemple, la formation d'une avalanche est liée à la combinaison d'une couche fragile et d'une plaque aux propriétés mécaniques spécifiques. Une meilleure compréhension et caractérisation de la neige en tant que matériau et du manteau neigeux en tant qu'interface entre l'atmosphère et le sol est critique pour de nombreuses applications telles que la prévision des avalanches ou l'estimation du bilan d'énergie et de masse de la surface de notre planète.

Ce document synthétise ma contribution à l'étude de la neige et, en particulier, à la mécanique de la neige à différentes échelles. Ce paragraphe réduit huit années de recherche à quelques lignes. La compréhension de la mécanique de la neige est intimement liée à une caractérisation détaillée de sa microstructure. Cette caractérisation est aujourd'hui possible à une résolution micrométrique et en trois dimensions grâce à la tomographie. J'ai contribué à l'installation d'un tomographe à rayons X dans une chambre froide et au développement d'outils de traitement d'images dédiés. Des modèles de calcul peuvent exploiter la richesse des données tomographiques et reproduire les propriétés de la neige en partant de l'idée que la neige n'est qu'une structure de glace poreuse. J'ai notamment travaillé à la mise en œuvre de cette approche dans des modèles par éléments finis et discrets, ce qui a permis de mieux comprendre et quantifier la rupture fragile de la neige. La combinaison de la tomographie et des modèles de calcul semble essentielle pour déchiffrer le lien entre la microstructure de la neige et ses propriétés effectives. Cependant, cette stratégie n'est pas adaptée pour caractériser, en pratique, l'ensemble du manteau neigeux. Pour combler le fossé entre la microstructure et les tests de terrain, j'ai travaillé sur la compréhension du test de pénétration du cône dans la neige et son interprétation en indicateurs de la microstructure. Étant donné la variabilité spatiale de la couverture neigeuse, la caractérisation détaillée des profils du manteau neigeux peut sembler vaine. Cependant, j'ai développé un algorithme de correspondance entre les profils de neige qui permet de suivre efficacement des minuscules couches de neige au travers d'un pan de montagne. En outre, la stratigraphie du manteau neigeux détermine si une avalanche est susceptible de se déclencher sur une pente. Les connaissances fondamentales sur la formation des avalanches et ce contrôle ont considérablement augmenté au cours des dernières décennies, mais leur mise en œuvre dans des outils de prévision des avalanches reste en retrait. J'ai contribué à la modélisation des conditions nivologiques dans les Alpes françaises et à l'évaluation de la stabilité du manteau neigeux et du danger d'avalanche associé, en me basant sur la physique de la neige et l'apprentissage automatique

Mes travaux futurs se concentreront sur la finalisation des projets en cours et sur l'exploration de questions scientifiques nouvelles mais connexes dans le domaine de la neige. Certains de ces travaux sont déjà en cours, d'autres pourraient rester utopiques. Dans mon travail et en général, la tomographie caractérise la neige dans des expériences de laboratoire. L'un de mes objectifs est d'amener la tomographie sur le terrain et de suivre l'évolution saisonnière du manteau neigeux à une résolution jamais atteinte auparavant, ce qui constituerait la base du développement d'une nouvelle génération de modèles de manteau neigeux. En parallèle, je prévois d'utiliser les modèles de calcul développés et les nombreuses données tomographiques recueillies pour constituer une bibliothèque des propriétés effectives de la neige en fonction de sa microstructure. L'objectif est d'aller au-delà d'une compréhension qualitative de la physique et de la mécanique de la neige et de fournir des relations quantitatives qui seront utilisées par la communauté dans des modèles à grande échelle. Mon intérêt pour la mécanique de la neige s'est concentré sur le régime de déformation fragile, qui est limité aux taux de déformation élevés et ne s'applique pas à de nombreuses applications telles que le tassement de la neige. Je souhaite explorer la mécanique de la neige à de faibles taux de déformation où d'autres mécanismes, tels que le frittage, la visco-plasticité de la glace et le métamorphisme, jouent un rôle. Ce projet nécessitera de nouveaux modèles de calcul spécialisés et la mesure tomographique de séries temporelles de l'évolution de la neige dans des conditions de température et de contrainte contrôlées. Enfin, les montagnes et, en particulier, leurs composantes cryosphériques sont fortement affectés par le changement climatique. J'utiliserai les outils de modélisation développés pour évaluer l'évolution des risques d'avalanche en fonction du réchauffement climatique et fournir des lignes directrices pour l'atténuation des risques dans les territoires de montagne.

Contents

Chapter 1

Introduction

Preamble

The *Habilitation à Diriger des Recherches* - habilitation to supervise research (HDR) is a national higher education diploma. It corresponds to peer evaluation of the scientific merit and aptitude to supervise young researchers. It is required to be the principal supervisor of Ph.D. students and apply for a higher professional position in the French Corpse of Engineer. The HDR thesis summarizes my contribution to snow mechanics and the training of students. This chapter introduces the broader context of my activities and my research topic.

Contents

1.1 Context of my research

1.1.1 Professional context

I obtained an engineering degree in 2009 at Ecole Polytechnique, where I first experienced snow science with an internship with John Pomeroy at the University of Saskatchewan about blowing snow. I then studied environmental sciences at Ecole Nationale du Génie Rural des Eaux et des Forêts (ENGREF) and graduated in 2011 in material sciences at Ecole Normale Supérieure (ENS) de Cachan - ParisTech. I did my Master's thesis with M. Schneebeli and T. Theile at WSL Institute for Snow and Avalanche Research (WSL-SLF) about snow brittle failure. I then went to Institut national de recherche pour l'agriculture, l'alimentation et l'environnement (Inrae) between 2011 - 2014 to get my Ph.D. under the supervision of Mohamed Naaim and Guillaume Chambon. My Ph.D. focused on snow mechanical modeling based on tomographic data.

Since then, I have worked as a researcher at the Centre d'Etudes de la Neige (CEN), which is part of the Centre National de Recherche Metéorologique (CNRM). The CNRM laboratory is a joint unit between Météo-France and the Centre National de la Recherche Scientifique (CNRS). One mission of Météo-France is to survey the snowpack, forecast its evolution, and diffuse the

corresponding information to the public, including avalanche danger. In this context, the objective of the CEN as a research unit is to provide new knowledge and tools to achieve this mission. In particular, the CEN works on (i) understanding snow-related processes, including observation at different scales, (ii) developing detailed snowpack models to assist in the forecasting of snow avalanche hazards, and (iii) studying climatic, hydrological and socio-economic issues related to the snow cover. From 2015 to 2019, I worked in a team focused on snow modeling and observation, supervised by Samuel Morin (until 2015) and Marie Dumont. My research mainly dealt with snow mechanics from the snow grain scale (microns) relevant to studying the physical processes to the mountain scale (km) relevant to evaluating the avalanche danger. This research aligned with the expertise I gained during my Ph.D., but with a broader range of scales and various involved processes and observation tools.

Since 2020, I have been the leader of the team "Snow Material" (*Matériau Neige*). This research team comprises three permanent researchers, one technician, and five to ten non-permanent positions (Master and Ph.D. students, postdoctoral fellows, and invited researchers). We study snow at the microscale and its subsequent behavior at the macroscopic scale, including avalanche formation processes. In particular, we conduct experimental studies based on X-ray tomography, microscale modeling of physical processes, and homogenization to the macroscopic scale. We try to understand the processes (mechanics, metamorphism, mass and energy transfer) that occur in a coupled manner at the microscale. We complement process-based models with machine learning to forecast the avalanche danger. My research remained in line with the studies I conducted before 2020, but I also gained interest in microstructural processes controlling snow evolution (heat and mass transfer) and climate change impacts on the cryosphere. My role as a team leader requires me to follow all the research my team is doing. However, this manuscript focuses on my research after my Ph.D. graduation.

In addition to these pure research and management activities, I am involved in various tasks related to my expertise in snow and avalanches:

- *referee* for international peer-reviewed journals (e.g., The Cryosphere, Natural Hazards and Earth System Science, Cold Regions Science and Technology, Journal of Glaciology, Geophysical Research Letters, Frontiers in Earth Science) and international projects (e.g., Swiss National Science Foundation, American National Science Foundation). I review about 5-8 papers and 2-3 projects a year.

- *editor* for Frontiers in Earth Sciences (topic editor of a special issue) and the magazine *Neige et Avalanches* from the Association Nationale de l'Etude de la Neige et des Avalanches (ANENA). This magazine popularizes snow science for snow professionals and mountain practitioners.

- *author or co-author* of 28 papers in peer-reviewed international journals. I contributed to more than 60 communications (oral and print), including three invited (funded) presentations. All my publications are listed in the bibliography [1].

- *supervisor* of young researchers or students, as described in detail in Sect. 1.1.2. I was also involved in the advisory committee of Ph.D. students: M. Belen-Heredia from Inrae and K. Fourteau from Institut des Géosciences de l'Environnement (IGE). I reviewed the Ph.D. thesis of G. Bobillier from WSL-SLF.

[1] The work I contributed to is cited in red in this document (dark blue otherwise).

- *scientific animator* of the *Atelier Neige* from the Observatoire des Sciences de l'Univers de Grenoble (OSUG) that brings together the main contributors (CNRM, Inrae, IGE, etc.) to snow science in Grenoble, one of the best places in France for cryospheric research.
- *representative* of Météo-France and secretary of the Pole Alpin pour la prévention des Risques Naturels (PARN). The PARN is an association at the interface between researchers, state administrations, and operators regarding mitigating natural risks in mountain areas.
- *expert* and contributor to national and international working groups on avalanche hazards or mountain climates, notably for the french public administration and the European Avalanche Warning Services (EAWS) association.
- *teacher* of mechanics and avalanche formation to forecasters (or broader public), and referent for the mechanical model *Modèle Expert d'aide à la Prévision du Risque d'Avalanche* (MEPRA) that provides a proxy for snowpack stability and is used operationally during the winter season as a decision support tool.

Being a team leader or a snow and avalanche expert means that a significant portion of my working time is dedicated to institutional or administrative tasks and management rather than pure research. These tasks are undoubtedly valuable for disseminating knowledge and organizing research. However, I try to maintain moments with an uninterrupted face-to-face with snow science and creative scientific discussion with students and colleagues.

1.1.2 Role as research supervisor

As explained above, the supervision of young researchers is an essential and integral part of a researcher's work and requires different skills from those needed for pure peer research. Writing papers or drawing figures with students might be more time-consuming than doing it oneself. However, the interactions with students asking apparently naive but critical questions help clarify my thoughts or identify some shortcomings in my reasoning. In addition, it is a real pleasure to see students gain autonomy and provide original and personal contributions to science. Most of the results presented in this dissertation would not have been possible without their work. Over the past eight years, I supervised or co-supervised ten graduating students, four Ph.D. students, and three postdoctoral fellows. The work we have done together is detailed below.

Graduating students:

1. **Tijan Mede**. Master's degree from Université Grenoble Alpes in Geomechanics. February 2014 - June 2014. Co-supervision (60%) with Guillaume Chambon (40%, Inrae). We worked on a discrete element model to reproduce the snow mechanical behavior based on ice mechanics and snow microstructure. Tijan conducted a sensitivity analysis of the model to its parameters. This internship was my first experience as a supervisor during my Ph.D. at Inrae. Tijan stayed at Inrae for a Ph.D. on the same topic, and I was one of his Ph.D. supervisors.
2. **Thibault Pilloix**. Master's degree from Institut de Géographie Alpine in Geography. January 2015 - June 2015. Supervision (100%). We compared hardness profiles measured with different penetrometers with a dedicated field campaign. Thibault presented our results to snow professionals with a technical paper [Pilloix and Hagenmuller, 2015]. We also

formalized the idea that snow profile variability mainly originates from layer thickness variations due to natural heterogeneity or depth measurement errors. I continued developing this idea up to a publication [Hagenmuller and Pilloix, 2016]. Thibault then worked as a ski patroller in a ski resort.

3. **Rémi Granger**. Master's degree from ENS Cachan in Geosciences. January 2016 - June 2016. Co-supervision (80%) with Laurent Arnaud (20%, IGE). In order to find how field tests relate to snow stratigraphy, we explored 30 years of snow profile observations collected by Météo-France (400 000 snow layers) and high-resolution profiles of penetration resistance and specific surface area. Rémi showed that the literature is sometimes too optimistic about the performance of reverse analysis algorithms. This internship showed the need for further detailed analysis of the cone penetration test (e.g., Ph.D. of Isabel Peinke). Rémi stayed at CEN for a Ph.D. about snow microstructure and fabric.

4. **Coline Bouchayer**. Master's degree from Université Grenoble Alpes / Université de LaSalle Beauvais in Geosciences. February 2017 - July 2017. Co-supervision (50%) with Vincent Vionnet (50%, CEN). This internship aimed to synthesize the wealth of data provided by detailed snowpack simulations based on a matching algorithm I previously developed. We provided a new methodology to synthesize the data produced by the future operational snow model under development in Météo-France [Hagenmuller et al., 2018c], [Hagenmuller et al., 2018]. Coline is currently a Ph.D. student at the University of Oslo and works on glacier friction.

5. **Léo Viallon-Galinier**. Engineer's degree from Ecole Polytechnique in Mechanics. March 2017 - July 2017. Co-supervision (60%) with Matthieu Lafaysse (40%, CEN). We worked on evaluating the snowpack model Crocus with measured snow profiles. Léo used the matching algorithm to deal with stratigraphic mismatches and compare simulated and measured snow profiles. We also developed a method to re-initialize the snowpack model with measured snow profiles [Viallon-Galinier et al., 2020]. Léo is now a Ph.D. student under my supervision.

6. **Bruno Poirier**. Bachelor's degree from Ecole de Technologie Supérieure de Montréal (Canada). January 2018 - May 2018. Co-supervision (40%) with Isabel Peinke (60%, CEN). We investigated snow metamorphism by interpreting cone penetration tests performed with the Snow Micro-Penetrometer (SMP). Bruno set an efficient experimental protocol and provided new results, which Isabel used for her Ph.D. [Peinke, 2019]. This internship also gave Isabel a chance to experience supervision.

7. **Adrien Didier**. Master's degree from Ecole Normale Supérieure de Lyon in Geosciences. January 2019 - March 2019. Co-supervision (60%) with Guillaume Chambon (20%, Inrae) and Maurine Montagnat (20%, IGE). We tried to simulate a cone penetration test in snow based on a microstructure captured by tomography. Adrien managed to run preliminary simulations and provide a proof of concept of the methodology. I worked a lot to clarify the code so that this first step will not block future students (e.g., postdoc Clémence Herny). Adrien is currently a Ph.D. student at Institut National des Sciences Appliquées Lyon in material sciences.

8. **Oscar Dick**. Engineer's degree from Ecole Nationale Supérieure des Techniques Avancées Paris in Mechanics. September 2020 - March 2021. Co-supervision (20%) with Léo Viallon (50%, CEN) and Marie Dumont (30%, CEN). We studied the impact of dust-on-snow

events on snowpack stability. Oscar ran the snow model with or without dust deposition on the snow surface and presented the results at an international conference [Dick et al., 2021]. Besides, we wrote a magazine paper together in the magazine *Neige et Avalanche* [Dick et al., 2021] and a scientific paper is about to be submitted. My contribution was mainly to interpreting and modeling the simulated snow profiles regarding avalanche problems. This internship also gave Léo a chance to experience supervision. Oscar is now completing an internship at the WSL-SLF about avalanches.

9. **Louis Védrine**. Master's degree from Ecole Normale Supérieure Paris Saclay in Civil Engineering. March 2022 - July 2022. Co-supervision (60%) with Lionel Gélébart (20%, Commissariat à l'énergie atomique et aux énergies (CEA) Saclay) and Maurine Montagnat (20%, IGE). We studied the visco-plastic behavior of snow with a microstructure-based model. The model uses a solver based on the fast Fourier transform and takes the three-dimensional (3D) snow microstructure decomposed into individual snow crystals as input. We will evaluate the model on cold-lab creep experiments and focus on the role of the mechanical anisotropy of each ice crystal on the macroscopic mechanical behavior. Ongoing work.

10. **Loïc Guazzetti**. Technician's degree from Ecole Nationale de la Météorologie. May 2022 - July 2022. Co-supervision (40%) with Jean-Michel Panel (60%, CEN). This internship aimed to test and improve a prototype of a cryogenic cell adapted to cold-room tomographs. This cell is required to precisely control the temperature of snow samples along metamorphism experiments captured by X-ray tomography. This short internship also aimed to promote the CEN activities among Météo-France technicians for future open positions. Ongoing work.

Ph.D. students: Note that my HDR graduation formally requires the supervision of the equivalent of one complete (100%) Ph.D. student who has already obtained his final degree. The co-supervision of Isabel Peinke and Tijan Mede fulfills this condition.

1. **Tijan Mede**. Degree from Université Grenoble Alpes in Geomechanics. Co-supervision (30%) with Guillaume Chambon (50%, Inrae) and Francois Nicot (20%, Inrae). October 2015 - December 2018. Defended on 6/02/2019 [Mede, 2019]. Delivered by Université Grenoble Alpes. Funded by LabEx TEC21 (grant agreement ANR-11-LABX-0030). This Ph.D. aimed to develop a computational model taking as input the 3D snow microstructure and the ice properties to simulate the mechanical behavior of snow. The model is based on the discrete element method and can reproduce the brittle behavior of snow at high-loading rates. We improved the representation of a 3D microstructure with a limited number of discrete elements [Mede et al., 2018a]. We then explored the macroscopic mechanical response of different snow samples to mixed-mode loading. We observed three distinct failure modes [Mede et al., 2018b]. We characterized the microscale mechanisms leading to volumetric collapse [Mede et al., 2020]. Tijan then worked as a postdoc at the Institute of Metals and Technology in Ljubljana, Slovenia.

2. **Isabel Peinke**. Degree from Université Grenoble Alpes in Environmental Fluid Mechanics. Main supervisor (70%) with Guillaume Chambon (30%, Inrae). March 2016 - June 2019. Defended on 28/06/2019 [Peinke, 2019]. Delivered by Université Toulouse 3 - Paul Sabatier. Funded by Météo-France and the European Space Agency (Contract No. 4000112698/14/NL/LvH). This thesis aimed to understand the interaction between the

cone of a penetrometer and the snow. The final objective was to invert penetration profiles into microstructural properties. We analyzed cone penetration tests characterized by the progressive formation of a compaction zone. We successfully developed a non-homogeneous Poisson shot noise model explicitly accounting for this transient compaction. We used the model to characterize snow sintering with cone penetration tests under controlled cold-lab conditions [Peinke et al., 2019]. The second part of the thesis consisted of cold-lab experiments combining cone penetration tests and X-ray tomography. High-resolution 3D images of the snow samples before and after the cone test were measured. A new tracking algorithm was applied to determine granular displacements induced by the test and quantify the size of the compaction zone [Peinke et al., 2020]. Isabel is now a data scientist at meteo*swift.

3. **Léo Viallon-Galinier**. Degree from Ecole Polytechnique in Civil Engineering and Mechanics. Main supervisor (60%) with Nicolas Eckert (40%, Inrae). October 2019 - October 2022. Funded by the french ministry for the environment. This thesis aimed to combine the pros of physically-based snow models and machine learning to propose new avalanche hazard indicators. The main idea is to combine our knowledge of mechanical processes in the snowpack and machine learning with past observations. First, we implemented mechanically-based indices of snow stability in the snowpack modeling chain of Météo-France (paper in press). Then, we combined simulated data of the snowpack evolution with observed avalanche occurrences within a Random Forest approach to predict avalanche days. On the Haute-Maurienne massif (French Alps) and over the last 58 years, we showed the added value of considering snowpack modeling and mechanical stability indices instead of using only simple meteorological and bulk information (paper submitted). Last we will apply this methodology to other domains and sources of past avalanche activity. Ongoing work. Léo will join the CEN as a permanent researcher in autumn 2022.

4. **Antoine Bernard**. Degree from Ecole Normale Supérieure Paris Saclay in Material Sciences. Co-supervision (30%) with Maurine Montagnat (40%, IGE) and Guillaume Chambon (30%, Inrae). October 2019 - December 2022. Funded by Institut Polytechnique de Grenoble. Snow mechanical behavior is highly strain-rate dependent: ductile at low strain rates and brittle at high strain rates. This Ph.D. investigated this transition with controlled mechanical testing and aimed to identify the driving microscale mechanisms with tomography. We first analyzed snow oedometric tests captured by tomography. We could decompose the contributions of snow metamorphism and ice matrix creep on the snow microstructure evolution (paper submitted). We also designed a specific compression stage to conduct displacement-controlled tests in the space-limited tomographic cabin. We used this compression stage to explore various strain rates and simultaneously capture stress-strain curves and microstructure evolution. Ongoing work.

Postdoctoral fellows:

1. **Kévin Fourteau**. Ph.D. from the Institut des Géosciences de l'Environnement in Paleoclimatology. Co-supervision (60%) with F. Domine (40%, Unité Mixte Internationale de Takuvik). October 2019 - December 2020. Funded by Fondation BNP Paribas. This project investigated the potential bias of measuring snow thermal conductivity with heated needle probes. We conducted cold-room experiments combined with X-ray tomography and numerical experiments with a finite-element model. We showed that the needle probe

technique is flawed due to an unadapted asymptotic development of an analytical formula commonly used to invert the temperature signal and poor thermal contact between the inserted needle and snow [Fourteau et al., 2022]. While working on this topic, we noticed the absence of a theoretical framework accounting for the coupling of heat conduction and latent heat transport carried by water vapor. With numerical experiments on 3D snow microstructure, we showed how these processes scale to effective macroscopic diffusion [Fourteau et al., 2021b] and conduction [Fourteau et al., 2021a]. Kévin then did a 1-year postdoctoral fellowship at WSL-SLF and is now applying for a CNRS permanent position at CEN.

2. **Clémence Herny**. Ph.D. from Laboratoire de Planétologie et Géosciences in Planetary Science. Co-supervision (70%) with Guillaume Chambon (30%, Inrae). December 2020 - February 2022. Funded by Agence Nationale de la Recherche (ANR) on project Mimesis-3D. Recent numerical mechanical models based on 3D snow microstructures have provided new insights into snow mechanical behavior but have lacked experimental evaluation. This project aimed to evaluate these models using experimental data. We combined tomographic imaging and cone penetration tests conducted in a cold room. We developed a model to reproduce the experimental tests. The model reproduced the penetration profile and the displacement field of the grains around the cone. Paper to be submitted soon. Clémence, after some time off, is looking for a new job.

3. **Julien Brondex**. Ph.D. from the Institut des Géosciences de l'Environnement in Glaciology. Co-supervision (30%) with Marie Dumont (40%, CEN) and Neige Calonne (30%, CEN). May 2021 - May 2024. Funded by European Research Council (ERC) on project IVORI. The overall project's objective is to build a snow-firn model based on microstructure that includes all relevant physical variables and processes to improve the modeling of seasonal and perennial snow. The postdoc started reviewing all the governing equations of snow evolution. Some equations needed to be re-built with the homogenization of microscale processes. The main challenge we face now is the development of numerical and rigorous schemes adapted to the evolution equations we want to implement in the snow model. Ongoing work.

1.2 Short introduction to snow mechanics

1.2.1 Definition of snow mechanics

Shapiro et al. [1997] define snow mechanics as "the theoretical and applied science of the mechanical behavior of snow; it is that branch of mechanics concerned with the response of snow to the force fields of its environment." For Mellor [1975], snow mechanics also "embraces the underlying physics of processes relevant to the mechanical behavior." In other words, the general objective of snow mechanics is to provide constitutive equations that relate strain ε and stress σ and explain the fundamental processes by which these relationships originate. Mellor [1975] also includes "the useful but disconnected empiricism associated with snow engineering, avalanche prediction, etc." Thus, his definition goes beyond formal material sciences. My research somewhat embraces these contours of snow mechanics: knowledge of the fundamental microscopic processes affecting the macroscopic mechanical behavior and a more practical and empirical methodology to predict the avalanche danger.

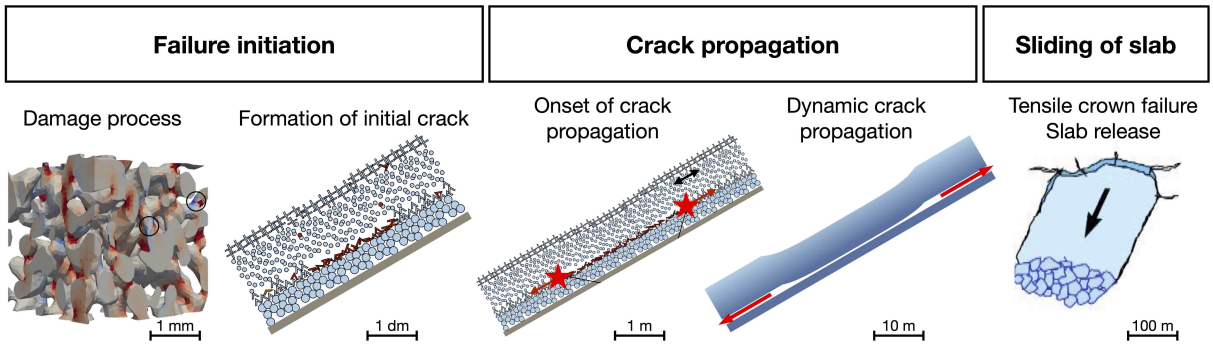

Figure 1.1: Different processes and scales involved in dry-snow slab avalanche release. Conceptual model from [Schweizer et al., 2021] adapted with inputs from [Hagenmuller et al., 2014c] and [Hagenmuller, 2017b]. The bar scale indicates the typical scale of the process considered.

1.2.2 Importance of snow mechanics

Knowledge of snow mechanics was primarily motivated by preventing avalanche hazards that endanger people and infrastructure in snow-covered mountain regions [Bader, 1962]. Indeed, the mechanical properties of the snow control the avalanche release and the avalanche flow [e.g., Schweizer et al., 2003; Ancey, 2006]. According to Shapiro et al. [1997], apart from avalanche forecasting and hazard mapping, the use of snow mechanics remained relatively infrequent due to the scarcity of commercial or governmental activities that require knowledge of snow properties and processes. For these authors, this is the reason for the limited funding for snow mechanics research. However, optimizing the mobility of military, industrial, or recreational vehicles on snow-covered terrain also led to active research in snow mechanics in the last decades [Shoop et al., 2006]. More recently, snow mechanics has also gained importance in understanding the natural evolution of snow. Indeed, snow is an essential component of the Earth's climatic system at the interface between the atmosphere and the ground [e.g., Brun, 2006]. It stores, when highly compacted, the history of the chemical composition of the atmosphere [e.g., Barnola et al., 1987]. It constitutes an important water stock for agriculture and hydroelectricity [e.g., DeBeer and Pomeroy, 2017]. It is the basis of the ski industry [e.g., Spandre et al., 2016; Hasler et al., 2016]. Last, its weight may represent a critical load on structures [e.g., Le Roux et al., 2020]. These applications do not primarily require snow mechanics. However, mechanics is a prerequisite to predicting the natural evolution of snow and its properties relevant to the considered problem. For example, interpreting greenhouse gas records in polar ice cores requires understanding how gas is trapped and, thus, how porous snow evolves into bubbly ice with closed pores [Burr et al., 2019; Fourteau et al., 2020]. Knowledge of snow evolution with, e.g., ice dislocation creep and metamorphism is not the main objective in this case but constitutes an essential intermediate step. Therefore, a better understanding of snow mechanics would benefit many applications.

Many of my research results on snow mechanics are versatile. However, the final application in mind is mainly avalanche release, whose forecasting is one of the missions of Météo-France. Two types of avalanche release can be distinguished: loose snow avalanches and slab avalanches. Loose snow avalanches start from a point on the snowpack surface and gain volume with a down-slope domino effect and the erosion of the underlying snow by the avalanche flow. Slab avalanches involve the release of a cohesive slab maintained on a slope by a metastable weak layer [Schweizer et al., 2003]. This avalanche type causes the most damage and fatalities because

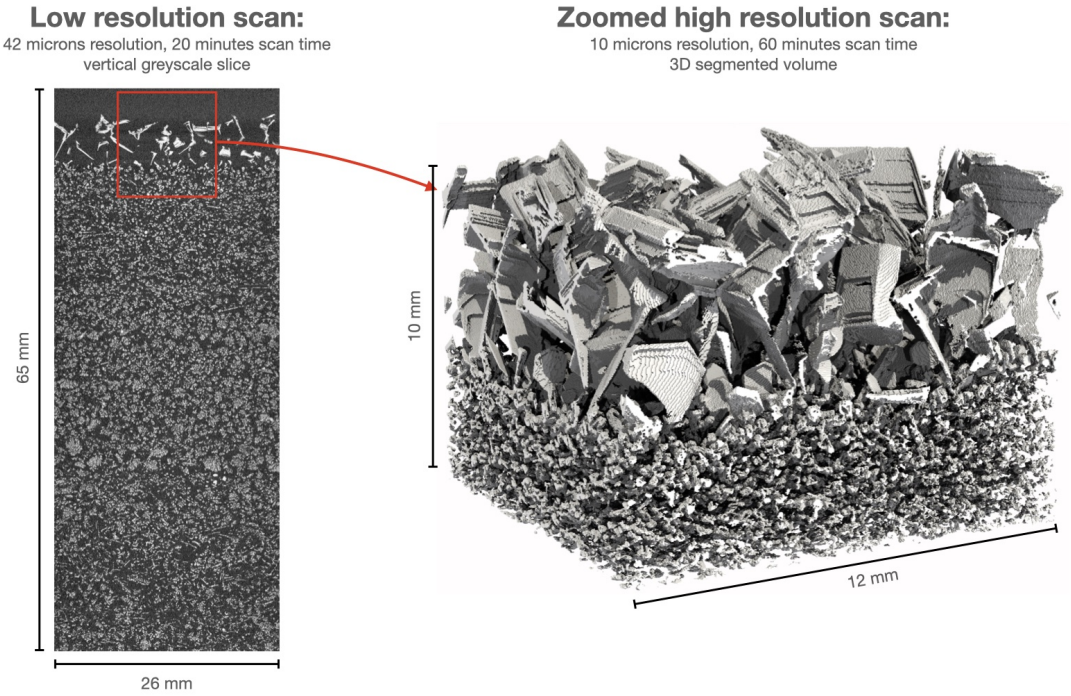

Figure 1.2: Snowpack layering revealed by X-ray tomography. Sampling at Col de Porte, 14/12/2021. The upper layer consists of surface hoar (SH). Below, a mixture of precipitation particles (PP), including graupel (PPGp), and decomposing and fragmented snow (DF) can be found. Unpublished.

the associated release volume is generally much higher, and the trigger (e.g., a skier) is in the middle of the released slab. In France, 95% of fatalities are caused by slab avalanches, according to the ANENA. Figure 1.1 presents the main mechanisms involved in the release of dry-snow slab avalanches. Failure initiation originates from the coalescence of damage in the ice matrix in competition with healing through sintering [Reiweger et al., 2009]. Depending on the strain rate considered (e.g., spontaneous release or artificial triggering), different microscopic processes need to be taken into account (see Sect. 1.2.4). In terms of snow mechanics, this process is generally up-scaled at a mesoscopic scale within a strength-of-material approach [e.g., Hagenmuller et al., 2014c]. When damage localizes in a crack of a few centimeters, the material strength approach is no longer adapted, and fracture mechanics formalism is required. Generally, linear elastic fracture mechanics is used to capture the onset of crack propagation in the so-called anti-crack mode [Heierli et al., 2008]. During dynamical crack propagation, the crack expands without additional load at high speed, and the driving mechanism may evolve [Bobillier et al., 2021]. Lastly, tensile stresses caused by the movement of the slab cause the opening of a crown crack in the slab [Jamieson and Johnston, 1992]. As expected, a better understanding of snow mechanics is thus of great interest in modeling the processes involved in avalanche release.

1.2.3 Snow microstructure diversity

The lack of budget might not be the main reason for the absence of explicit constitutive equations that describe snow mechanics. I believe the reason is more related to the diversity of snow microstructural patterns that exist naturally on Earth (Fig. 1.2). Compared to rocks, snow

is characterized by a relatively simple composition: mostly air, a bit of hexagonal-ice crystals, sometimes a touch of liquid water, and traces of impurities. Challenges arise from the 3D arrangement of these constituents, the so-called snow microstructure. There exists no single snow material but an infinite number of different materials composed of air and ice [e.g., Hagenmuller, 2014]. For example, the snow density typically ranges between 30 and 550 kg m^{-3} (perennial snow of higher density is called firn or porous ice) [Theile, 2010]. Its specific surface area, defined as the ratio between the air-ice interface area and the ice mass, ranges between 2 and 160 m^2 kg^{-1} [Kerbrat et al., 2008]. Furthermore, the international classification for seasonal snow on the ground distinguishes nine main classes of grain shape and 37 subclasses [Fierz et al., 2009]. Even if this number of classes is already large, this classification relies on a single criterion describing snow: the shape of snow grains individualized on a crystal card [Mallett, 2021].

The different snow types originate from the intermittent and variable nature of precipitation, the action of wind and gravity, and the permanently ongoing metamorphism of snow. These distinct layers of snow create a stratified snowpack (Fig. 1.2). This diversity first arises from the formation of snowflakes in the atmosphere. The shape of a snowflake that generally grows by deposition of water vapor onto a nucleus depends on temperature and humidity [Nakaya, 1954]. Precipitation particles already comprise nine different snow classes such as columns, needles, and stellars [Fierz et al., 2009]. The general public knows this as "no two snowflakes are alike." However, once on the ground, the story of snow does not end, and snow continues to evolve. Snow is one of the most brittle materials known to man [Schweizer et al., 2004], and it evolves mechanically. Gravity (and the weight of the overlying layers) induces progressive compaction through the creep of the ice matrix [Schleef et al., 2014]. Wind can break snow grains into smaller particles, forming a more compact and sintered structure [Comola et al., 2017]. Besides, snow is a porous material with a high specific surface area and is generally close to its melting temperature. Therefore, it is very active thermodynamically with continuous localized phase changes and mass transport through liquid or vapor phases [Colbeck, 1982]. These processes lead to rapid changes in grain size and shape. Under dry isothermal conditions, metamorphism is driven by the curvature of the ice-air interface [Bader and Niggli, 1939]. This equilibrium metamorphism tends to round the grain shape and increase the grain size and bond size. When there is a strong temperature gradient (e.g., > 10 K m^{-1}), vapor fluxes are mainly controlled by the local temperature gradient [Marbouty, 1980]. This kinetic metamorphism tends to reveal the hexagonal crystalline structure of ice with the formation of sharp edges and flat facets. It also generally leads to a weak and anisotropic microstructure. Finally, wet snow metamorphism is active when the snow temperature is at its melting temperature. This metamorphism can be fast compared to dry snow metamorphism and depends on the liquid water content [Colbeck, 1975]. It generally creates large roundish grains connected with capillary or icy bonds. These processes contribute to the diversity of snow microstructural patterns, making snow science rich.

Due to this diversity, understanding the mechanics of snow is closely related to its microstructural characterization [Brown, 1989]. It has long been recognized that density alone is insufficient to describe the mechanical behavior of snow at a given temperature. For example, Keeler and Weeks [1968] showed that two samples with the same density but different microstructures might have strengths that differ by a factor of four. Jamieson and Johnston [1990] observed that the snow with a faceted microstructure was approximately half as resistant as partly settled or rounded snow of the same density. More recently, Hagenmuller et al. [2015] observed the same ratio within numerical experiments based on snow tomographic data. However, numerous experimental studies only reported the mechanical properties of snow as a function of density [e.g., Mellor, 1975; Shapiro et al., 1997]. Figure 1.3 presents the values of Young's modulus compiled

from different studies. Linear elasticity is described by a simple formalism, namely a linear relationship between stress and strain. However, the characterization of the elastic modulus suffers from a huge scatter for a given density. For example, the elastic modulus of snow ranges on two orders of magnitude for a density of 200 kg m^{-3} (Fig. 1.3). One may incorrectly claim that this variability entirely arises from the snow microstructure variability at a given density. A large part of the scatter is rather probably due to experimental biases. However, within a given study with constant bias, the scatter remains up to one order of magnitude for low-density snow. Therefore, mechanical properties should always be associated with a detailed and possibly quantitative description of the snow microstructure.

The diversity of snow types is generally first characterized by the class of grain shape [Fierz et al., 2009]. This description is adapted to manual field observations with a simple crystal card and a magnifying glass (8x magnification minimum). However, codification in discrete classes cannot render the continuum of microstructural patterns found in nature. This technique also inevitably involves subjectivity. This description can hamper the development of detailed snowpack models, which describe snow evolution with differential equations [Löwe et al., 2016]. Since the pioneering work of Good [1987] and Brzoska et al. [1999], X-ray tomography now allows for a complete capture of the 3D snow microstructure at a resolution of around 10 μm. It provides a way to characterize the diversity of snow but is restricted to small samples and generally to lab experiments. Therefore, intermediate measurement techniques are required to characterize the snow microstructure in the field. The cone penetration test measured with high vertical resolution provides promising information on the microstructural layering of the snowpack [Schneebeli and Johnson, 1998; Löwe and van Herwijnen, 2012]. Measurements of the interaction of light and snow grains also comprise exciting metrics at the microstructure scale [Libois et al., 2014]. Measurements of thermal conductivity might also constitute an indirect way to capture the bond system in the snow microstructure since narrow constrictions limit thermal fluxes in the ice matrix [Domine et al., 2011]. In summary, the diversity of snow types is mainly captured by grain shape classification in the field and tomography in the lab, but promising intermediate tools are under development.

1.2.4 Deformation regimes

Another difficulty that arises when dealing with snow mechanics is its variety of mechanical behaviors, depending on the strain rate, the loading direction, the temperature, and the microstructure. Narita [1984] distinguished four types of deformations under tension according to the strain rate $\dot{\varepsilon}$. At high strain rates, $\dot{\varepsilon} > 10^{-4}$ s^{-1}, he observed a visco-elastic regime with the sudden occurrence of fracture, i.e., brittle failure. Hagenmuller et al. [2014c] observed that microstructural damage may already occur for infinitesimal strain and that the failure is not as sudden as it appears. At low strain rates $\dot{\varepsilon} < 5 \times 10^{-6}$ s^{-1}, snow deforms continuously without failure. Viscous deformation dominates, and the mechanical behavior resembles that of a fluid. In the ductile-to-brittle transition, Narita [1984] observed an average behavior between local damage (micro-cracks) and viscous deformation. The ductile-to-brittle transition becomes more complex when the applied deformation yields new contacts between snow grains. In particular, de Montmollin [1982] exhibited a two-step transition with an intermediate regime, the brittle regime of the first kind, between the viscous and brittle regimes. The focus on a specific regime depends on the application: for avalanche release, assuming snow is brittle might be sufficient for the moment. Considering snow as a viscous material for snow settlement is more relevant than as a brittle material. The mechanical behavior of the snow also depends on the direction of loading. For example, Reiweger et al. [2015] measured the failure envelope of weak snow layers

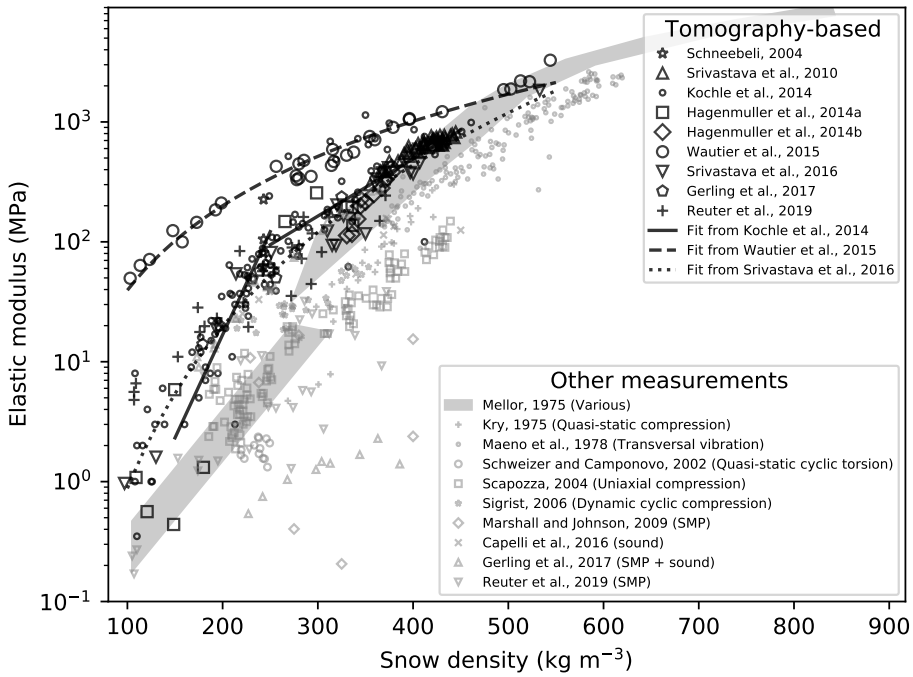

Figure 1.3: Elastic properties of snow as a function of density. Compilation of different studies including numerical experiments based on tomographic data. When the full elastic tensor is available, the equivalent isotropic Young's modulus is reported in this graph. Unpublished.

and described it with a Mohr-Coulomb model with a cap. The mechanical behavior of snow can also be anisotropic with different responses when the loading directions are rotated [e.g., Hagenmuller et al., 2014a].

The macroscopic behavior of snow can be interpreted by the behavior of its main solid constituent, ice. Ice in snow can be elastic, brittle, quasi-brittle with the progressive build-up of damage before failure, or visco-plastic. In addition, sintering can heal damage in the ice matrix or form new cohesive contacts. The prevalence of one of these processes mainly depends on the strain rate. At high strain rates, elastic deformation of the ice matrix, failure of bonds, and potential granular rearrangement of snow particles can explain the elastic or pseudo-plastic macroscopic behavior [Hagenmuller et al., 2014c, 2015]. The anisotropic behavior originates from the anisotropy of the microstructure [Srivastava et al., 2016]. Mechanical behavior under mixed-mode loading conditions may result from the Mohr-Coulomb-like behavior of ice and the complex redistribution of stresses within the ice matrix [Hagenmuller et al., 2014c]. The visco-plastic behavior of snow originates from the dynamics of dislocation in individual ice crystals, typically modeled with Glen's law (Norton-Hoff). It is not yet evident how this local behavior of ice crystals scales up to the macroscopic scale [Theile et al., 2011]. However, it is sufficient to explain the ductile-to-brittle transition: above a critical strain rate, the dislocation cannot accommodate the deformation smoothly anymore, and the local stresses exceed the material strength [e.g., Löwe et al., 2020]. de Montmollin [1982] explained the double brittle-to-ductile transition by the sintering process. Sintering produces the adhesion of two ice surfaces in contact [Hobbs and Mason, 1964]. The build-up of adhesion strength is time-dependent: the longer the particles remain in contact, the stronger the cohesive bond created [Szabo and Schneebeli, 2007]. As shown by Löwe et al. [2020], incorporating this time-dependent behavior is sufficient to explain singular stick-slip cycles at specific strain rates. Overall, even if the snow mechanical behavior appears to be complex, the individual processes at play at the microscopic scale appear relatively simple. The complexity and sometimes the apparent order here arise from the aggregate of a considerable number of uncoordinated interactions between elements of the system [Ladyman et al., 2013].

1.2.5 Scientific challenges

The following overarching scientific challenges and questions shaped my research:

- *Snow microstructure, a key to understanding snow mechanics.* Quantitative knowledge of snow mechanics remains rather limited due to the diversity of snow types and the insufficient characterization of the link between snow microstructural patterns and its mechanical behavior. Snow microstructure characterized by tomography thus appears as a key to understanding snow mechanics at the material scale. How do we make tomography systematic and convenient to characterize snow microstructure in a lab? How do we use the wealth of data produced by tomography to understand the link between microstructure and snow mechanics or related thermo-dynamical processes? In particular, how does snow fail, and how does snow settle under gravity or evolve through water vapor transport?

- *Snow microstructure in the field and the snowpack model.* Tomography describes the 3D arrangement of ice and pores of small samples at a micrometric level. This time-consuming measurement technique appears unadapted to the monitoring of seasonal snowpack evolution. Furthermore, this description is sometimes overkilling for current snowpack models affected by other sources of uncertainty and running on large spatio-temporal domains

(mountain ranges and decades). Is there an alternative to tomography to capture snow microstructural proxies directly and quickly in the field? Do cone penetration tests constitute this alternative, and can the penetration signal be inverted into microstructural proxies? What does the cone precisely measure, and how do the snow grains interact with the penetrometer tip? Could the heated needle probe that measures thermal conductivity be a convenient way to capture the snow bond system? By the way, what does the needle precisely measure? Do we really need high-resolution profiles, and does the spatial variability of the snowpack reduce the benefit of these profiles to zero? How can we combine different profiles and use them to evaluate detailed snowpack models? Has the current description of snow microstructure in snowpack models reached its limits?

- *Avalanche formation.* Our understanding of the processes involved in avalanche formation has increased significantly over the past decades. With mechanical models dedicated to simplified problems and specific measurements, we now better understand the snow mechanics at work at different scales. However, the view seems less attractive when looking at "real life" modeling tools designed as a decision aid to avalanche forecasters (e.g., the modeling chain of Météo-France). What models of snowpack stability could we adapt to our tools? Most of these models are based on physics and assume that the input simulated snowpack is free of errors. How can we combine these models with machine learning to provide relevant indicators of snowpack stability, benefiting from past observations of avalanche activity?

The three main scientific challenges listed above correspond to the following three chapters. Some are intimately related (e.g., Chapters 2 and 3) and benefit from each other. For others, the gap remains too big for a bridge, or they do not necessarily share connected objectives (e.g., Chapters 2 and 4). At the end of each chapter, the ongoing work and my research plan for the next five years are presented for these central challenges. A last shorter chapter summarizes my past research contribution and future perspectives.

Chapter 2

Snow microstructure, a key to understanding snow mechanics and physics

Preamble

This chapter is dedicated to understanding the link between the snow microstructure and the snow properties. First, I present the tomographic setup and image processing tools we developed. Second, I describe how tomographic data can be used to feed computational models that reproduce the mechanical properties of snow. In particular, we will focus on brittle properties modeled with two different approaches. Third, I show how computational approaches and detailed observation allowed by tomography help understand features of snow evolution, namely the coupling of heat and mass transfer and the combination of metamorphism and ice creep during snow settlement. Finally, some guidelines for future research are drawn.

Contents

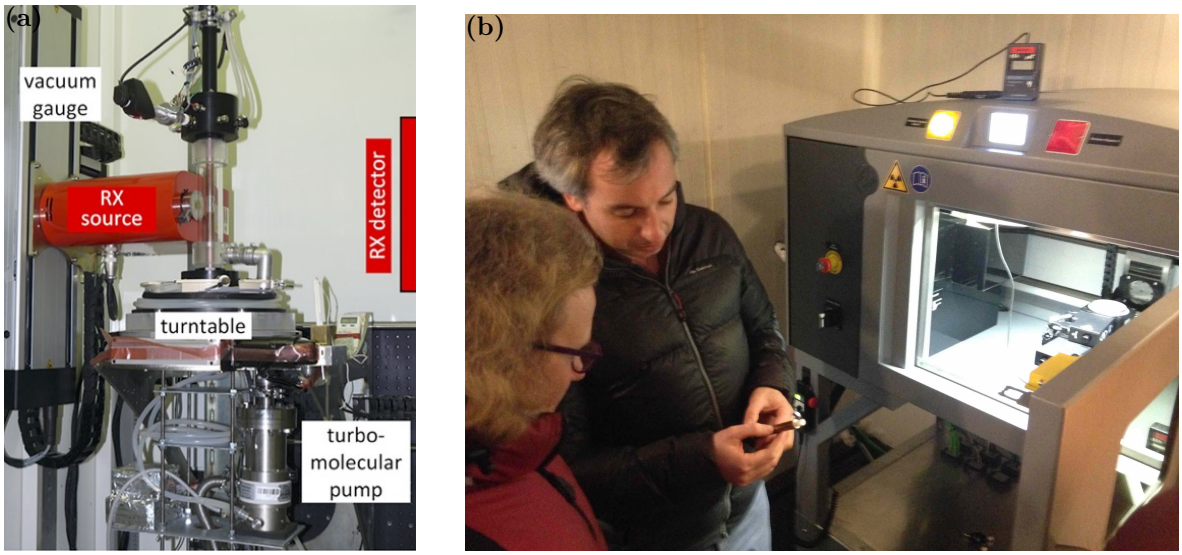

Figure 2.1: Two complementary strategies to perform tomographic scans of frozen materials: a) CellDyM: a miniaturized cryogenic cell compatible with standard tomographs operating at ambient temperature [Calonne et al., 2015], and b) TomoCold: a tomograph directly adapted to operate down to -30° C.

2.1 Snow tomography

2.1.1 Tomography of frozen materials

X-ray tomography uses the ability of X-rays to penetrate objects. When the X-rays pass through an object, part of the radiation is absorbed. Depending on the object size and the attenuation coefficient of the material, more or less energy escapes on the opposite side, which a detector can measure as a radiograph. When the photoelectric effect is the dominant contributor to absorption, the attenuation coefficient μ can be approximated as a function of the density of the material ρ, its atomic number Z and the radiation energy E (typically 10 to 40 keV) as [Alvarez and Macovski, 1976]:

$$\mu = K\rho\frac{Z^4}{E^3} \tag{2.1}$$

where K is a constant. X-ray radiation, therefore, easily distinguishes air from ice, but the contrast between liquid water and ice remains small (Eq. 2.1). For tomography, hundreds (typically 1500) of two-dimensional radiographs are taken in sequence, measuring objects in various rotational positions. On standard tomographs, the object is located on a rotation stage. In contrast, a medical X-ray scanner turns around the patient body. The relation between attenuation and absorption, the Beer-Lambert law, is then used in advanced numerical schemes (filtered-back projection algorithm) to invert the sequence of radiographs into 3D images. The value of each voxel in the 3D image is proportional to the attenuation coefficient (Fig. 2.2a).

The 3D measurement of the snow microstructure is a relatively new research field. Good [1987] first superposed photographs of thin sections of snow that were progressively cut in a casted sample. In a certain way, the method provided 3D images of snow but was never applied again because it is extremely time-consuming, and the cutter resolution (>100 μm therein) limits the image resolution. Brzoska et al. [1999] from CEN (!) provided the first 3D images of the

snow microstructure at a resolution of 10 μm. They benefited from the ID19 beamline of the European Synchrotron Research Facility (ESRF) in Grenoble. Since then, the methodology has developed, and tomography has become a standard material and snow science tool. In Grenoble, notably under the impulse of my colleague F. Flin, miniaturized cryogenic cells were improved and developed to maintain small snow samples at a given temperature in an environment at ambient temperature (Fig. 2.1a) [Calonne et al., 2015]. This strategy enables us to take advantage of the performance of any tomograph, such as synchrotron beamlines. However, the manipulation of snow samples at room temperature is limited. This strategy has been applied mainly to capture the time evolution of the snow microstructure under controlled temperature conditions [e.g., Calonne et al., 2014a]. Other snow labs such as the WSL-SLF in Switzerland [Schneebeli and Sokratov, 2004], the Alfred Wegener Institute in Germany [Freitag et al., 2013], the Dartmouth College [Baker, 2019] or the Montana State University in the USA [Lebaron and Miller, 2014] adopted another strategy. They installed a slightly modified tomograph directly in a cold room.

For my research, the limitations of the cryogenic cell do not allow us to easily perform mechanical tests combined with tomography and scan large samples. We decided to buy a new tomograph (TomoCold) dedicated to snow and ice studies and located in a cold room. Between 2017 and 2019, I was in charge of funding (CNRM: 160 k€, OSUG: 79 k€, LEFE-INSU: 20 k€, [Hagenmuller, 2018]), instrument selection, administrative public market procedure, and on-site evaluation. The DeskTom130 tomograph from RXSolutions company appeared to be the best solution (Fig. 2.1b). Table 2.1 summarizes its technical specifications. In particular, it operates at cold temperatures down to -30°C and up to a resolution of 5 μm. I am responsible for the general operation and maintenance of the system. Since April 2019, we have used 1300 h of X-ray radiation for about 500 3D images and thousands of single radiographs. The system benefits my research, my students (postdocs of K. Fourteau, C. Herny, Ph.D. of A. Bernard, Master of L. Vedrine), but also, more broadly, my lab (projects ANR Mimesis-3D, ANR Alpalga, ERC IVORI) and the snow community in Grenoble (IGE, Inrae).

2.1.2 Image processing

The output of the tomograph is a 3D image whose grayscale value represents the X-ray attenuation coefficient (Fig. 2.2a). These data do not directly quantify the snow microstructure. In particular, an essential processing step involves reducing the grayscale image to a binary image object/background (Fig. 2.2a, red contour). This step is called binary segmentation and affects all subsequent quantitative analysis of the snow microstructure [Hagenmuller et al., 2016]. Unfortunately, the grayscale image is noisy, and the transition between materials is generally fuzzy (Fig. 2.2a). Thus, binary segmentation is not straightforward. This step has long been recognized as a weak point in the image processing of snow tomographic data and a time-consuming process if each slice must be manually corrected [Lesaffre et al., 2003]. Snow segmentation techniques are usually based on global thresholding [Coléou et al., 2001; Flin et al., 2003; Schneebeli and Sokratov, 2004; Kerbrat et al., 2008; Heggli et al., 2009]. However, this technique is not robust and biased if the threshold value is determined visually [Boykov and Funka-Lea, 2006; Iassonov et al., 2009]. During my Ph.D., we developed a new technique [Hagenmuller et al., 2013, 2016] which we then continuously improved [Hagenmuller et al., 2019; Dumont et al., 2021]. The algorithm is implemented in C++ with a Python interface and can be easily used by students [e.g., Peinke et al., 2020; Fourteau et al., 2021b,a] [e.g., Granger et al., 2021] at CEN or in other labs [e.g., Willibald et al., 2020].

The main idea behind this segmentation technique is to take advantage of some basic knowledge about the physics of X-ray radiation and snow metamorphism. First, the distribution of

Scanning capabilities	
Operating temperature	[-30, +2] °C
Highest true resolution	5 μm
Typical scan time (highest resolution, single field)	1 h
Maximum scanned volume (diameter × height)	180 mm × 250 mm
Maximum sample weight	2 kg
Mechanical specifications	
Cabinet dimensions	1800 mm × 1250 mm × 800 mm
Total weight	650 kg
Vertical axis stroke	150 mm
Horizontal axis stroke	150 mm
Zoom axis stroke	520 mm
Focal point to detector distance (FDD)	610 mm
Min. focal to object distance (FOD)	13 mm
X-ray source (Hammamatsu microfocus stealed tube)	
Maximum voltage	130 kV
Maximum power	39 W
Minimum focal spot size	5 μm
X-ray detector	
Pixel matrix	1920 x 1536
Pixel pitch	127 μm
Frame rate	1-60 fps

Table 2.1: Technical specifications of TomoCold.

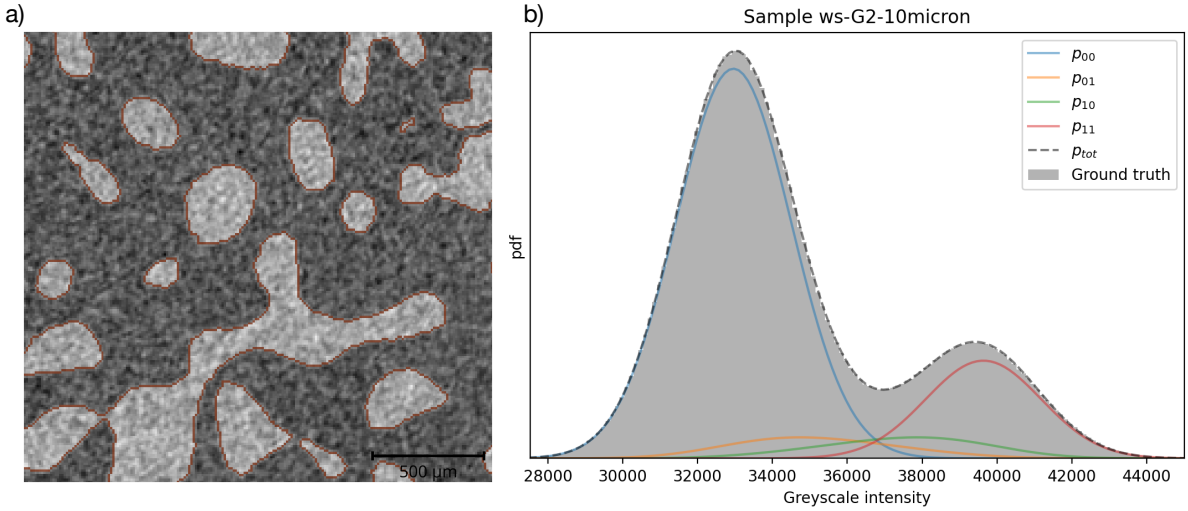

Figure 2.2: Image segmentation: a) Typical grayscale attenuation image of a snow sample reconstructed from radiograms. The ice appears in clear gray (high attenuation), and the air appears in dark gray (low attenuation). The red contour represents the segmented ice domain. b) Measured histogram of the grayscale image ("Ground truth") and associated statistical model p_{tot}. Distributions p_{00} and p_{11} represent the intensity distribution of pure air and ice. The symmetric distributions p_{01} and p_{01} represent the intensity distribution of mixed voxels (air mixed with ice or ice mixed with air).

the grayscale value or intensity I is modeled with a statistical model (Fig. 2.2b). The statistical model assumes that the noise in the image depends only on the tomographic settings and not on the scanned material. Noise is described by a Gaussian distribution with a standard deviation σ. With this assumption, the intensity distribution can be modeled with a sum of two Gaussian distributions whose means (μ_0, μ_1) and normalization factors (λ_0, λ_1) correspond to the attenuation coefficients, and relative proportions of material 0 and 1, respectively. This model is known as the Gaussian mixture model [Choi et al., 1991]. This model does not account for partial volume effects, i.e., the presence of voxels containing a mixture of different materials because the limit between the materials does not exactly follow the voxel grid and because of blur in the reconstructed image. Knowing the interaction of X-rays with the matter, we can assume that the intensity of mixed voxels is proportional to the quantity of material in the voxels. The intensity distribution of mixed voxels can thus be described by the convolution of a Gaussian distribution (noise) and a uniform distribution (proportion of one material). This model is called the partial volume mixture model [Bromiley and Thacker, 2008; Brenne et al., 2021] and describes the full distribution p of the grayscale intensity I as:

$$p(I) = \lambda_0 \mathcal{N}(\mu_0, \sigma)(I) + \lambda_1 \mathcal{N}(\mu_1, \sigma)(I) + \frac{1 - \lambda_0 - \lambda_1}{\mu_1 - \mu_0} \left[\operatorname{erf}\left(\frac{I - \mu_0}{\sigma\sqrt{2}} \right) - \operatorname{erf}\left(\frac{I - \mu_1}{\sigma\sqrt{2}} \right) \right] \tag{2.2}$$

with $\mathcal{N}(\mu, \sigma)$ a Gaussian distribution of mean μ and standard deviation σ, and with the error function defined as $\operatorname{erf}(x) = 2/\sqrt{\pi} \int_0^x \exp(-u^2) du$. This model is then fitted to the grayscale histogram using the least-square approach (Fig. 2.2). The five parameters of the distribution are related to the scanning procedure and the microstructure of the object. In particular, they determine the snow density as $\rho = \rho_{ice}(1 + \lambda_1 - \lambda_0)/2$ and are related to the area of the ice-air interface S and the thickness d of the blurred transition as $S \times d = 1 - \lambda_0 - \lambda_1$.

Second, we exploit the information derived from the grayscale distribution model to segment the grayscale using an energy-based approach. The main idea is to define the cost of assigning one voxel to the air or the ice phase. The best segmentation minimizes this cost. This energy or cost function comprises a data fidelity term and a regularization term. The data fidelity term is related to the likelihood that a voxel of a given intensity is composed of one of the two materials. It can be directly derived from the statistical model described above. For example, in Figure 2.2, it is rather unlikely that a voxel with an intensity of 40 000 is mainly composed of air, and it will cost "a lot" to segment it as air. The data fidelity term depends only on the local grayscale value. Iassonov et al. [2009] showed that adding regional information improves the segmentation performance. We add this information through the regularization term that penalizes the segmentation in different phases of neighboring and similar voxels. More precisely, we define the cost C_{ij} of segmenting two neighboring voxels i and j in different phases as:

$$C_{ij} = r \cdot w_{ij} \left(1 + \alpha \exp\left(-\frac{(I_i - I_j)^2}{2\sigma^2} \right) \right) \tag{2.3}$$

with σ the noise amplitude, r the amplitude of the regularization term, α the relative cost of the gradient, and w_{ij} factors depending only on the relative position of the two voxels in the image grid. For $\alpha = 0$, Hagenmuller et al. [2013] showed that the global regularization term is proportional to the ice-air interface area and that the regularization amplitude defines the effective resolution of the segmented image. The regularization term penalizes large interface areas. This penalization is particularly interesting for snow, where metamorphism naturally reduces surface energy. For $\alpha > 0$, the algorithm will also preferentially locate the ice-air interface where the grayscale gradients are the highest [Boykov and Funka-Lea, 2006]. Minimizing the

energy function on billions of binary variables is carried out with cuts in a well-chosen graph [Boykov and Kolmogorov, 2004; Jamriska et al., 2012]. The precision of the initial method was demonstrated on synthetic snow images [Hagenmuller et al., 2013], and the method is now commonly applied to snow tomographic data. Its main advantage is that it benefits from local spatial information and is almost automatic, with only two "free" parameters that the user can choose: the effective resolution r and the gradient cost α. The whole procedure was generalized to samples composed of more than two materials (e.g., air, ice, and mineral dust) and to 4D images (e.g., 3D time series) by Hagenmuller et al. [2019].

2.1.3 Database

The hands-on tomograph and the associated efficient image processing framework produce a considerable amount of data. Building a robust database with clear and systematic meta-data is necessary to use these data efficiently. Together with my colleague N. Calonne, we adapted the formalism of ITK/MetaIO (`https://itk.org/Wiki/ITK/MetaIO/Documentation`) to tomographic snow data. Figure 2.3 shows some of the meta-data fields. I will not go into the details of this technical work, but it is essential to ensure that the data become FAIR: findable, accessible, interoperable, and reusable [Jacobsen et al., 2020].

2.2 Snow mechanical properties

An approach frequently applied in my research is predicting the macroscopic mechanical properties of snow based on the 3D snow microstructure and the properties of ice. The goal is to find the homogeneous material that behaves like the heterogeneous material made of ice and pores. This approach is called homogenization and provides a powerful tool that complements difficult experiments on fragile and evolutive snow. Homogenization formally requires that the characteristic dimension of the volume of material or the phenomenon is much larger than the characteristic dimension of the heterogeneities (e.g., grain or pore size) [Auriault, 1991]. In this section, two different modeling strategies are used to reproduce the snow elastic and brittle behavior: finite elements and discrete elements. Finite elements are suited to model elastic and strength properties. Discrete elements are suited to model the entire stress-strain curve, including the post-peak softening involving granular rearrangements.

2.2.1 Homogenization of elastic properties

At high strain rates and low strain amplitudes, snow exhibits an elastic behavior [Narita, 1984]. The stiffness tensor $\boldsymbol{E}$ characterizes the linear elastic relation between stress $\boldsymbol{\sigma}$ and strain $\boldsymbol{\varepsilon}$ as: $\boldsymbol{\sigma} = \boldsymbol{E}\boldsymbol{\varepsilon}$. Numerical homogenization is a convenient way to estimate $\boldsymbol{E}$. Moreover, it can be seen as a solution to obtain reproducible results with scatter only attributed to microstructural effects. However, the elastic modulus values obtained with this technique are as scattered as those measured directly, especially for low densities (Fig. 1.3, black points). The isotropic elastic modulus values reported in the literature span two orders of magnitude for a given density. Meanwhile, each density-based parameterization fits the corresponding data points well [Köchle and Schneebeli, 2014; Wautier et al., 2015; Srivastava et al., 2016] (Fig. 1.3, lines). Therefore, only a small part of the overall scatter can be attributed to microstructural effects. Where does this scatter come from?

Homogenization yields apparent macroscopic properties of the sample tested. However, apparent properties are not necessarily effective, i.e., representative of the material and unaffected

key	description	comments
imageID	Unique identifier of the image	Generally projectName + _ + imageName + _ + imageType
pathFile	Complete path to mhd file	Needs to be re-generated from individual mhd file via dedicated python functions, if directory changes. Not present in mhd meta data as redundant.
projectName	Name of the associated project	forbidden characters: _, /, space Preferred format : YYYY_familyName_projectName
imageName	Name of the image	PROCESSED + / + projectName + / + Images + / + imageName + _ + imageType + '.raw' gives the name of the raw file.
imageType	Image type	- grey: grey volume - seg: segmented volume - roi: segmented sub-volume inhomogeneous - roi-hom: segmented sub-volume homogeneous (e.g. can be used for macro. properties computations
pixelType	Binary encoding of the raw image	Preferred is ushort for grey images, uchar for segmented images
pixelEndian	Bytes order	
dimX	Image dimension in x [pixel]	X is horizontal in the tomograph
dimY	Image dimension in y [pixel]	Y is horizontal in the tomograph
dimZ	Image dimension in z [pixel]	Z is vertical in the tomograph
resoX	Voxel size in x [microns]	X is horizontal in the tomograph
resoY	Voxel size in y [microns]	Y is horizontal in the tomograph
resoZ	Voxel size in z [microns]	Z is vertical in the tomograph
originX	Physical position of voxel (0,0,0) in absolute coordinate system in x [microns]	Used to register series or to crop sub volumes
originY	Physical position of voxel (0,0,0) in absolute coordinate system in y [microns]	Used to register series or to crop sub volumes
originZ	Physical position of voxel (0,0,0) in absolute coordinate system in z [microns]	Used to register series or to crop sub volumes
motherImage	Name of the image used to create this one	For instance XXX_seg generally inherits from XXX_grey
snowTypePrimary	Snow type	if snow: choose the primary snow type (valid entries are the abbreviations of the main seasonal snow types classification)
snowTypeSecondary	Snow type	if snow: choose the main snow type (valid entries are the abbreviations of the main seasonal snow types classification)
sampleType	Sample description	If pure homogeneous snow indicate « snow », otherwise free text
impregnation	Has the sample been impregnated?	If yes, indicate field impregnationInfo
impregnationInfo	Description of impregnation (if yes)	Free text
field	Has the sample been collected in the field and has not been modified since (e.g. sieving, very long rest time)?	If yes, indicate field fieldInfo
fieldInfo	Description of the field sampling (if yes)	Free text
timeSeries	Is the sample part of a time series?	Same snow block
inVivoSeries	Is the sample part of a in vivo time series?	Note that a in vivo series is also always a time series
sampleDate	Date and time at which the sample was scanned or impregnated. If non impregnated, corresponds to time of first projection	To access the sample age in the time series) format: YYYY-MM-DDThh:mm:ss
experiment	General description of the experiment / work	Free text
tomograph	Name of the tomograph used	
voltage	Voltage [kV]	
current	Current [microA]	
focalMode	Type of focus used	
frameRate	Frame rate (number of image per second)	
avrFrame	Number of image for averaging	
imagerMode	Mode of imager (e.g. binning / sensitivity)	For DeskTom13, 0 means full high sensitivity, 1 means 2x2 binning.
nbProjection	Number of projections	
nbTurns	Number of turns for stack scans	Only used for stacked scans. 1 otherwise
scanDuration	Duration of the projections acquisition in minutes (warm-up and reference projections not accounted for)	
reconstructed	Whether the projections where reconstructed (almost always True)	
imageProcessing	Description of the different image processing steps between the original image (or the tomograph output) and the considered image	Free text e.g. : - person who did the segmentation - reference paper (if applicable) - details
material	Association between segmented image value and material	Represented as a list of string L with L[i] the material name associated to value i [air, ice, sand] means voxels of value 0 are air, voxels of value 1 are ice, and voxels of value 2 are sand.
imageQuality	Overall quality (confidence) of the image	
density	Density computed from image [kg/m3]	Density of ice is chosen as 917 kg/m³ when snow sample
ssa	Specific surface area from image [m2/kg]	
ssaMethod	Method used to compute SSA	
reference	Reference papers: - on image acquisition, sample preparation, data computed from image etc	
doi	doi of the data (optional)	
access	Is the image private or public?	
auxiliaryData	If any, description of the auxiliary data associated to the tomo data (measurements, logbook, etc).	
comments	Any other comment	

Figure 2.3: Chosen meta-data format of 3D tomographic images. The associated information is saved in a meta-header format (.mhd) separated from the binary data according to https://itk.org/Wiki/ITK/MetaIO/Documentation.

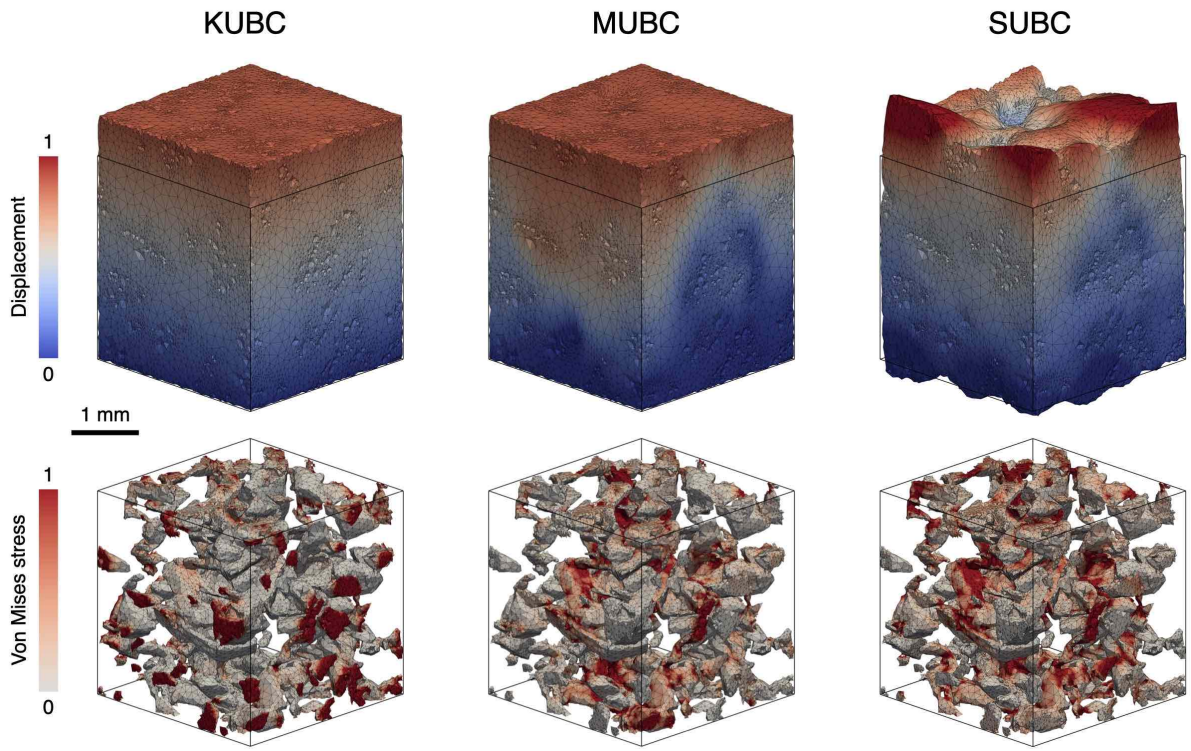

Figure 2.4: Impact of boundary conditions on the homogenization of the elastic properties of snow. A sample composed of faceted crystals is deformed along the vertical axis according to three different boundary conditions: Kinetic Uniform Boundary Conditions (KUBC), Mixed Uniform Boundary Conditions (MUBC), and Stress Uniform Boundary Conditions (SUBC). The resulting stresses and displacements were scaled to the same average value. The air was supposed to be elastic with a very small elastic modulus. Unpublished.

by size effects or boundary conditions. Homogenization using the volume-averaging method relies on Hill's lemma [Hill, 1963]. The lemma ensures that the mechanical work density (or energy) at the microscale is preserved while scaling up to the macroscopic level:

$$< \boldsymbol{\sigma} >:< \boldsymbol{\varepsilon} >=< \boldsymbol{\sigma} : \boldsymbol{\varepsilon} > \tag{2.4}$$

where $\boldsymbol{\sigma}$, $\boldsymbol{\varepsilon}$, and $< \cdot >$ are the local stress and strain tensors, and the average operator on the material volume, respectively. Hazanov [1999] showed that this condition can be generalized to heterogeneous materials as conditions on the sample boundary Γ:

$$\int_\Gamma (\boldsymbol{t}(\boldsymbol{x}) - < \boldsymbol{\sigma} > \boldsymbol{n}) \cdot (\boldsymbol{u}(\boldsymbol{x}) - < \boldsymbol{\varepsilon} > \boldsymbol{x})\, d\Gamma = 0 \tag{2.5}$$

where $\boldsymbol{t}, \boldsymbol{u}, \boldsymbol{n}, \boldsymbol{x}$ are traction, displacement, normal vector, and position, respectively. Volume-averaging homogenization on a heterogeneous body makes sense only if the loading conditions satisfy this equation [Pahr and Zysset, 2008]. Three main types of boundary conditions that satisfy this criterion are considered. They are defined as follows with σ_0 and ε_0 two constant tensors and for all $\boldsymbol{x}$ on Γ [Pahr and Zysset, 2008]:

- uniform displacement (KUBC): $\boldsymbol{u}(\boldsymbol{x}) = \boldsymbol{\varepsilon}_0 \boldsymbol{x}$
- uniform traction (SUBC): $\boldsymbol{t}(\boldsymbol{x}) = \boldsymbol{\sigma}_0 \boldsymbol{n}$
- uniform displacement-traction (MUBC): $(\boldsymbol{t}(\boldsymbol{x}) - \boldsymbol{\sigma}_0 \boldsymbol{n}) \cdot (\boldsymbol{u}(\boldsymbol{x}) - \boldsymbol{\varepsilon}_0 \boldsymbol{x}) = 0$

Periodic uniform boundary conditions may also be considered on periodic microstructures. For infinitely large volumes, all these boundary conditions will yield the same apparent elastic tensor $\boldsymbol{E}$ defined as $< \boldsymbol{\sigma} >= \boldsymbol{E} < \boldsymbol{\varepsilon} >$, which can thus be considered effective. In practice, homogenization is applied to finite volumes. Hazanov and Huet [1994] showed that the effective stiffness tensor E is bounded (matrix bounds) by those calculated with KUBC (upper bound) and SUBC (lower bound). With a well-chosen displacement-traction mixture, the value in MUBC converges the most quickly with volume to the effective value [Pahr and Zysset, 2008].

On small snow samples loaded in the vertical direction, these different boundary conditions yield very different stress and strain patterns close to the sample boundary (Fig. 2.4). These localized stress or strain patterns would not affect the volume-average values for large volumes. For relatively small volumes considered in the literature, they can affect the computed apparent properties [Köchle and Schneebeli, 2014; Wautier et al., 2015; Srivastava et al., 2016]. More quantitatively, different boundary conditions and snow samples were tested (not shown, unpublished). For low-density snow and relatively large volume for snow tomography ($10 \times 10 \times 10$ mm^3), the apparent properties with KUBC and SUBC do not yet converge. For example, on a sample composed of precipitation particles (PP) with a low density of about 100 kg m^{-3}, the equivalent isotropic Young's modulus depends on the boundary conditions: $\boldsymbol{E}_{KUBC} = 22.3$ MPa, $\boldsymbol{E}_{MUBC} = 3.1$ MPa and $\boldsymbol{E}_{SUBC} = 1.7$ MPa. For very dense snow, the discrepancy between KUBC and MUBC is smaller. Overall, the speed of convergence with volume depends not only on density but also on snow microstructure. For example, it is faster for small rounded grains than for large depth hoar for a given density.

Previous studies reporting elastic properties derived from 3D micromechanical simulations used various boundary conditions such as uniform displacement, periodic boundary conditions, and non-uniform conditions. Therefore, it is very likely that the reported values are affected by the boundary conditions chosen (Fig. 1.3). Homogenization is a powerful tool, but apparent properties are not necessarily effective.

2.2.2 Finite element modeling of brittle properties

Above a certain load or deformation, the snow behavior is no longer elastic, and damage progressively occurs in the ice matrix. The stresses in the bonds exceed the strength of the ice, and the bonds fail one after the other. The broken bonds form a failure surface that propagates into the complete sample fracture. The maximum stress supported by the sample corresponds to its strength. A way to reproduce this elastic brittle deformation regime is to mesh the ice matrix with finite elements and to set the local material law as elastic with a maximum stress criterion in each bond [Hagenmuller et al., 2014c]. I started this project during my Master's internship at the WSL-SLF in 2011, where I developed and evaluated the methodology on tensile experiments. Since then, we have also applied the model to reproduce the snow failure envelope.

Snowpack layers lying on a slope are subjected to simultaneous compressive and shear stresses due to their weight and additional loads related, for instance, to the presence of a skier. These loading conditions are often called mixed-mode loading and are essential to understanding failure initiation in avalanche release. The proportion of shear and compression, related to slope angle, affects the maximum stress the sample can support before failure. The failure envelope is the ensemble of failure points in the (shear, compression) stress space. Perla and Beck [1983]; Zeidler and Jamieson [2006] measured the effect of normal load on shear strength with shear frame tests. They observed an increase (almost linear) of shear strength with normal loading, which a Mohr-Coulomb model can reproduce. Reiweger and Schweizer [2013] measured the failure of weak layers for different angles and also observed failure for pure compression. Reiweger et al. [2015] further analyzed the loading experiments and described the failure behavior with a modified Mohr-Coulomb with Cap model that accounts for the possible compressive failure of snow. Chandel et al. [2015] determined the failure envelope of two samples of faceted snow (FC) using a micromechanical approach. They did not observe a significant increase in shear strength with normal loading. The failure envelope resembled a Mohr-Coulomb with a Cap but without Mohr-Coulomb.

We conducted numerical experiments similar to Chandel et al. [2015] with a slightly different strategy. We both used finite element meshes of the 3D microstructure. Chandel et al. [2015] described the ice matrix with an elastoplastic constitutive law with damage. We described snow with an elastic constitutive law where the bonds can fail in a brittle manner according to a maximum stress criterion. The first constitutive law is richer but requires an explicit solver whose enormous computing expense limits the simulation to small samples or rough meshes. In our case, the whole simulation consists of a sequence of elastic simulations. Figure 2.5 shows the failure envelope simulated for three different samples. The samples were composed of precipitation particles (PP), rounded grains (RG), and faceted crystals (FC). The amplitude of the failure envelope increased with snow density. The shape of the failure envelope also depends on the snow microstructure. Shear strength ($\tau_c = (0.12, 12, 20)$ kPa for samples PP, RG and FC, respectively) is about two to four times lower than compressive strength ($\sigma_c = (0.24, 36, 82)$ kPa for samples PP, RG and FC, respectively) and about two times lower than the tensile strength ($\sigma_t = (0.24, 18, 24)$ kPa for samples PP, RG and FC, respectively). We did not observe an increase in shear strength with normal load for sample PP, but we observed it for RG and FC samples. Notably, the anisotropy of the failure envelope correlates with the anisotropy of the elastic tensor [Hagenmuller, 2017]. Complementary simulations would be required to develop a mixed-mode shear-compression failure criterion that can be used in avalanche release models.

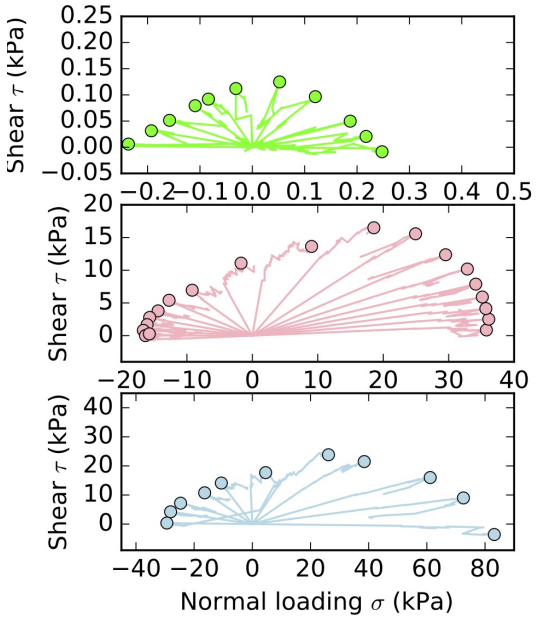

Figure 2.5: Failure envelopes of different snow samples: a) precipitation particles (PP) with a density of 120 kg m^{-3}, b) rounded grains (RG) with a density of 240 kg m^{-3} and c) faceted crystals (FC) with a density of 311 kg m^{-3}. The line represents the loading path (strain-controlled) in the stress space and the dot indicates the point of failure. Taken from [Hagenmuller, 2017].

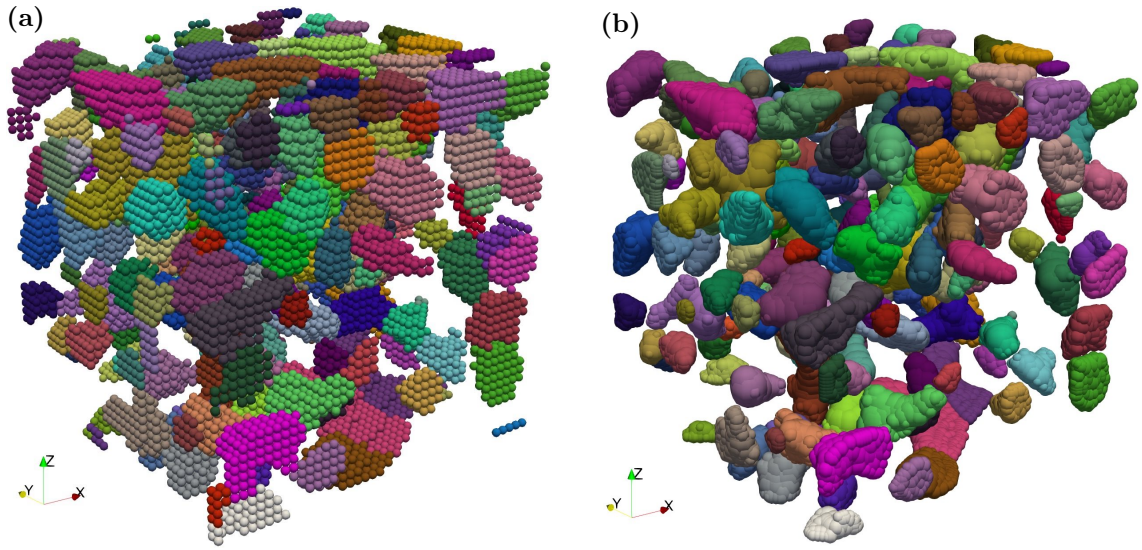

Figure 2.6: Two different strategies to describe the granular microstructure of snow with a set of spheres are used: a) identical spheres distributed on a regular grid and b) interpenetrating spheres of different sizes and located on the structure medial axis. Sample side length is 3 mm.

2.2.3 Modelling snow as a granular material

When snow fails under mixed-mode loading (with a positive compression component), the microstructure experiences large strains and the creation of new contacts. These changes generally appear once the maximum stress value has been reached. Post-peak softening affects the way cracks propagate in snow [Gaume, 2013] and is therefore crucial. Finite elements are no longer appropriate to model this deformation regime. Indeed, granular rearrangements and contacts between rigid snow grains mainly control this regime. The discrete element method is best suited to model granular material [Cundall and Strack, 1979].

The ice matrix is a continuously connected volume of ice. The 3D microstructure of snow (e.g., Fig. 1.2) captured by tomography does not explicitly contain individual grains. To describe snow as a granular material, we need to describe the snow microstructure using a set of rigid elements that interact through localized contacts. We also need to describe each grain with elements that the discrete element framework can handle. During my Ph.D., I developed a grain segmentation algorithm to identify individual snow grains defined as zones separated by regions of potential mechanical weakness [Hagenmuller et al., 2014b] and used it to perform discrete element simulations [Hagenmuller et al., 2015]. However, the simulations were numerically costly and needed to be improved. We worked on this aspect during the Ph.D. of T. Mede, which I present below.

In the discrete element method, granular materials are generally modeled as a set of spherical elements [Radjai and Dubois, 2011]. Adjusted contact law parameters, such as rolling friction, can indirectly account for irregular grain shapes [Ai et al., 2011]. However, this approach is limited when the grain shape deviates significantly from a sphere. The exact grain shape can also be modeled with polyhedrons [e.g., Hogue, 1998] but at the cost of numerically-expensive contact detection and contact force calculation. Clumping together different spheres, whose contact detection is simple, appears to be more efficient in capturing the grain geometry [Kruggel-Emden et al., 2008]. Hagenmuller et al. [2015] adopted a straightforward approach by placing small spheres instead of voxels along the grain boundary (Fig. 2.6a). This approach faithfully reproduces the grain shape but requires many spheres.

We developed an alternative approach based on interpenetrating spheres [Mede et al., 2018a] (Fig. 2.6b). The approach is mainly based on the medial axis transformation, which defines the spheres needed for exact grain reconstruction [Coeurjolly and Montanvert, 2007]. The number of spheres is then further diminished by approximating the grain shape. This decimation step is controlled by the minimal sphere radius and a parameter defining how close two spheres can be. We showed that the mechanical behavior of a snow sample could be well reproduced even with a relatively small number of spheres. This efficient procedure was later improved by sphere decimation based on the Laguerre diagram [Coeurjolly and Montanvert, 2007]. It enabled us to simulate the granular behavior on larger samples than ever before (see Sect. 2.2.4 and 3.1.2).

2.2.4 Weak layer collapse under mixed-mode loading

The discrete element model was used to explore the failure of snow under mixed-mode loading [Mede et al., 2018b] and to understand the micromechanism at the origin of normal collapse [Mede et al., 2020]. In particular, during the Ph.D. of T. Mede, we investigated the origin of the initial failure in avalanche release, whether it is in shear, as assumed for years, or compression, which is still a matter of debate [Reiweger et al., 2015].

The model takes 3D images of snow as input, and the shape of every grain is modeled by packing its volume with a set of overlapping spheres. The initial contacts are then modeled as

elastic, brittle, and frictional (cohesion of 1 MPa, Young's modulus of 100 MPa, friction coefficient of 0.2). The contacts created by grain rearrangement are described by the same contact law but with a cohesion set to zero. A global damping coefficient of 0.02 is used to dissipate energy and stabilize the system. Rigid boundary conditions are applied to the top and bottom faces of the cubic samples. Periodic boundary conditions are applied to all four lateral faces. The samples are loaded by applying a constant shearing velocity of 1 cm s^{-1} and a normal stress p to the top surface while keeping the bottom surface fixed. The normal stress p is varied between experiments to change the angle of mixed-mode loading. Three different samples were used, covering different densities and snow types.

Figure 2.7 shows the evolution of the microstructure of one sample under varying normal stresses. Three qualitative failure modes were observed in all snow samples tested, depending on the normal stress applied. However, the magnitude of stress that leads to failure is different between samples. The lowest density sample fails at the lowest load, and the faceted crystals fail at a stress lower than that of rounded grains with the same density. At low normal stresses (mode A, Fig. 2.7), the sample fails on a narrow horizontal band which concentrates all the damage. The sample can still support the normal load and does not collapse vertically. At moderate normal stresses (mode B, Fig. 2.7), shear failure also localizes at the bottom of the sample, but the post-peak softening in shear is abrupt. Here, shear failure weakens the sample in the normal direction. The sample can no longer support the normal load and collapses. If shearing is stopped at shear failure, the sample collapses anyway. At high normal stresses (mode B, Fig. 2.7), the sample directly fails in compression and collapses vertically.

The internal mechanisms that lead to volumetric collapse are further examined on the microscale. Normal shear-induced collapse occurs when the applied normal stress exceeds a critical value. Interestingly, this value coincides with the point on the failure envelope with the highest shear strength (i.e., the top point of the failure envelope). Just before sample collapse, the force chains that support the normal load are no longer stabilized laterally by the cohesive contacts that just failed. They start to buckle, which leads to the sample collapse.

The discrete element model offers insights into the failure of snow under mixed-mode loading. In particular, we unveil the interplay between shear failure and normal collapse. Depending on the slope angle, a weak layer may simply fail in compression or shear, which induces a visible normal collapse. However, the substantial collapse observed indifferently on all snow types and leading to density up to 600 kg m^{-3} appears overestimated and should be considered with care. The model does not include any physical dissipation processes and may simulate too "nervous" systems.

2.3 Snow microstructure evolution

In the previous Section 2.2, we wanted to relate a given microstructure to its mechanical properties. In practice, this microstructure is associated with a particular history of temperature and stress conditions, which shapes the ice matrix and subsequent snow properties. In particular, metamorphism and ice creep are two natural mechanisms driving the evolution of dry snow. In this section, I describe my contribution to this research field, mainly conducted during the Ph.D. of A. Bernard, the postdoc of K. Fourteau, and the ANR project EBONI.

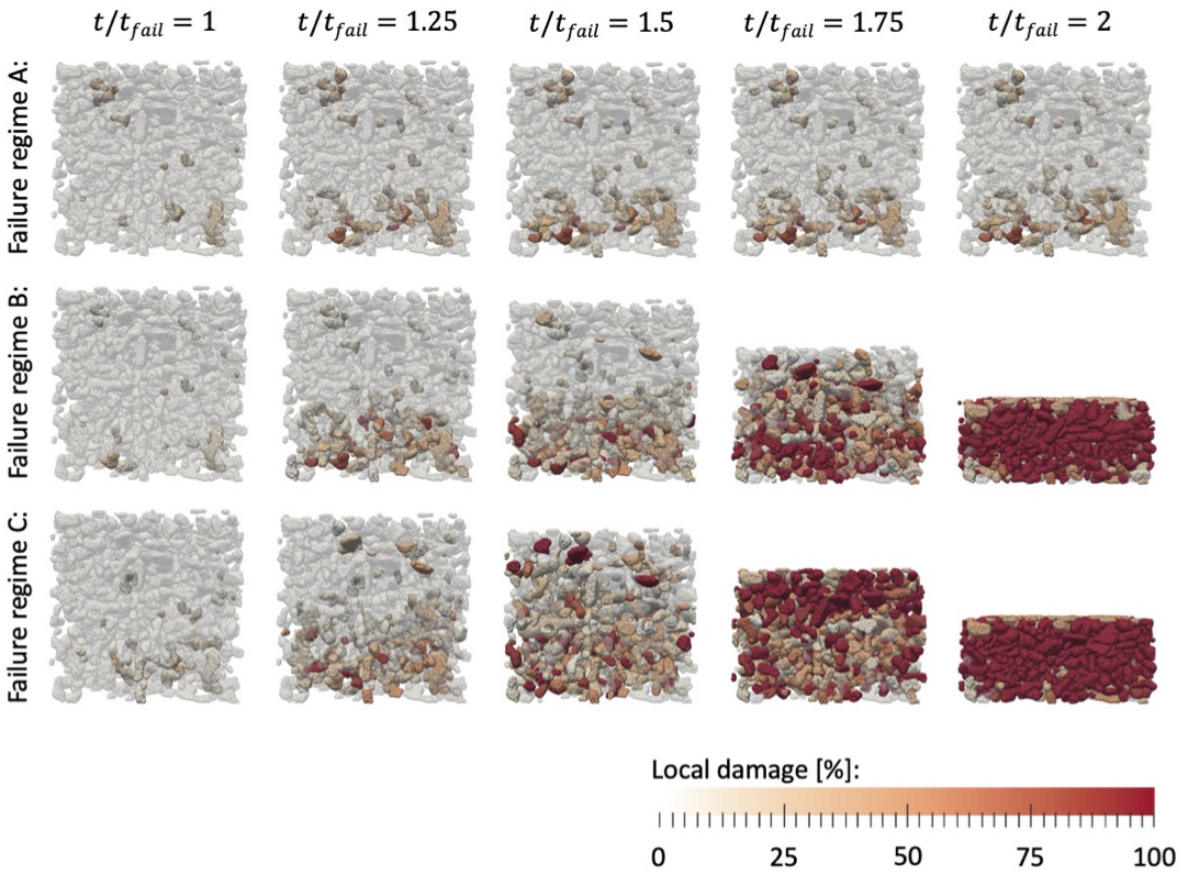

Figure 2.7: Damage state of a sample of rounded grains (5 mm side length) under mixed-mode loading at different loading stages and for different normal pressures (1, 2 and 9.5 kPa from top to bottom raw). The sample is composed of rounded grains (RG) with an initial density of 250 kg m^{-3}. Local damage is defined for each grain as the ratio of broken cohesive bonds with neighboring grains. Taken from [Mede et al., 2020].

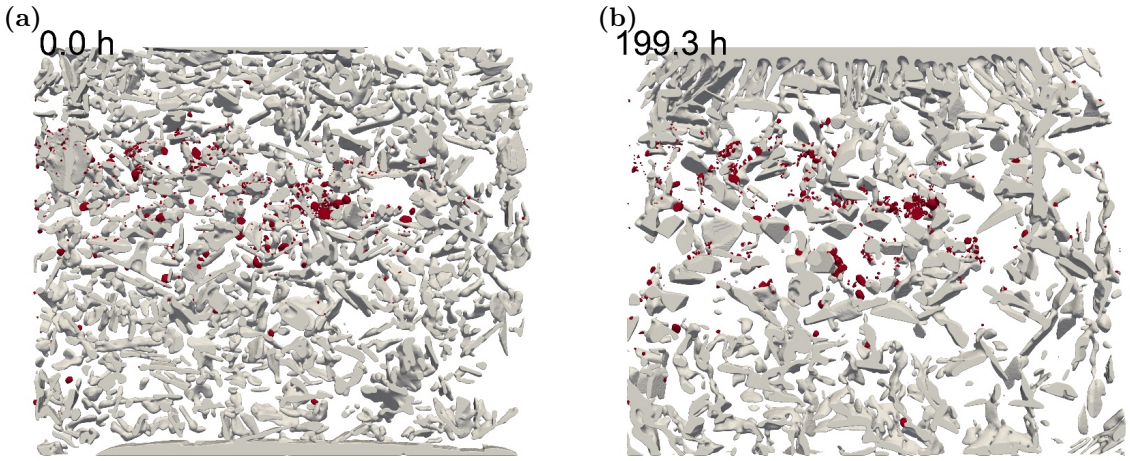

Figure 2.8: Evolution of a snow sample contaminated with mineral dust, evolving from a) decomposed and fragmented snow to b) faceted crystals under a temperature gradient of 20 K m^{-1} during about one week. A vertical slice of 8 mm in side length is shown. Ice is represented in gray, and dust is in red. See also `https://youtu.be/R1bo_m0LE40`. Adapted from [Hagenmuller et al., 2019].

2.3.1 Heat and vapor transport in snow

The snowpack is generally subject to a temperature gradient: close to the melting temperature on the ground and very cold on the top open surface. This gradient yields coupled heat and water vapor transport in the snowpack. At the microscale, snow grains typically grow on the colder side and sublimate on the warmer side [Colbeck, 1982]. This process, known as kinetic or temperature-gradient metamorphism, causes drastic changes in the snow morphology, thereby influencing its macroscopic physical properties [e.g., Schneebeli and Sokratov, 2004; Calonne et al., 2014a]. Understanding the driving mechanisms at the microstructural scale is of primary importance to model these morphological changes but also the mass and heat transport at the macroscopic scale [Calonne et al., 2014b; Hansen and Foslien, 2015]. The driving mechanisms of crystal growth during kinetic metamorphism are still under debate [Krol, 2017]. Studies considered that crystal growth is diffusion-limited or reaction-limited (i.e., limited by surface kinetics) [e.g., Libbrecht, 2005; Flin and Brzoska, 2008; Calonne et al., 2014b]. The prevalence of one or the other process is related to the condensation coefficient α, which describes the likelihood of water molecules being incorporated into the nearby ice lattice. Understanding the driving mechanisms of metamorphism requires 4D time-lapse data of snow microstructure evolution and associated modeling at the microstructure scale [Krol and Löwe, 2016]. However, existing 4D data suffer from a low signal-to-noise ratio, which limits any subsequent analysis [Krol, 2017].

With cryogenic cells, we measured one of the most resolved time series of snow evolution: 7.5 µm spatial resolution and 3 h average temporal resolution [Hagenmuller et al., 2019]. The evolution of snow composed of decomposing and fragmented particles (DF) with an initial density of about 220 kg m^{-3} was captured under isothermal metamorphism for 100 h and temperature-gradient metamorphism ($\nabla T = 20$ K m^{-1}) for 200 h. With the image processing tools described in Section 2.1.2, this considerable amount of data could be efficiently analyzed. Figure 2.8 or this movie `https://youtu.be/R1bo_m0LE40` show the evolution with temperature gradient. The

movie of isothermal metamorphism is here: https://youtu.be/Bm_8JTJhsuU. These data enabled us to quantify the local growth of ice crystals. Interpretation in terms of driving mechanisms is ongoing. Note that we contaminated the snow samples with dust particles because our initial goal was to investigate the motion of dust particles under temperature-gradient metamorphism. Indeed, we provided the first observational evidence that the temperature-gradient metamorphism induces the motion of dust particles in the snow while isothermal metamorphism does not yield any dust movement. The resulting self-cleaning effect of the snow surface might reduce the radiative impact of dust in snow, particularly in arctic regions where temperature-gradient metamorphism prevails and precipitations are scarce [Hagenmuller et al., 2019].

In addition, with the same homogenization procedure used for snow mechanics, we investigated how the coupling between phase change and water vapor-heat diffusion upscales to the macroscopic level [Fourteau et al., 2021b,a]. The temperature gradient in the snowpack causes water vapor fluxes. These macroscopic vapor fluxes result from vapor diffusion in pores, which is affected by phase changes (sublimation, condensation) on the ice surface acting as sources and sinks of vapor [Yosida, 1955; Colbeck, 1982]. Whether local phase changes enhance vapor diffusion in the snow was still debated. Indeed, Yosida [1955] introduced the "hand-to-hand" mechanism, which states that a water molecule deposing on one side of an ice grain and another molecule sublimating on the other side is equivalent to the same molecule instantaneously crossing the ice grain. With that idea in mind, the vapor fluxes in snow could be larger than in "free" air because the presence of the ice matrix shortens the diffusion paths. Since then, no clear consensus has emerged [e.g., Hansen, 2019]. We proved this idea is wrong: a mass flux is always associated with individual molecules explicitly crossing a fixed surface, which is not the case in the previous example. Moreover, we evaluated the effective diffusion coefficient in the snow with numerical homogenization experiments. Diffusion in the snow is enhanced by phase changes but remains smaller than in free air (Fig. 2.9) [Fourteau et al., 2021b]. We also showed that vapor fluxes are not neutral in heat conduction in snow. In particular, the effective thermal conductivity of snow can be underestimated by up to 30% if the transport of vapor is neglected [Fourteau et al., 2021a].

2.3.2 Snow settlement

In Section 2.2, we focused on how snow microstructure affects its mechanical properties. Here, the question is the other way round: how does the mechanical deformation of snow affect its microstructural evolution? The snow on the ground settles naturally under gravity. Obviously, its density increases, but other subtle microstructural changes may also occur. Dry seasonal snow settles under two main mechanisms. Isothermal metamorphism rounds the "elongated" snow grains into more compact shapes [Schleef and Löwe, 2013] and makes some bonds disappear [Flin, 2004]. The visco-plastic creep of ice induces the deformation of the ice matrix [Wautier et al., 2017]. During the Ph.D. of A. Bernard, we investigated the interactions between these two mechanisms and their signatures on snow microstructure evolution.

We monitored oedometric compression tests of different snow samples at a temperature of -8°C. The microstructure evolution was continuously captured by tomography at a resolution of 8.5 μm for about a week for each sample. The evolution of one sample is shown here: https://youtube.com/shorts/KMROXsUFxqI. We compared the microstructural evolution without load and loads between 2.1 kPa and 4.7 kPa. We characterized the microstructure by density and specific surface area and also proxies of the bond network. In particular, we used the min-cut surface [Hagenmuller et al., 2014a] to quantify the number and size of bonds (Fig. 2.10a). The creep of the ice matrix induced a significant increase in the number of bonds but, surprisingly,

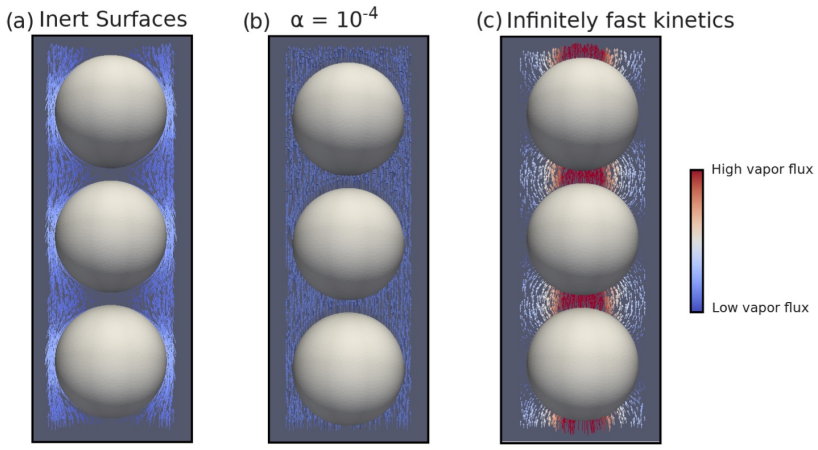

Figure 2.9: Vapor flux around a very simple ice microstructure (sphere diameter is 3 mm) under a temperature gradient of 50 K m^{-1} simulated with different assumptions on the ice surface kinetics. The heat fluxes are enhanced by active surface kinetics (sublimation-condensation) (c) compared to the case where the ice is considered as an inert material (a). Taken from [Fourteau et al., 2021b].

was not associated with an increase in bond size, even in the loading direction (Fig. 2.10b). The evolution of bond size and grain size, related to the specific surface area, was mainly driven by isothermal metamorphism. However, these results need to be extended to a wider variety of snow samples and loads to draw general conclusions.

2.4 Ongoing and future work

2.4.1 In-situ tomography

Tomography has become a standard technique to measure the snow microstructure in laboratory conditions [e.g., Hagenmuller et al., 2016]. Time-series of snow evolution under controlled conditions notably gives new insights into microscale mechanisms and their impact on the microstructure morphology [e.g., Hagenmuller et al., 2019]. Moreover, homogenization methods can now provide estimates of several essential but difficult-to-measure snow properties related to thermal conduction [Calonne et al., 2011], vapor diffusion [Fourteau et al., 2021b], elasticity [Schneebeli, 2004], brittle failure [Hagenmuller et al., 2014c], viscosity [Wautier et al., 2017], interaction with electromagnetic waves [Kaempfer et al., 2007]. A new generation of snow models with an explicit representation of the snow microstructure is currently being developed to benefit from this wealth of data [e.g., Löwe et al., 2016] (project ERC IVORI, where I am in charge of the tomography and microstructure package). Characterizing the evolution of the snow microstructure in the field is required to develop and evaluate these new models. I brought tomography to my lab cold-room. Now the goal is to *bring tomography to the field* as an almost routine measurement technique. This ongoing work can be decomposed into three main parts:

- One goal of the CEN is to build a snow model as universal as possible. Especially, we would like a model that correctly reproduces the snowpack in Arctic regions, which is essential to understanding the Earth's climatic system. The model Crocus typically fails to reproduce the snow conditions in these regions. The Arctic snowpack appears very different from the

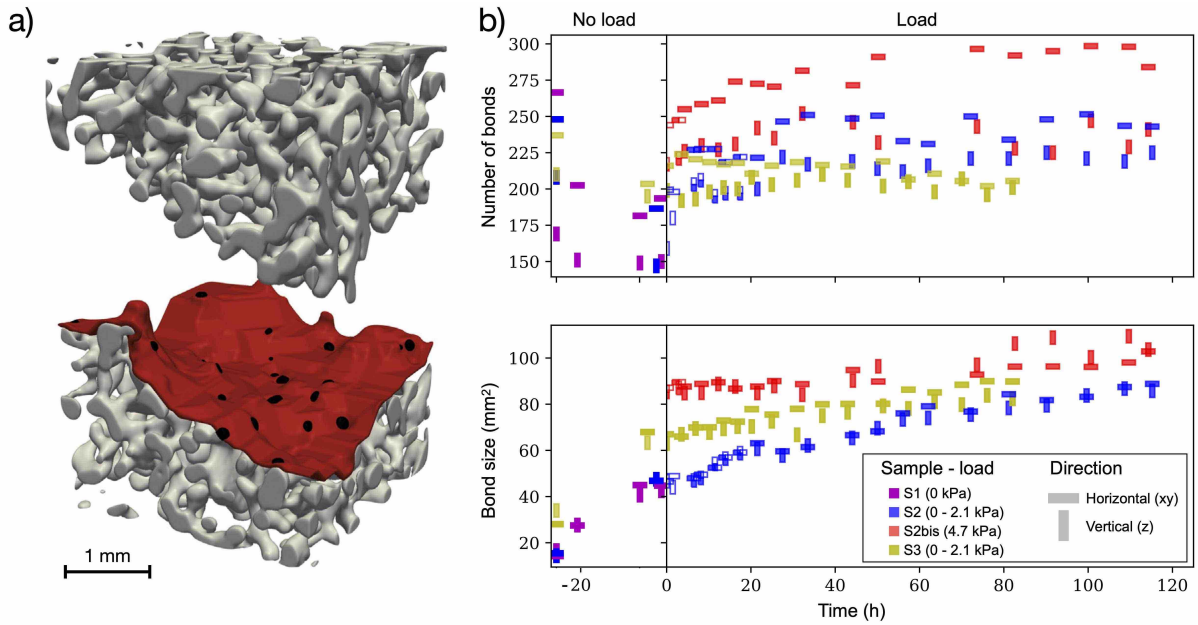

Figure 2.10: Evolution of the bond network with creep and isothermal metamorphism. a) Characterization of the bond system with the min-cut surface. This surface (red surface) separates the two faces of the sample with a minimal broken ice surface area (black surfaces). It is characterized by a number of bonds with a certain area. Adapted from [Hagenmuller et al., 2014a]. b) Evolution of the number of bonds and their size for different samples and loads. Unpublished.

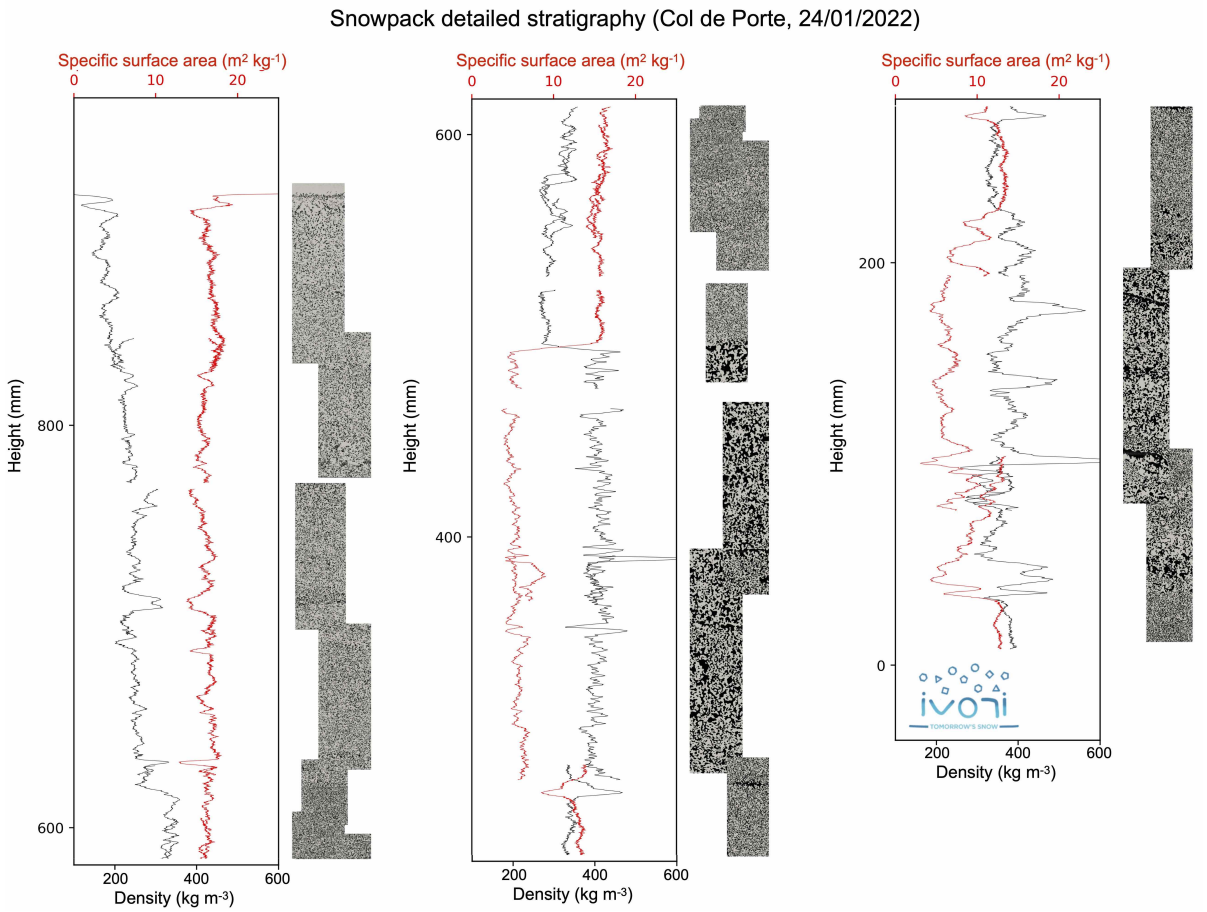

Figure 2.11: A very detailed snow profile. Full snowpack captured by X-ray tomography and associated profiles of density and specific surface area. Collected at Col de Porte on 24/01/2022. Under development. Unpublished.

alpine snowpack (rather shallow with a wind-packed slab on the top and depth hoar close to the ground). We plan to buy a new tomograph and conduct a field campaign directly in the region to capture this particular snow structure. We will visit the Canadian High Arctic Research Station in the winter 2023-2024 with a new tomograph. I led the design of new tomograph specifications and active discussions with different companies on the market. In particular, we paid attention to ease of transport (transport cabin incorporated in the instrument, fragile pieces easy to dismantle, cabin as light as possible, etc.), maintenance that we could perform on our own at sites that are difficult to access (robust equipment, easy installation, availability of competent engineers for remote conference, spare components) and high tomographic performances (large samples up to 25 cm height and high resolution up to 2 μm). We ordered the instrument in the summer of 2021. Covid delayed the delivery, which is now planned for mid-2022.

- Before going to the Arctic, we focused on the microstructure of alpine snow and developed a dedicated protocol. Using tomography to capture the seasonal evolution of the snowpack is a great challenge. To date, tomography has been mainly limited to small volumes of snow, mostly harvested under laboratory conditions. The goal is to design an experimental protocol to capture the entire snowpack microstructural stratigraphy in the field within one working day (Fig. 2.11). To do so, we developed a versatile sampling protocol. "Versatile" here means, for example: "how do I sample without damage the column composed of a crust lying on light, fresh snow with bits and pieces." To reduce the scanning time, we combined two types of tomographic scans. Each snow sample is entirely scanned at a resolution of 42 μm (2 min scanning time per centimeter height). Only a sub-volume of interest is scanned at a higher resolution of 10 μm (1 hour per centimeter height). The protocol was tested and improved during the winter season 2021-2022 at Col de Porte (France), and we succeeded in completing a complete tomographic snow profile. For us, it is a real game-changer. The Winter season 2022-2023 will be dedicated to adjustments and systematic measurements using this protocol.

- Last, faster scans or scans of large volumes of snow with standard tomographs means scanning at a resolution close to the size of the microstructural heterogeneity. The image quality is, therefore, far from ideal. We usually segment tomographic grayscale images into binary images that describe in a deterministic way the material to which the voxels belong (see Sect. 2.1.2). This procedure is suited for high-resolution scans. It is no longer adapted to low-resolution scans, mainly composed of mixed voxels, i.e., voxels affected by blur or partial volume effects. Indeed, we lose essential information during binary segmentation. For example, a mixed voxel composed of 45% ice and 55% air will be segmented as air, regardless of whether it contains a significant portion of ice. We thus need a paradigm change in image processing. We are currently developing image processing techniques that allow quantifying high-order proxies of the snow microstructure (density, specific surface area, curvature, bond size, etc.) without ever segmenting the grayscale image [e.g., Bruns et al., 2017; Brenne et al., 2021]. In addition, we explore methods to incorporate mixed voxels into homogenization computational methods.

2.4.2 Brittle to ductile

As explained in the short introduction to snow mechanics (Sect. 1.2.4), snow exhibits a ductile to brittle behavior with increasing strain rate. We have focused mainly on the homogenization of

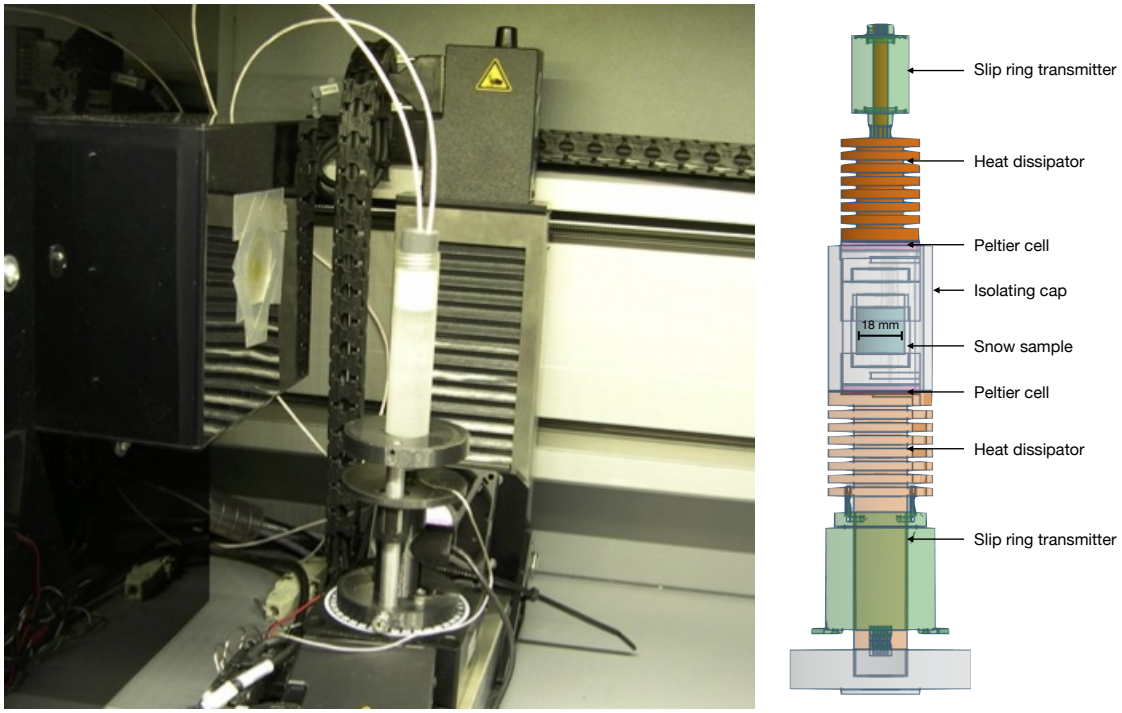

Figure 2.12: Different installations used to capture the evolution of the snow microstructure under different conditions. a) Compression device used to explore the different mechanical regimes of snow with strain-rate and installed in the tomograph. A piston moves up from the bottom of the sample at a controlled speed. Vertical force and displacement are recorded. The sample size is typically 16 mm in height and 14 mm in diameter. It can be continuously scanned up to a resolution of 7.5 μm. b) Blueprints of the temperature cell, CellCold. The boundary temperature of a snow sample is imposed with Peltier cells. The installation is compact enough to scan at a resolution up to 7.5 μm.

brittle properties so far (Sects. 2.2.2, 2.2.3) because these properties are essential for avalanche release and are "easier" to simulate. However, the low-strain rate behavior of snow is also critical for many applications, such as the simple but essential knowledge of snow evolution under gravity. Three main objectives will guide my future research:

- The methodology to reproduce brittle snow properties (Sect. 2.2.2) has not been applied to many snow data. This limited application is partly due to the high computing cost of these approaches and the absence of dedicated working time. One goal would be to systematically explore the existing database (including international partners) and apply the computational models developed. In particular, we may systematically compute mechanical properties such as the elastic modulus, the failure envelope, and the normal strain under a given compression and thermodynamical properties such as heat conductivity or vapor diffusion coefficient. With these data, models could be developed that relate snow microstructural proxies (not only density, as currently) and snow properties. Besides, if the computing efficiency is prohibitive, we may explore alternative numerical solvers that can efficiently benefit from the power of high-performance computing facilities (e.g., 21 petaflops at Météo-France).

- The dependence of the snow mechanical behavior on strain rate has long been known [e.g., Narita, 1984]. However, limited knowledge exists on how the snow microstructure evolves under different imposed strain rates. During the Ph.D. of A. Bernard, we developed a compression cell that enables one to vary the strain rate from 10^{-6} s^{-1} to 10^{-2} s^{-1} and to capture the evolving microstructure with tomography (Fig. 2.12a). The final goal is to quantitatively relate the observed microstructural mechanisms to the macroscopic stress-strain curves in the different brittle to ductile regimes.

- Two time-dependent micromechanisms can no longer be neglected at a low strain rate. First, sintering between snow grains is not considered in our discrete element models (Sect. 2.2.3): the contacts created during deformation are only elastic ("repulsive") and frictional. However, grains in contact can sinter very rapidly [e.g., Szabo and Schneebeli, 2007] which can affect the snow mechanical behavior even at relatively high strain-rates (e.g., around 10^{-3} s^{-1}) [Capelli et al., 2020]. The idea is to include sintering in the discrete element model to evaluate its role in snow mechanics (e.g., post-peak softening) and widen the range of validity of the model. This development can be inspired by active work in the domain of powder sintering for industrial purposes [e.g., Martin et al., 2006, 2016]. Second, the visco-plastic behavior of ice plays a dominant role at low strain rates ($<10^{-3}$ s^{-1}) [e.g., Wang and Baker, 2013; Burr et al., 2017]. To date, no micromechanical model can correctly reproduce this behavior, which is essential in the compaction of snow and firn. Existing models are either based on a too simplified representation of the snow microstructure [Theile et al., 2011] or ignore the highly anisotropic properties of individual crystals [Wautier et al., 2017], which cannot be simplified to homogeneous polycrystalline ice due to the presence of pores. We are currently working on a new approach based on the explicit representation of dislocation planes of the ice crystal [e.g., Lebensohn et al., 2009; Steinbach et al., 2016] in a fast-Fourier based numerical solver [Gélébart and Dérouillat, 2017]. The association of the experimental work (previous bullet point) and this micromechanical approach is of great interest in gaining knowledge on the visco-plastic behavior of snow. Moreover, the modeling approach is also of great interest for very slow firn compaction that is difficult to reproduce in controlled experiments [Burr et al., 2019].

2.4.3 Coupling between mechanics and thermodynamics

Parallel to snow micromechanical models, models describing the physics at the microscale (phase change and vapor and heat diffusion) can now mimic metamorphism on 3D images of snow [Flin et al., 2003; Kaempfer and Plapp, 2009]. The absence of mechanical deformation due to gravity has long been identified as the main bottleneck of these thermodynamical models [Flin et al., 2003; Vetter et al., 2010]. To date, no 3D model can efficiently and realistically couple these mechanisms. The creep of the ice matrix and the failure of bonds weakened by local sublimation are especially active during the short-term metamorphism of recent snow. In particular, the absence of mechanical processes in the metamorphism models hinders their detailed evaluation with tomographic data of controlled experiments where gravity can unfortunately not be set to zero. We will try to address the coupling of thermodynamics and mechanics.

- State-of-the-art metamorphism models [Flin et al., 2018], [Bretin et al., 2015] rely on phase-field reactive approaches. These approaches are based on discrete geometry: a microstructure seen as a collection of voxels on a regular grid [e.g., Flin et al., 2005]. In contrast, the discrete element approach is generally based on spherical elements, and the finite element approach is generally based on tetrahedrons. The meshing of the 3D microstructure is required to reduce the number of degrees of freedom of the simulated geometry. The direct coupling between two different representations of the snow microstructure remains possible, but the permanent "remeshing" step might be too expensive numerically or yield numerical instabilities. A common numerical structure would be of great interest to conduct these numerical experiments on snow evolution. We will explore using alternative and efficient voxel-based mechanics (Ph.D. project to be funded).

- To develop and evaluate these microscale (previous bullet point) or mesoscale models (new model by ERC IVORI, postdoc of J. Brondex), high-resolution tomographic time series of snow evolution under controlled temperature and stress conditions are required [e.g., Chen and Baker, 2010a]. This type of data already exists but lacks spatial/temporal resolution [e.g., Krol, 2017] or does not span very different conditions (e.g., CEN database). In CEN, this lack of diversity is partly because we relied on tomographs from other labs with higher user pressure. For instance, an experience at ESRF (European Synchrotron Research Facility) lasts a time slot, i.e., 24/24h during five days max., and that is all. With the new tomographs at CEN (TomoCold and the one to be received in mid-2022), we can now systematically explore snow evolution under different boundary conditions. However, the temperature in the tomograph cabin cannot be precisely controlled without dedicated devices. The existing cryogenic cells are not adapted to cold-room tomographs. Their isolation system is unnecessary and too bulky. We are developing a dedicated system (Fig. 2.12b). The 3D time series obtained with this device will then be used to infer closing relations of the time evolution of snow microstructural proxies. Indeed, relating microstructural proxies to macroscopic properties is not enough for a snowpack model. One must model how these proxies evolve with boundary conditions and macroscopic properties (postdoc J. Brondex).

Chapter 3

Snowpack stratigraphy

Preamble

The snowpack is built from distinct snow layers whose evolution is driven by boundary conditions such as precipitation, wind, temperature, and load. As stated in the international classification of seasonal snow on the ground, "each stratigraphic layer differs from the adjacent layers above and below by at least one of the following characteristics: microstructure or density" [Fierz et al., 2009] (Fig. 3.1). Microstructure with the thermal state and impurities content fully defines a snow layer. Tomography can capture the snow microstructure, but its application in operational observation networks is beyond reach. Nevertheless, the ability to efficiently capture proxies of snow microstructure layering and combine numerous snow profiles into relevant information remains essential. This chapter is dedicated to measurement techniques that can capture snowpack stratigraphy and methods for processing snow profiles. First, I present cone penetration testing in the snow. The force required to insert a cone into the snowpack has long been used as a proxy of snow mechanical properties. Using more sophisticated penetrometers now requires better knowledge and models of the snow-cone interaction. Second, I describe the characterization of the snowpack with the thermal conductivity measured by a heated needle probe. Thermal conductivity is related to the connections between grains. Then, I describe a matching algorithm of snow profiles that allows one to correct for stratigraphic mismatch due to variable layer thicknesses. I show how this algorithm can be used on measured and simulated profiles. Last, I draw some guidelines for future research.

Contents

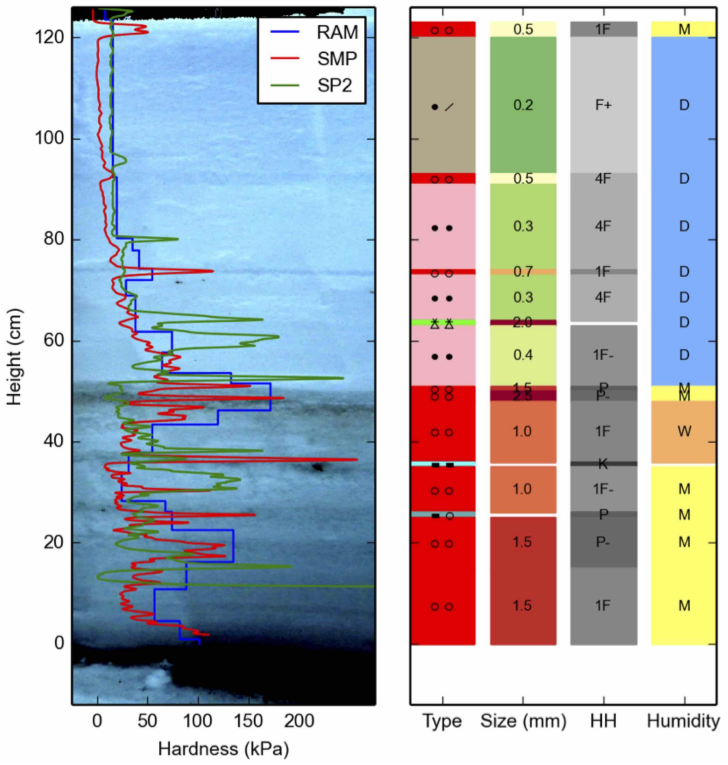

Figure 3.1: Example of snow stratigraphy: picture of the snowpit wall, hardness profiles measured with different penetrometers (ramsonde, Avatech Snow Probe 2 (SP2), and SMP), and manual profile with grain shape and size, hand hardness (HH, F: fist, 4F: four fingers, 1F: one finger, P: pen, K: knife) and humidity classes (D: dry, M: moist, W: wet, V: very wet, S: soaked). Measurement at Col de Porte, France, on 11/03/2016. The profiles measured with SP2 and SMP were smoothed with a 0.5 mm running mean. Adapted from [Hagenmuller et al., 2018].

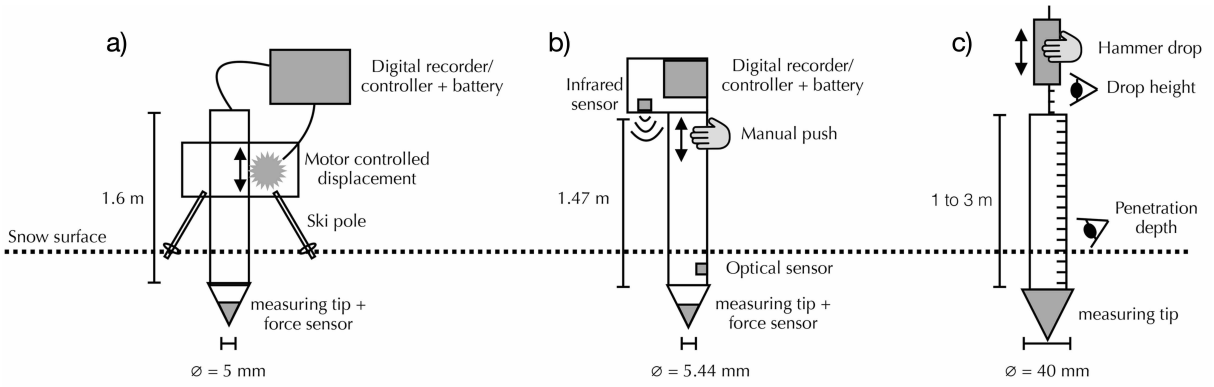

Figure 3.2: Main features of three different penetrometers commonly used in the snow and avalanche community: (a SMP, b) SP2, and c) Ramsonde. Adapated from [Hagenmuller and Pilloix, 2016].

3.1 Cone penetration test in snow

3.1.1 Ramsonde, Avatech Snow Probe 2, and Snow Micro-Penetrometer

Snow stratigraphy is generally estimated manually (Fig. 3.1). Even if they follow a strict procedure [Fierz et al., 2009], such manual measurements are partly subjective and observer-dependent. Hardness is defined as resistance to penetration of an object in snow and has long been considered a relevant stratigraphic indicator [Bader and Niggli, 1939]. It can be estimated manually (hand hardness is divided into five classes: fist, four fingers, one finger, pen, knife) or measured by a penetrometer as vertical profiles of penetration resistance (Figs. 3.1 and 3.2). Since the 1930s, avalanche warning services have measured hardness profiles with the ramsonde. The ramsonde is a simple and robust probe driven into the snow by mechanical hammer blows on its top (Fig. 3.2c). In the operational observation network of Météo-France and in support of avalanche forecasting, these stratigraphic measurements are performed about once a week at 100 sites in the French mountains during the winter season. We (internship of R. Granger) investigated the layer measurements reported in Météo-France from 1983 to 2014. It represents about 400 000 layers characterized by seven variables (ram hardness, density, hand hardness, grain size, liquid water content, humidity class, and temperature; see Figs. 3.1 and 3.3). Only two components of a principal components analysis explain 75% of the variance of this dataset. The first component is called "cohesion" and is mainly related to density, ram hardness, and hand hardness. The second component is called "thermal sate" and is mainly related to liquid water content, humidity class, and temperature (Fig. 3.3). This analysis confirms the importance of hardness measurement in the existing characterization of snowpack stratigraphy.

Ramsonde measures vertical profiles of penetration resistance, providing an overview of the snowpack structure. For example, it can help to roughly classify the snowpack structure as potentially stable or unstable [Schweizer and Wiesinger, 2001]. However, the vertical resolution and the hardness resolution of the profiles measured with ramsonde are too low to capture thin weak layers and small hardness variations in soft snow layers. Therefore, the ramsonde profile does not help capture stratigraphic features missed by manual observation or accurately assess the snowpack stability. The Snow Micro-Penetrometer (SMP), originally developed by Schneebeli and Johnson [1998] is a digital penetrometer with high vertical and force resolutions (Fig. 3.2a). The latest version can characterize snow layers at a millimeter-scale [e.g., Proksch et al., 2015]

and capture the overall mechanical stability of the snowpack [e.g., Reuter et al., 2015]. However, this research instrument is expensive, fragile, and heavy. Thus, it does not yet constitute an alternative to the ramsonde for operational snowpack monitoring.

A new digital hand-driven penetrometer, the Avatech Snow Probe 2 (SP2), was developed to provide highly-resolved penetration profiles without the disadvantages of the SMP. We precisely evaluated this instrument. Our goal was not only to provide a qualitative evaluation [Lutz and Marshall, 2014], [Pilloix and Hagenmuller, 2015] but to quantitatively compare the profile measured by the instrument with those measured by the SMP and the ramsonde. To this end, we (internship of T. Pilloix) measured different snowpack types with these penetrometers and compiled measurements for other research groups. In addition, we developed a matching algorithm, which allows us to decompose differences between profiles into differences in layer hardness and differences in layer depth [Hagenmuller and Pilloix, 2016]. We further developed this algorithm and used it in different applications (details in Sect. 3.3). Even if the SP2 can reproduce the general shape of the hardness profile measured by the SMP (Fig. 3.1), the SP2 measurements are not well repeatable with a profile variability higher than the spatial variability measured by the SMP [Hagenmuller et al., 2018]. The depths of the layer measured by the SP2 are shifted by -10 to 22 cm with a standard error of 7.4 cm. Hardness measured by the SP2 is in fair agreement with the hardness measured by the SMP with no significant bias but a standard difference of 34 kPa. The SP2 resolution, as the ramsonde resolution, is too low to detect a weak layer in new snow but high enough to qualitatively identify a weak layer in an old snow problem [Hagenmuller et al., 2018]. Overall, these results guided the absence of investment by Météo-France in this instrument.

3.1.2 Measurement of the 3D displacement around the cone

As explained above, the SMP measures the penetration resistance of snow at a high vertical resolution ($\sim$4 μm) and stress resolution ($\sim$50 Pa). This resolution yields "noisy" hardness profiles with high-frequency fluctuations around the global hardness trend due to the snowpack layering. These fluctuations are not white noise but are related to failure at the bond scale and thus contain information about snow microstructure [e.g., Johnson and Schneebeli, 1999]. Interpreting hardness fluctuations as microstructural proxies requires understanding interactions between the penetrometer and snow [Floyer and Jamieson, 2010; van Herwijnen, 2013; Lebaron et al., 2014].

During the Ph.D. of I. Peinke, we measured the three-dimensional displacement of snow grains induced by the cone penetration with X-ray tomography [Peinke et al., 2020]. We did not have a tomograph in a cold room at that time. However, with a careful manipulation of the snow samples and dedicated experimental protocol, we combined X-ray scanning in a cryogenic cell at Laboratoire Sols, Solides, Structures, Risques (3SR) lab and cone penetration testing in our cold lab on the same samples. We measured the displacement induced by the penetration of a conic tip with a radius of 2.5 mm in eight different snow samples at a temperature of -10°C. We calculated the three-dimensional displacement induced by the cone penetration from the tomographic images measured before and after the test. Standard image correlation techniques cannot recover these displacements. At the high strain rate induced by penetration (speed of 1 cm s^{-1}), snow deforms as a granular material [Narita, 1984]. Thus, we can use the idea that "no snow grains are alike" to associate each grain of the initial image to the same grain in the final image but at another position [Andò et al., 2012]. We combined this tracking algorithm with particle image correlation on the grayscale 3D images to improve the deduced displacement resolution. The developed algorithm captured most granular displacements and

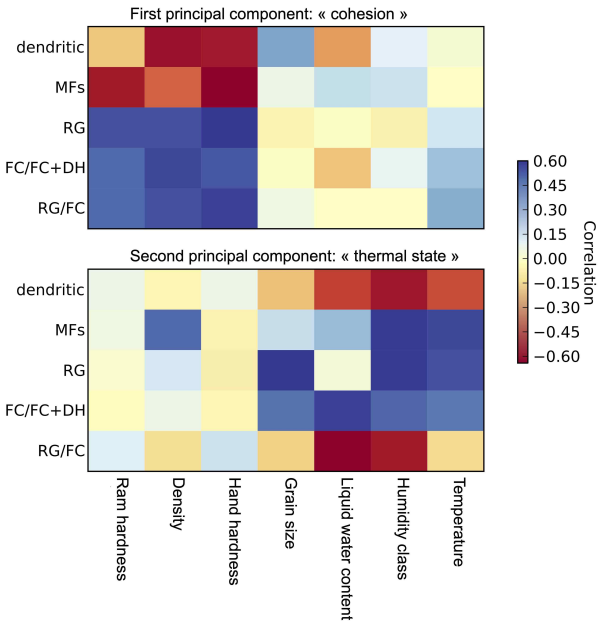

Figure 3.3: Principal component analysis on the characteristics of 400 000 snow layers measured in France from 1983 to 2014. The characteristics of each layer are measured according to the international classification [Fierz et al., 2009] (see Fig. 3.1). The principal component analysis is conducted separately on each class of grain shape (dendritic: precipitation particles (PP) and decomposed and fragmented snow (DF); MFs: melt forms, RG: rounded grains, FC + DH: faceted crystals and depth hoar; RG/FC mixture of rounded grains and faceted crystals). Unpublished.

accurately reproduced the volumetric strain, which is also directly measurable from local density changes. Figure 3.4 shows the displacement field and the corresponding density changes for two different snow samples (out of eight). The cone pushes snow grains away in both the vertical and horizontal directions. The movement is downward at the tip apex and upward near the sample surface. Snow is generally compacted in front of the cone and on its sides, but for the sample composed of depth hoar, we also observed dilation, probably due to size effects in this shallow penetration test. The displacement varies with distance to the cone, and no solid plug forms in front of the tip. The size of the deformed or compacted zones did not show any trend with density.

These results enable us to discuss the fundamental assumption of models used to interpret penetration profiles in snow. We showed that the density continuously increases from intact snow to compacted snow in contact with the penetrometer. Thus, the simple model of Johnson [2003] that assumes that the compacted snow reaches a constant critical state cannot accurately estimate the size of the compaction zone. The cavity expansion model [Yu and Carter, 2002] reproduced the progressive evolution of density with distance to the cone. Moreover, the force profiles simulated with this model agreed relatively well with those measured. However, this model describes snow as a continuum and it thus failed to reproduce the force fluctuations. In addition, it did not capture vertical movements as it assumes that the displacement induced by the penetration of the cone is only radial. The Poisson shot noise model introduced by [Löwe and van Herwijnen, 2012] somehow assumes that snow grains do not contribute to the penetration resistance once their bonds fail. Here, we confirmed, at the microscale and in 3D, the measurements of van Herwijnen [2013]; Lebaron et al. [2014]: the penetration creates a compaction zone in front of the tip, which may significantly affect the overall resistance force and subsequent interpretation.

3.1.3 Statistical model of the cone penetration process

The high-frequency fluctuations in penetration resistance with depth, measured by the SMP, have long been thought to contain information about snow microstructure. Johnson and Schneebeli [1999] first developed a model of penetration in snow. They assumed that the resisting force results from the brittle rupture of microstructural elements. These elements were supposed to be identical but randomly distributed in space. They empirically derived the number of ruptures from the number of peaks in the SMP signal. Marshall and Johnson [2009] extended this model to account for simultaneous rupture events and provided a more robust inversion method based on Monte-Carlo simulations. In parallel, Satyawali et al. [2009]; Satyawali and Schneebeli [2010] used the moments of the SMP signal (running mean and standard deviation) to classify snow types from penetration profiles. Löwe and van Herwijnen [2012] unified these two approaches. They described the penetration force as a Poisson shot noise process with single events described as ideal elastic-brittle elements (subplot of Fig. 3.5). With this formalism, the microstructural parameters of the model, namely the intensity (or the number of failure events) λ, the microscopic rupture force f, and the deflection at rupture δ, can be directly estimated from the cumulants κ_n of the penetration signal $F(z)$. In particular, Löwe and van Herwijnen [2012] obtained the following relations:

$$\kappa_n(z) = \frac{f^n \delta \lambda}{n+1} \quad \text{and} \quad C(z, z+r, |r| < \delta) = f^2 \delta \lambda \left(\frac{1}{3} - \frac{1}{2}\frac{|r|}{\delta} + \frac{1}{6}\frac{|r|^3}{\delta^3} \right) \tag{3.1}$$

where κ_n is the cumulant of order n (e.g., κ_1 is the mean, κ_2 is the variance) and C is the two-point correlation function. We call this model, the Homogeneous Poisson Process (HPP)

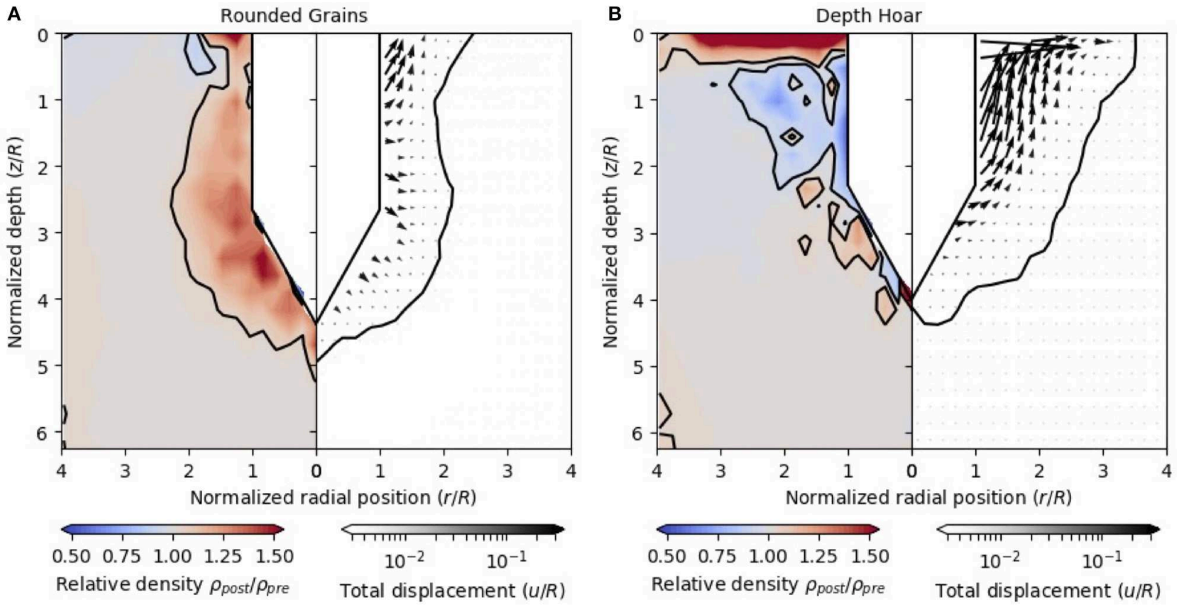

Figure 3.4: Deformation induced by a cone penetration test in snow. Average density change (left side) and displacement field normalized by tip radius R (right side) around the cone tip for two types of snow: (A) rounded grains, (B) depth hoar. The contours show the deformation and compaction zones around the tip. Displacements are plotted only if more than 30% of the grains in the corresponding subvolume are successfully tracked. The cone radius R is 2.5 mm. Taken from [Peinke et al., 2020].

model. The model is applied on small analysis windows (typically $\Delta z = 5$ mm) where λ, δ and f are supposed to be constant.

We further extended this relation [Peinke et al., 2019]. As explained in the previous subsection, a compaction zone progressively forms in front of the cone. This compaction zone somehow increases the apparent size of the cone, which affects the number of rupture events due to penetration. More practically speaking, the direct application of the HPP model did not work on our SMP data on small snow samples of a few centimeters in height. Thus, we needed a model capable of accounting for this transient behavior of the penetration profile. Based on mathematical developments (not detailed here), we showed that Eq. 3.1 holds, even if the intensity $\lambda(z)$ now depends on the position z:

$$\kappa_n(z) = \frac{f^n \delta \lambda_z(z)}{n+1} \quad \text{and} \quad C(z, z+r, |r| < \delta) = f^2 \delta \lambda_z(z) \left(\frac{1}{3} - \frac{1}{2}\frac{|r|}{\delta} + \frac{1}{6}\frac{|r|^3}{\delta^3} \right). \tag{3.2}$$

With this model, called the Non Homogeneous Poisson Process (NHPP) model, we separated the scale of variation of snow properties (f and δ) and the scale of variation due to the penetration process (λ) (Fig. 3.5). The calculation of the microstructural parameters from the penetration signal $F(z)$ is also modified. We need to define the function $\widetilde{F}$ as:

$$\widetilde{F} = \frac{F - \kappa_1(F)}{\kappa_1(F)^{1/2}} \tag{3.3}$$

Assuming the ergodicity of the process, the microstructural parameters can be calculated as follows

$$f = \frac{3}{2}\overline{\widetilde{F}^2}, \qquad \delta = -\frac{3}{2}\frac{C(0)}{C'(0)}, \qquad \lambda_z(z) = \frac{4}{3\delta}\frac{\kappa_1(F)}{\overline{\widetilde{F}^2}} \tag{3.4}$$

where $\overline{\bullet}$ denotes the mean over depth, κ_1 is the first cumulant (mean) and C is the two-point correlation function. We showed that this model is of clear interest when the transient part of the penetration profile is dominant but does not add much to the HPP model, if the penetration process is in a permanent regime with a fully developed and constant compaction zone in front of the cone.

We used the NHPP model on cone penetration tests to investigate snow sintering at microscopic and macroscopic scales [Peinke et al., 2019]. Sintering, i.e., the creation and growth of bonds between snow particles [Blackford, 2007], has long been recognized as a dominant process in snow strengthening [Gubler, 1978]. As stated in the general introduction (Sect. 1.2), characterization of the bond system is essential in snow mechanics. On simplified geometries composed of ice spheres, experimental and theoretical work described the evolution of bond size as a power-law [Kingery, 1960; Kuroiwa, 1961; Hobbs and Mason, 1964; Maeno and Ebinuma, 1983; Chen and Baker, 2010b]. Different studies quantitatively investigated the macroscopic strengthening of real snow with sintering [Ramseier and Keeler, 1966; de Montmollin, 1982; Matsushita et al., 2012; van Herwijnen, 2013; Podolskiy et al., 2014]. However, no studies measured the evolution of the bond size at the microscopic scale and the associated strengthening at the macroscopic scale. With the SMP and the NHPP statistical model, we analyzed the evolution of sieved snow for 24 h at -10°C. We showed that the evolution of the macroscopic force F is mainly due to strengthening microstructural bonds (an increase of f). Both macroscopic and bond rupture forces followed a power law with an average exponent of 0.28. Our analysis essentially confirmed the previous work of van Herwijnen [2013] but also showed that the NHPP model could reveal the underlying physics of snow sintering. In addition, we extended the analysis on longer time

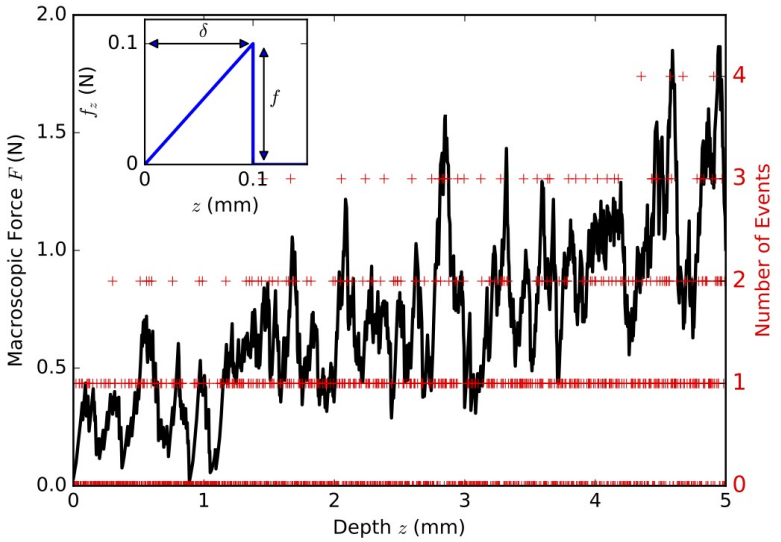

Figure 3.5: Simulated force penetration profile obtained as the superposition of uniform elastic brittle events (inset) whose number of occurrence follows a non-homogeneous Poisson distribution whose intensity increases linearly with depth. Taken from [Peinke et al., 2019].

scales of snow evolution under isothermal and temperature-gradient conditions. Under isothermal conditions, the macroscopic strengthening of the sample was again mainly explained by the microscopic strengthening of the bonds. Interestingly, under temperature gradient conditions, the bond strength was shown to slightly increase, and the drastic reduction of the number of bonds explained the weakening of the sample over time [Peinke, 2019].

3.2 Heated needle probe

The snowpack is mainly composed of air that is not entirely free to move in pores due to the tortuosity of the ice matrix. It thus does not conduct much heat and plays an essential role in the thermal regime of the underlying ground and associated feedback with the environment (e.g., permafrost, hydrology, vegetation) [Zhang, 2005]. The processes leading to heat transfer through snow comprise conduction through the ice matrix and the pores, latent heat transfer due to sublimation-condensation cycles and vapor diffusion, and ventilation due to forced air advection or thermal convection [Sturm et al., 1997; Domine et al., 2011]. Different studies identified conduction through the ice matrix as the dominant heat transfer mechanism [e.g., Sturm et al., 1997; Kaempfer et al., 2005; Calonne et al., 2011]. Like mechanical strength, which depends on the bonds between grains where stresses concentrate, heat conduction may be limited by the narrow constrictions between the ice grains [Colbeck, 1997]. Domine et al. [2011] showed that the effective thermal conductivity of snow is correlated with density but also depends on microstructure and, in particular, the snow bond system. Therefore, measuring snow thermal conductivity is not only essential to understanding the role of snow in the Earth's climatic system but also provides an indirect proxy of the snow microstructure.

The heated needle probe technique is commonly used to measure the thermal conductivity of materials [Blackwell, 1954]. This method is based on measuring the temperature rise of a

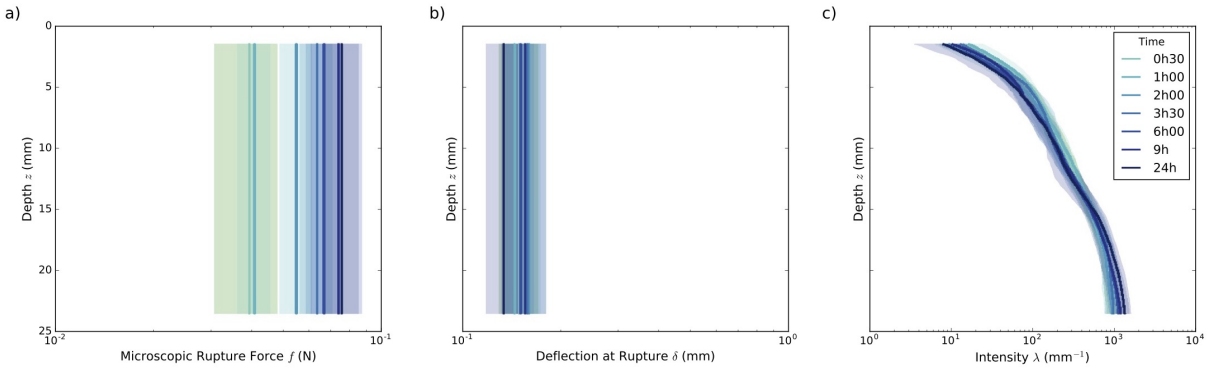

Figure 3.6: Vertical profiles of the micromechanical properties estimated by the NHPP model on a sample of rounded grains for different sintering times. The density of the sample is 500 kg m^{-3}, and its specific surface area is 18 m^2 kg^{-1}. The shaded area around the curves represents the standard deviation obtained for the different profiles at one sampling time. Taken from [Peinke et al., 2019].

needle inserted into the material and heated with a known power (for about 50-100 s in snow). The transient temperature evolution is related to heat conduction in the material: the lower the thermal conductivity, the higher the resulting temperature rise. The technique initially developed for soils has long been applied to snow studies in the field [e.g., Morin et al., 2010] and the cold lab [e.g., Sturm and Johnson, 1992]. It provides a convenient way to monitor the snowpack evolution and possibly capture its stratigraphy. However, Calonne et al. [2011]; Riche and Schneebeli [2013] reported systematically underestimated values of thermal conductivity when measured with heated needles and compared to other techniques. During the postdoc of K. Fourteau, we investigated different reasons for this discrepancy [Fourteau et al., 2022].

First, Riche and Schneebeli [2013] hypothesized that the heterogeneous nature of snow at the microscale might affect the theoretical model of the needle temperature rise [Jaeger, 1956], which treats snow as a continuum. We tested this hypothesis by explicitly simulating heat conduction around a heated needle (Fig. 3.7b). We then compared the simulated transient temperature evolution to the one calculated on a snow sample considered homogeneous (Fig. 3.7c) with an effective thermal conductivity derived from a homogenization simulation (Fig. 3.7a). The simulations performed on the same snow sample modeled as a heterogeneous or homogeneous material lead to very similar temperature evolution with time and subsequent estimation of thermal conductivity. Therefore, it is unlikely that the heterogeneous nature of snow explains the systematic underestimation of thermal conductivity with the heated needle probe technique.

Second, we investigated whether the damage caused to the snow when the needle is inserted or ice accretion on the needle when it is permanently installed in the field can affect the measurement. Indeed, Riche and Schneebeli [2010] hypothesized that damage around the needle affects the estimation of thermal conductivity. In contrast, Morin et al. [2010] simulated the impact of an air gap between the probe and the snow material and did not observe any impact on the shape of temperature evolution after 30 s of heating. We conducted similar numerical experiments to reproduce the temperature evolution of a heated needle inserted in a homogeneous snow sample (Fig. 3.7c). We tested two simplified cases: the presence of an air gap around the probe and the presence of an ice block stuck to the bottom of the needle. We observed that an air gap greatly influences the estimation of the effective thermal conductivity, especially for the denser and more conductive snow. The thermal conductivity estimated with or without an

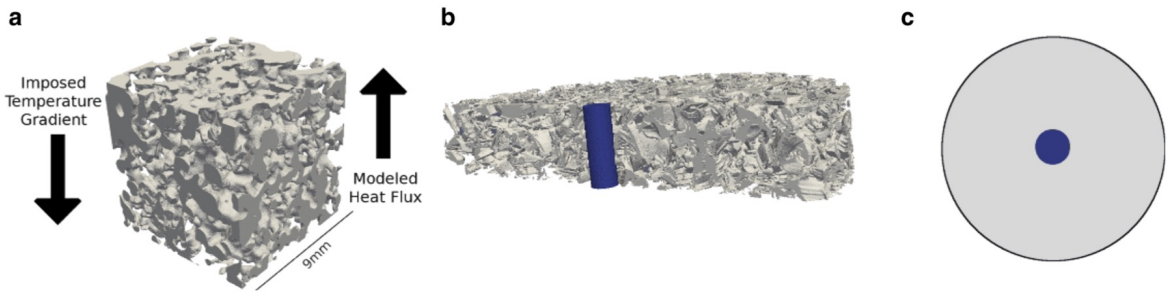

Figure 3.7: Schemes of the three different numerical simulations. (a) 3D homogenization simulation used to estimate the thermal conductivity of a snow sample based on its microstructure (ice phase shown in gray). (b) 3D heterogeneous needle probe simulation, modeling the temperature increase of a probe (in blue), taking into account heat transfer through both phases composing a snow sample (ice phase shown in gray). (c) 2D homogeneous needle probe simulation, modeling the temperature increase of a probe (in blue) in which the external medium is considered homogeneous. Taken from [Fourteau et al., 2022].

air gap of 0.2 mm thickness differs by 20% on snow with a density of 400 kg m^{-3} (for a 75 s heating duration). In contrast, the block of ice did not significantly affect the estimation of the effective thermal conductivity. We did not obtain the same result as Morin et al. [2010] because we did not neglect the heat storage by the needle. This simplification is possible for materials with a large heat capacity but no longer suited for snow with a smaller capacity. The damage caused to the snow structure by the needle insertion yields significant under-estimation of the snow thermal conductivity.

However, this under-estimation of conductivity by the needle technique is also observed on permanent needles with "perfect" contact with the measured snow material. There is still one explanation missing. This last explanation can be found in the analytical model used to interpret the temperature rise. Jaeger [1956] modeled the temperature rise ΔT of the probe (Eq. 18 therein) as a function of the time t since the heating start, the heating rate Q, the thermal conductivity of the tested material k_T, the thermal contact resistance between the probe and the material, the thermal capacities of the probe and the material, and a characteristic time τ depending on the probe radius and the thermal diffusivity of the material. For $t \gg \tau$, the complex formula simplifies to:

$$\Delta T = \frac{Q}{4\pi k}\left[a + \frac{2Hk}{r} + \ln\left(\frac{t}{\tau}\right)\right] + O\left(\frac{\tau}{t}\ln\left(\frac{t}{\tau}\right)\right) \tag{3.5}$$

with $a = 0.810$. The thermal conductivity is thus only related to the variation of temperature with time and the heating rate Q:

$$k \approx \frac{Q}{4\pi}\left(\frac{\partial \Delta T}{\partial \ln(t)}\right)^{-1} \tag{3.6}$$

Equation 3.6 is used in practice to derive the thermal conductivity from the measured heated curve. The derivatives of ΔT with time are usually measured after about $t = 100$ s of heating. On snow, the typical time $\tau = 1.5$ s, it appears thus reasonable to consider that $t \gg \tau$ and that the approximation (Eq. 3.5) is valid. However, we showed that the convergence towards

the asymptotic development is rather slow and that snow thermal conductivity can be underestimated by up to 40% because of this discrepancy. Unfortunately, the heating time in snow cannot be extended because convection may appear after 100 s [Sturm and Johnson, 1992]. Fortunately, the errors related to the finite heating duration can be numerically predicted given the property of the heated needle probe. We provided the correction factors for the Hukseflux TP02 probe, one of the most common probes in snow science.

In summary, thermal conductivity can be conveniently measured with the heated needle probe. However, a correction factor must be applied to the standard methodology to account for the finite duration of the heating. Otherwise, the estimated thermal conductivity can be under-estimated by up to 40%. Nevertheless, the required correction remains unknown when the needle insertion damages the snow in contact with the probe. Therefore, we recommend using fixed needle probes to monitor snowpack evolution.

3.3 Matching of snow profiles

Snow profiles characterize the snowpack stratigraphy and represent the evolution of snow properties with depth. Snow scientists often observe that profiles measured a few meters from each other comprise the same information but are not directly comparable because some layers are shifted vertically. These shifts are due to variability in the layer thickness (e.g., wind effects) or errors in the measured depths. Such true and apparent spatial variability causes stratigraphic mismatches, even if continuous layers are present in the snowpack [Sturm and Benson, 2004]. In other words, layers at the same depth in different profiles are not necessarily at the same position in the stratigraphy. The layers of different profiles must be matched to correct these stratigraphic mismatches and compare "comparable" layers. A small number of profiles can be matched manually [Sturm and Benson, 2004; Calonne et al., 2020; Mayer et al., 2022]. However, the huge amount of data measured by high-resolution snow "profilers" such as penetrometers [e.g., Schneebeli and Johnson, 1998] and reflectance measurement tools [e.g., Arnaud et al., 2011], or simulated by detailed snowpack models [e.g., Lehning et al., 2002; Vionnet et al., 2012] requires the development of an automatic matching algorithm. Lehning et al. [2000] first implemented a mapping method accounting for deviating total snow depth and variable layer segmentation. However, this method was not robust and allowed the vertical inversion of layers. We thus developed a new one. The new method was applied to various problems during the internships of T. Pilloix, L. Viallon-Galinier, and C. Bouchayer. In this section, I first present a generic matching algorithm (Sect. 3.3.1). Then, I show how this algorithm applies to measured penetration profiles (Sect. 3.3.2) and simulated snow profiles (Sect. 3.3.3).

3.3.1 Main principles

The goal of matching is to retrieve the transformation of the layer position (depth) that best matches points of similar characteristics (Fig. 3.8). It requires three main ingredients: a similarity metric between profiles, an ensemble of transformation functions, and an optimizer that finds the best transformation in the ensemble according to the similarity metric. In Figure 3.8, one profile is locally shifted to minimize the standard deviation to the reference profile. Here, possible transformations include all functions that reduce the layer thickness by a maximum of 50% or extend it by a maximum of 100%.

There are different ways to solve this problem. In [Hagenmuller and Pilloix, 2016], we considered it as a general registration problem without a prior hypothesis on the form of the similarity

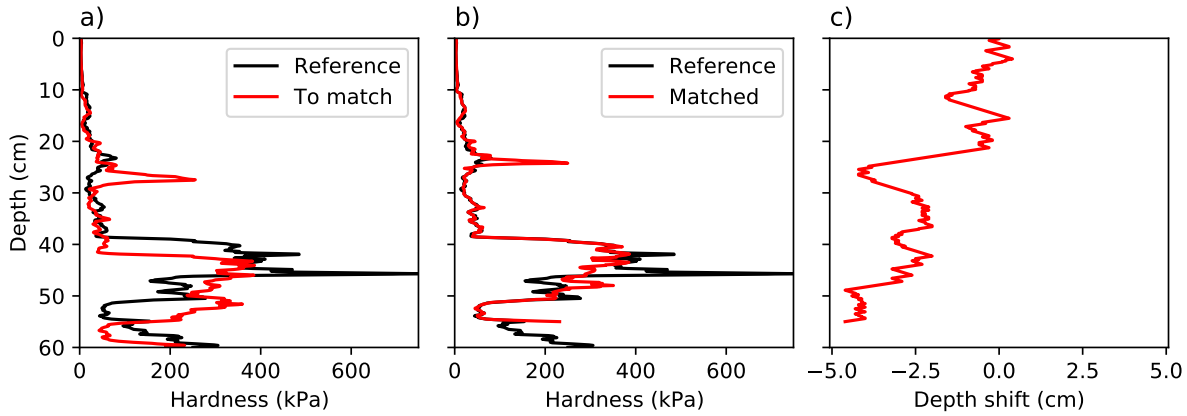

Figure 3.8: Example of matching two hardness profiles: a) the two initial profiles, b) the matched profiles, and c) the depth shift required to match the profiles.

metric and the transformation functions. We imposed that the layer order cannot be inverted and that one layer cannot disappear nor extend to the whole profile. The method SLSQP (Sequential Least-Squares Programming, implemented in python package scipy.optimize) can solve this constrained optimization problem [Kraft, 1988]. The limitations of this algorithm are its high computing cost and the fact that the optimizer can get stuck in a local minimum.

Inspired by the work of Schaller et al. [2016], we realized that, with limited additional constraints on the initial problem, the matching problem reduces to a much simpler one. This additional constraint states that the similarity metric is the sum of a local metric (i.e., a point-by-point comparison between the profiles without global variables). For instance, L_1 and L_2 distances (sum of the absolute or squared local differences) satisfy this criterion. Maximizing the correlation or minimizing the maximum difference between the profiles does not satisfy this condition. With these constraints, the problem can be efficiently solved by Dynamic Time Warping (DTW), introduced by Itakura [1975]; Sakoe and Chiba [1978] in speech recognition in the 1970s. The basic idea of this method is to discretize the two profiles P and P_{ref} into a set of points $(P_i)_{i=1..n}$ $(P_{ref,j})_{j=1..m}$ on the same depth grid with a step dz. Then the points of (P_i) are consecutively assigned to those of $(P_{ref,j})$ with simple rules related to the similarity metric. The rules define how many points (P_i) can be assigned to the same point of $(P_{ref,j})$ (this number, here equal to 2, defines the maximum squeeze of the initial profile) and how many successive points of $(P_{ref,j})$ are not associated with any points of (P_i) (this number, here equal to 1, defines the maximum extension of the initial profile). With this choice, the layer thickness is, at maximum, reduced by 50% or dilated by 100%. By choosing a sufficiently small value for dz, all continuous layer reduction/dilation functions within these bounds can be reproduced. The DTW algorithm enables finding the optimal matching with a computation complexity of $n \times m$. Details can be found in [Senin, 2008; Schaller et al., 2016].

The method described above does not apply directly to combining multiple (more than two) profiles into a representative profile. Indeed, no profile of the set can be arbitrarily considered as the reference profile. The goal is to construct a profile that maximizes its average similarity to all profiles in the set. Petitjean et al. [2011] introduced a global averaging strategy called DTW Barycenter Averaging (DBA). It is a heuristic strategy that has been shown to perform well. Its main idea is to iteratively match the profiles to the mean of the matched profile, which thus

evolves with the number of iterations. After a few iterations (typically 5 to 20), the mean of the matched profiles converges to the representative profile. In contrast to simply averaging the initial profiles, this representative profile preserves sharp vertical transitions between layers.

3.3.2 Application to measured penetration profiles

We first used the matching algorithm to evaluate a new penetrometer, the Avatech Snow Probe 2 (SP2). Indeed, DTW allows us to compare profiles measured with the SP2 and the SMP, considered the reference penetrometer. Furthermore, DBA applied to numerous profiles measured close to each other provides a way to quantify the spatial variability of the snow cover. With this approach, we can assess whether the differences between the SP2 and SMP profiles are due to measurement errors or to the natural spatial variability of the snowpack. The results of this study are detailed in Section 3.1.1 [Hagenmuller and Pilloix, 2016; Hagenmuller et al., 2018].

Quantifying the snowpack spatial variability is also essential for avalanche applications [Gubler and Rychetnik, 1991; Schweizer et al., 2008; Bebi et al., 2017]. For example, the continuity of a weak layer throughout a slope is a prerequisite to forming large avalanches [Schweizer et al., 2003]. Forests modify snowpack properties through interception of snowfall by the canopy, wind sheltering, and changes in the energy balance [Schneebeli and Bebi, 2004]. These processes and tree variability lead to large snowpack variability in mountain forests. The protective role of forests against avalanches is partially related to these spatial variations found in forests [Gubler and Rychetnik, 1991; Schneebeli and Bebi, 2004]. Quantifying the snowpack spatial variability is possible and convenient with hardness profiles measured with the SMP [Kronholm et al., 2004]. The DBA algorithm now enables us to quantify it on a large amount of data collected with the SMP, which would have been impossible manually [e.g., Kronholm et al., 2004; Sturm and Benson, 2004]. In particular, we wanted to evaluate how bark beetle attacks on forests affect snowpack spatial variability [Teich et al., 2019]. M. Teich and colleagues measured numerous (about 500) SMP profiles in different types of forests and at different times during the winter season. I processed the data with the DBA matching and analyzed the associated spatial variability (Fig. 3.9). We observed that the spatial variability in snow stratigraphy does not significantly differ between the green ("healthy" forest) and gray (forest after a beetle attack) stages of the spruce forest stands. This is shown qualitatively in Fig. 3.9 and quantified in [Teich et al., 2019]. We found that canopy cover (out of tested variables) is the main driver of heterogeneity in snow stratigraphy. The latter increased with increasing forest canopy cover. Surprisingly, the presence of foliage or the ground roughness did not affect spatial variability in this case. This goes beyond my expertise, but these results are essential to guide silvicultural measures after bark beetle disturbance in forests with a protective function.

3.3.3 Application to snowpack simulations

The matching algorithm applies to any data describing the evolution of snow properties with depth. These data can be measured or simulated. The profiles are not necessarily univariate: a layer can be characterized by several variables. Moreover, each layer property is not necessarily a floating scalar but can describe a class. The only requirement for the matching is that we can define one distance between the layers. For example, a layer of precipitation particles (PP) is more similar to a layer of decomposing and fragmented snow (DF) than a layer composed of melt forms (MF). Here, I describe two applications based on the generalization of the matching algorithm to more complex data.

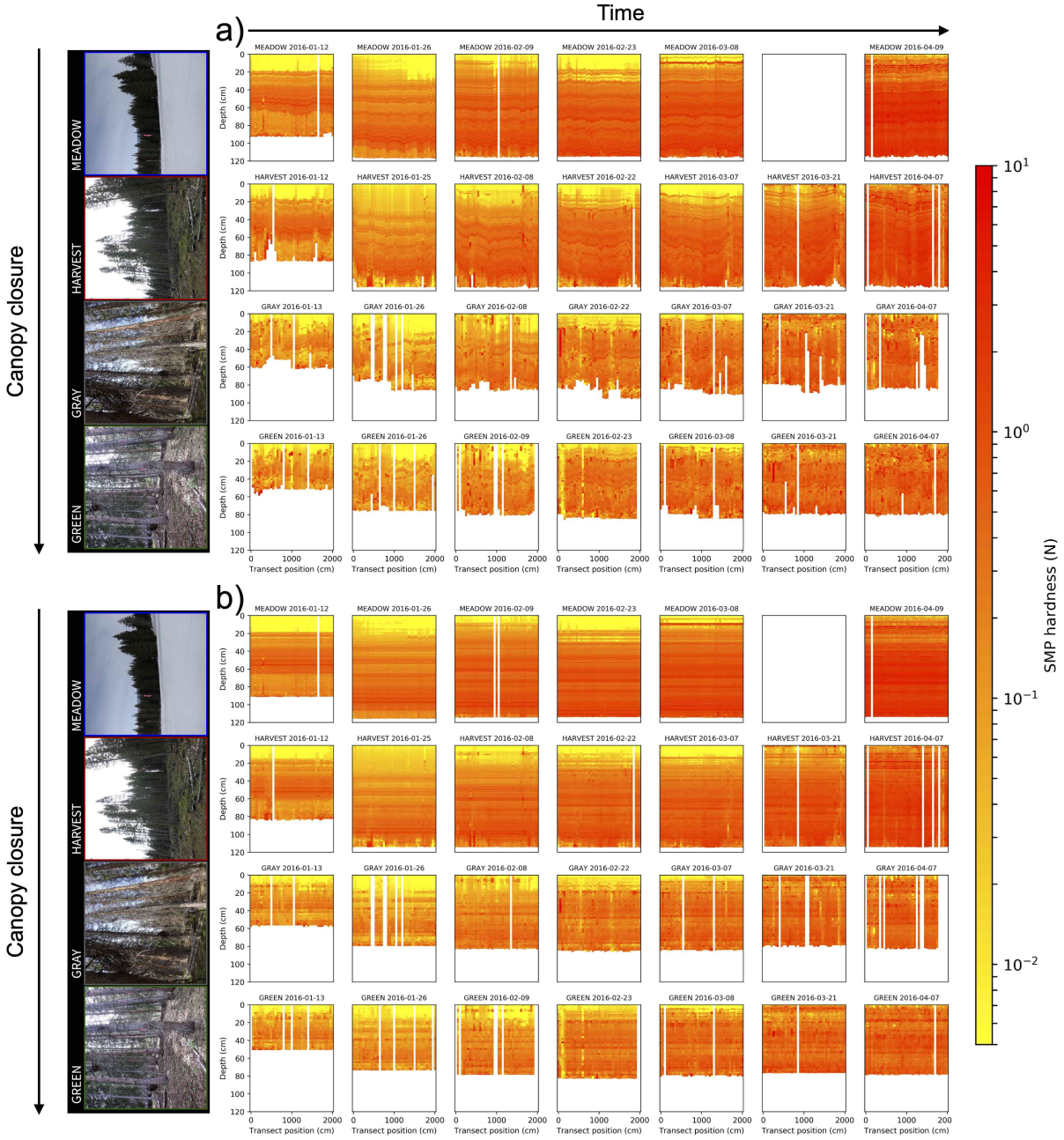

Figure 3.9: Hardness profiles measured along 20 m transects under different forest types (GREEN=green stand; GRAY=gray stage stand; HARVEST=salvage-logged stand; MEADOW=non-forested meadow area) and at different dates in Uinta Mountains in Utah, USA. a) Initial profiles b) Matched profiles. Adapted from [Teich et al., 2019].

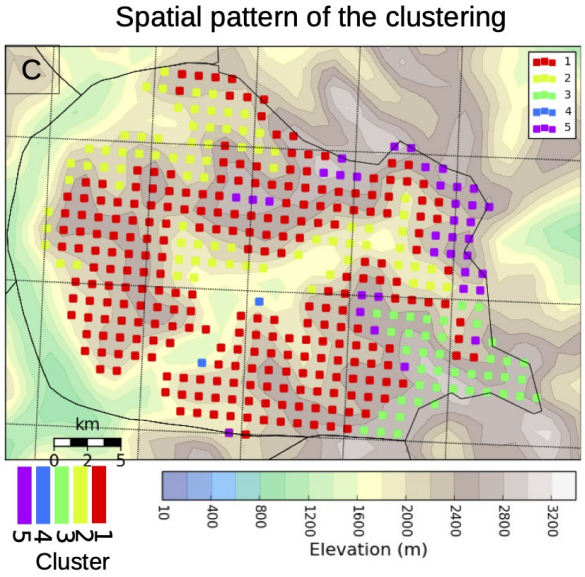

Figure 3.10: Clustering of snowpack profiles on the Queyras massif. Taken from [Hagenmuller et al., 2018].

One major challenge of the CEN in the following years is to provide simulated snowpack data at a spatial resolution of 250 m in the french mountains. The idea is to force the snowpack model Crocus [Vionnet et al., 2012] with the high-resolution numerical weather prediction model AROME [Seity et al., 2011; Brousseau et al., 2016] and to assimilate satellite data [Cluzet et al., 2020]. The high resolution produces numerous detailed snowpack profiles, which must be synthesized into relevant information, e.g., supporting avalanche forecasting. Two main approaches can be considered. The profiles can be reduced to scalar indicators, e.g., an index describing snowpack stability (see Chap. 4). Similar profiles can also be aggregated in a few groups [Hagenmuller et al., 2018]. This latter approach is developed here. We applied the matching algorithm on profiles of density and specific surface area simulated by Crocus forced by the weather prediction model AROME at 1.3 km resolution. We first computed the distance of each couple of profiles in the set with the DTW matching algorithm, thus accounting for potential depth shifts. Then agglomerative clustering is used on the calculated distance matrix to group similar profiles. Lastly, profiles belonging to the same cluster are matched together (DBA) to derive a representative profile of each cluster. This procedure was applied to the Queyras massif (France). It correctly identified the dependence of stratigraphy on elevation, but also the East-West gradient, typical of this mountain range (Fig. 3.10). This study case provided excellent proof of concept of the methodology for potential application in avalanche warning services [Hagenmuller et al., 2018]. Indeed, more recently, Herla et al. [2022] applied the same methodology on simulated profiles in Canada.

Snowpack models, such as Crocus or SNOWPACK, have generally been evaluated on bulk or surface properties, such as snow depth [e.g., Brun et al., 1989], snow water equivalent or surface albedo [e.g., Lafaysse et al., 2017]. However, these detailed snow models are initially designed to simulate the snowpack stratigraphy and have never been quantitatively evaluated for their capacity to do so. In parallel, to support avalanche forecasting, trained observers regularly report stratigraphic profiles [Fierz et al., 2009]. For instance, about 36 000 profiles were reported between 1990 and 2015 in the French mountains. How could this wealth of data be used to

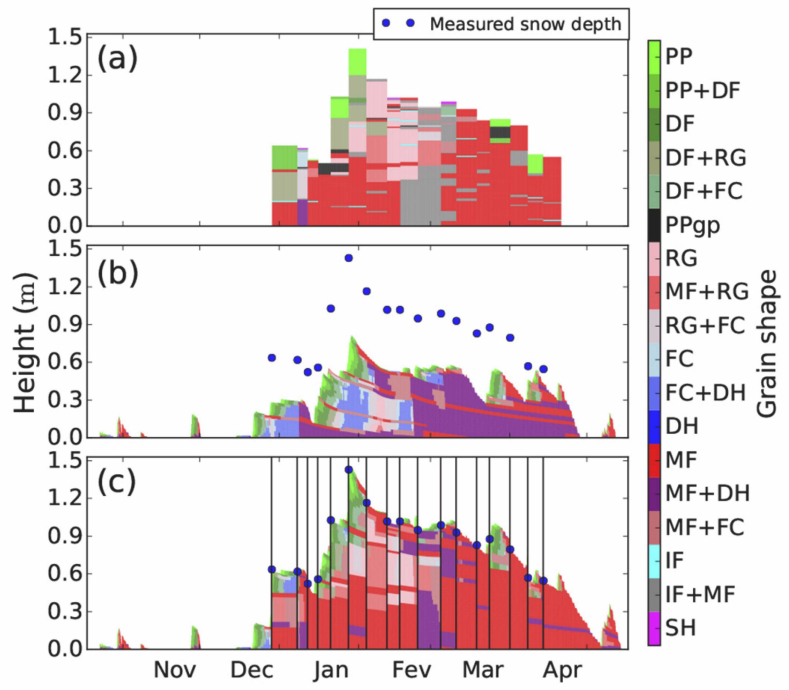

Figure 3.11: Application of the matching technique on the snowpack evolution at Col de Porte during winter 2003-2004. The plots represent the grain shape profiles at different dates during winter and obtained by different methods: (a measured snow profiles (b Crocus simulation initialized by a bare ground in August, and c) Crocus simulation with direct insertion each time an observed profile was available (almost every week). Taken from [Viallon-Galinier et al., 2020].

evaluate and improve the simulated stratigraphy? We developed a new method to compare the simulated and observed snow stratigraphy and use an observed snow profile as the initial conditions of the simulation. To this end, we adapted the matching algorithm [Hagenmuller and Pilloix, 2016] to deal with standard measured or simulated snow profiles, including multiple properties, sometimes described by classes (grain shape type, hand hardness, and humidity) [Viallon-Galinier et al., 2020]. We evaluated Crocus against 739 profiles observed on three alpine sites between 2000 and 2015. Crocus simulated snow depth with a median error of 12 cm, layer density with a median error of 50 kg m^{-3}, and layer grain shape with an error of 0.31 according to a dedicated metric (Fig. 3.11a,b). Direct insertion of snow observations into the model corrected the simulations. The median error of the simulation decreased to 6.8 cm for snow depth, 39 kg m^{-3} for density, and 0.25 for grain shape, one week after initialization with an observed manual profile (Fig. 3.11a,c). However, this improvement almost vanished one month after the insertion. This work provides the framework to evaluate consistently new developments of detailed snowpack models and constitutes a first step towards the assimilation of observed profiles in ensemble forecasting.

3.4 Ongoing and future work

3.4.1 Numerical cone penetration tests

Snow is characterized by a great diversity of microstructural patterns and complicated experimental manipulation (fragile material evolving with temperature). Therefore, we adopted a strategy based on numerical experiments in the previous chapter (Chap. 2). The discrete element model provided new insights into brittle failure and qualitatively agreed with previous experimental data (Sect. 2.2.4). However, we lack a quantitative evaluation of the model on experimental data.

The cone penetration test captured by tomography appears as a suitable choice to conduct this evaluation. Indeed, the initial microstructure captured before the tests can constitute the model's initial conditions. The model can be evaluated on the force profile and the deformation pattern captured with tomography. Cone penetration activates complex deformation patterns with a compression zone around the penetrometer apex and an expansion zone close to the sample surface. Being able to reproduce the force and displacement profiles for this mechanical test would constitute a strong validation of the micromechanical model. During the internship of A. Didier and the postdoc of C. Herny, we started this detailed evaluation by modifying the boundary conditions used in the numerical code of Mede et al. [2020]. The first results are promising: accounting only for the microstructure of snow and the properties of ice (without any fit), the model correctly reproduces the measured deformation and force profiles. The validation of the micromechanical model on the cone penetration gives confidence in the mechanical properties simulated on other loading conditions (e.g., systematic computation of snow failure envelope).

The Snow Micro-Penetrometer (SMP) can bridge the gap between laboratory-based techniques and field techniques. The link between snow microstructure and penetration profile remains empirical [e.g., Proksch et al., 2015]. Existing statistical models of cone penetration rely on assumptions that are not fulfilled (Sect. 3.1.2). The numerical experiments of cone penetration tests provide a convenient way to explore how snow microstructure affects the penetration profile. In particular, we can directly evaluate the statistical model on the simulated snow profile. This ongoing work will yield a new method to recover microstructural proxies from straightforward field measurements.

The development of a "light-weight and cheap SMP" also measuring reflectance and recording the sound of the cone penetration could be a game-changer. Leading this development would be out of reach for the CEN human resources. However, joint developments with private companies, such as the ones conducted for an instrument measuring liquid water content in the snow (WISE), might not be impossible.

3.4.2 Matching in support of snowpack modeling

The remaining work on the matching algorithm is mainly technical. It may include its incorporation, for instance, into the python package snowmicropyn, which constitutes an international toolbox for processing SMP data. Besides, support to the matching algorithm users on different operational applications in Météo-France is also part of the work.

On more scientific aspects, developing new snowpack models (e.g., project ERC IVORI) with a higher vertical resolution than that of the already detailed model Crocus or SNOWPACK requires a very detailed characterization of the snow layer. The highest the vertical resolution, the more crucial the vertical match. For instance, the RHOSSA intensive measurement campaign [Calonne et al., 2020] is currently used to evaluate the model Crocus and relies on the matching

algorithm. Due to the fragile nature of snow, the detailed characterization of the snow stratigraphy is generally conducted on disconnected snow blocks. The snow characterization is at a very high resolution, but the accuracy of the positioning of the whole block in the snowpack is generally very low (a few cm). We will use matching to correct this potential error (e.g., Fig. 2.11). All in all, the matching tools work and will be used.

Chapter 4

Avalanche formation

Preamble

Avalanche forecasting requires information on the current and future state of the snowpack [LaChapelle, 1977]. Snowpack modeling complements direct observations and weather forecasting by providing information otherwise unavailable [Brun et al., 1989]. In the past decade, numerous numerical models have been developed to understand the link between snowpack properties and the propensity of the snowpack to form an avalanche [e.g., Heierli et al., 2008; Reiweger et al., 2015; Reuter et al., 2015; Gaume et al., 2018; Bobillier et al., 2021]. The knowledge of avalanche formation subsequently increased [Schweizer et al., 2016]. However, there is still a gap between these computational tools designed to gain knowledge and the actual operational use of those by avalanche forecasters [Morin et al., 2020]. This chapter is dedicated to modeling tools predicting snow stability and avalanche activity. The snowpack modeling chain of Météo-France (S2M) is first described and illustrated on avalanche prediction. The existing methods for computing stability indicators from detailed snow stratigraphy based on a mechanical analysis are then summarized. Last, these physically-based models are complemented by machine-learning approaches.

Contents

4.1 Snow stability modeling

4.1.1 S2M: a tool to assess avalanche conditions

Forecasting the avalanche danger in the French mountain ranges partly relies on the numerical simulations of the physical properties of snow on the ground and assessment of its mechanical stability [Pahaut and Giraud, 1995]. The model chain SAFRAN – SURFEX/ISBA–Crocus – MEPRA (S2M) provides these simulations [Lafaysse et al., 2013], [Vernay et al., 2022]. The *Système d'Analyse Fournissant des Renseignements Adaptés à la Nivologie* (SAFRAN) is a weather analysis model providing the atmospheric conditions on an hourly basis [Durand et al., 2009]. It uses meteorological observations to adjust a guess from a large-scale numerical weather prediction model (ERA40 before 2002 and ARPEGE after 2002). The model is semi-distributed

over elementary areas representing the main drivers of the snow spatial variability in mountain areas. Each mountain massif, e.g., Chartreuse, is decomposed into 300 m elevation bands and eight different aspects for three different slope angles. The model SURFEX/ISBA-Crocus (or simply Crocus) is driven by SAFRAN and simulates the evolution of the snow stratigraphy. It accounts for precipitation, dry/wet metamorphism, settlement, and heat exchanges. It simulates up to 50 layers at time-resolution of 15 min [Brun et al., 1989; Vionnet et al., 2012] (e.g., Fig. 4.1). Crocus is coupled to the soil model ISBA-DIF to account for heat fluxes with the ground [Decharme et al., 2011]. Last, the *Modèle Expert d'aide à la Prévision du Risque d'Avalanche* (MEPRA) derives mechanical properties from the core variables of Crocus and provides hazard indicators related to spontaneous and triggered avalanches [Giraud, 1992]. The model chain S2M provides a meteorological and snowpack reanalysis from 1958 to 2021 [Vernay et al., 2022], short-time forecasting of the snow conditions [Morin et al., 2020] and can be adapted to project the snowpack evolution with climate change [Verfaillie et al., 2017]. I contributed to the S2M development by optimizing MEPRA, developed in the early 1990s, and implementing it into the surface modeling platform of Météo-France (SURFEX). However, I am mainly a user of the model chain. In particular, as described in the following paragraphs, we used the detailed stratigraphy simulated by S2M to gain knowledge in avalanche formation.

Deposition of Saharan dust on snow frequently occurs in the French mountain ranges and changes the color of snow [Dumont, 2017; Greilinger and Kasper-Giebl, 2021]. Previous qualitative studies have associated dust deposition events with increased avalanche activity [Landry, 2014; Chomette et al., 2016]. Even if the impact of dust on snow radiative properties has long been well-known [Wiscombe and Warren, 1980], there is no clear scientific evidence that dust deposition can significantly affect snowpack stability. Indeed, direct observation of avalanches starting from a dust-contaminated layer does not constitute evidence of the own effect of dust. This limitation is due to the absence, in the field, of a "reference" snowpack without dust. We (internship of O. Dick) used S2M to investigate the impact of dust deposition on snow properties and mechanical stability [Dick et al., 2021]. The S2M tool, which includes an advanced radiative transfer model [Libois et al., 2013], enabled us to compare simulations with and without dust deposition. Figure 4.1 shows this comparison on the grain type profiles. The presence of dust yielded the formation of a melt-freeze crust (red MF layer in Fig. 4.1), which changed the temperature gradient in the snowpack in the following days. This change led to increased temperature-gradient metamorphism and the formation of faceted crystals (blue FC layer in Fig. 4.1) known to favor slab avalanches. We quantitatively evaluated the changes in snow stability with the model MEPRA on the Thabor massif in the French Alps during the winter season of 2017-2018. We also conducted ensemble simulations with a multi-physical approach [Lafaysse et al., 2017] to ensure that our results were significant. We showed that dust deposition could decrease the snowpack stability with the phenomenon described in Figure 4.1. However, dust deposition can also increase the stability by creating a melt-freeze crust on the snowpack surface, reducing the stress applied on the underlying weak layers through the so-called bridging effect [Monti et al., 2016]. The dust-on-snow events also advanced the onset of wet avalanche activity by up to one month in spring, as already observed on the complete melt of the snow cover [Dumont et al., 2020]. Dust deposition thus impacts snowpack mechanical stability. Nevertheless, in contrast to a myth shared by mountain practitioners, this effect is not only negative (de-stabilizing) but also positive (stabilizing) depending on the conditions. In many cases, it is neutral. However, it remains to be clarified whether dust events are also an indirect indicator of weather conditions favoring avalanche activity.

The avalanche danger, communicated in the avalanche bulletin, is determined by the ease

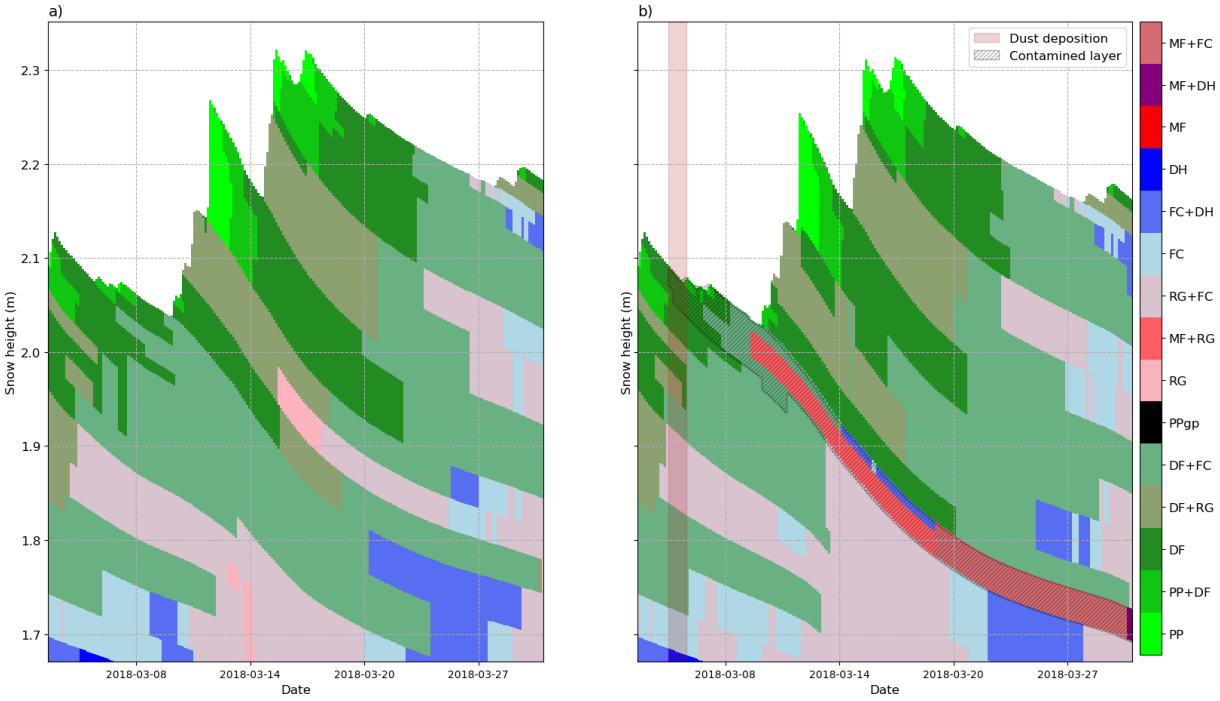

Figure 4.1: Evolution of grain shape profiles a) without or b) with a dust deposition. The simulation point corresponds to Thabor massif at 2400 m elevation on a North facing slope inclined by 40 degrees. The dust deposed on March 5^{rd} 2018. The hatches correspond to the layer contaminated with more than 0.1 mg g^{-1} of dust. Grain shape named after [Fierz et al., 2009]. Adapted from [Dick et al., 2021].

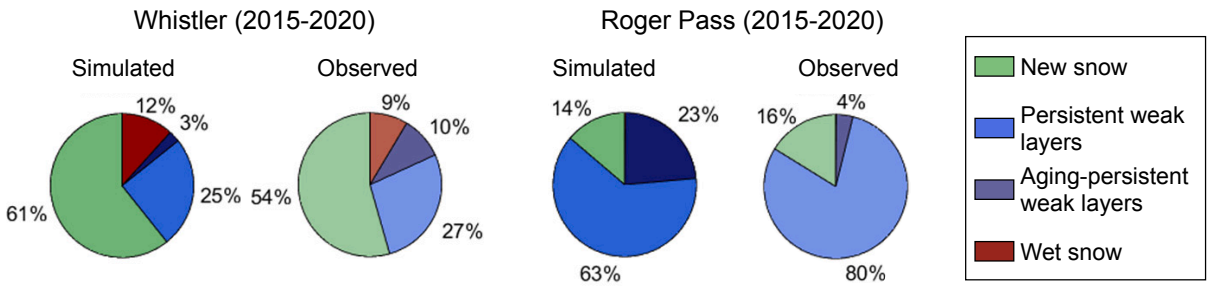

Figure 4.2: Frequency of avalanche problem types at two Canadian sites (Whistler and Roger Pass) for the winter seasons between 2015 and 2020, either derived from snowpack simulations or directly observed. Adapted from [Reuter et al., 2022].

of triggering an avalanche (i.e., snow instability), the spatial distribution of instability, and the amount of snow potentially involved in the avalanche (or avalanche size) [Statham et al., 2018]. Avalanche warning services in North America [Statham et al., 2018] and Europe [EAWS, 2017] formulated avalanche problem types to complement the avalanche danger level and provide helpful information to mountain practitioners. The European classification (New snow, Wind-drifted snow, Persistent weak layers, Wet snow, and Gliding snow) distinguishes the meteorological and snow drivers at the origin of avalanche-prone situations. These five typical problems support avalanche professionals and recreationists in their local hazard assessment. Snowpack models presently do not provide information on avalanche problem types. We modeled this classification on simulated snow stratigraphy [Reuter et al., 2022]. We developed an algorithm to detect and track weak layers in SNOWPACK (the Swiss detailed snowpack model) and Crocus simulations. The algorithm analyzes the temporal evolution of snow stratigraphy. It checks step-wise whether a slab buries a weak layer, whether this weak layer-slab structure is unstable, and how this instability evolves with time. We assess avalanche problem types from this analysis. We showed that the detection of an avalanche problem correlated well with avalanche activity recorded around Davos (Switzerland), and the problem types agreed with the ones reported by observers on Canadian sites (Fig. 4.2). The developed methodology could support avalanche forecasting and be used to assess past and future impacts of climate change on the characteristics of snow instability.

4.1.2 Review of stability models

Slab avalanches, whether they release naturally or are artificially triggered, result from a sequence of processes occurring in the snowpack [e.g., Schweizer et al., 2021] (Fig. 1.1). In particular, failure initiation and the onset of crack propagation describe the snowpack stability at the point scale [e.g., Reuter et al., 2015]. Low stability means the snowpack is prone to failure initiation and crack propagation. Snowpack stability paired with spatial information and avalanche size determines the avalanche danger [Statham et al., 2018]. On the one hand, stability tests can characterize point stability in the field. They mainly consist of loading a snow column with increasing stress until failure [Föhn, 1987a; van Herwijnen and Jamieson, 2007; Simenhois and Birkeland, 2009] or mimicking the progressive growth of a crack until self-propagation [Gauthier and Jamieson, 2006]. On the other hand, characterizing the mechanical stability of simulated profiles requires dedicated models: the so-called stability models.

During the Ph.D. of L. Viallon-Galinier, we summarized the broad spectrum of stability models developed since the pioneering work of Roch [1966]. We focused on models that were,

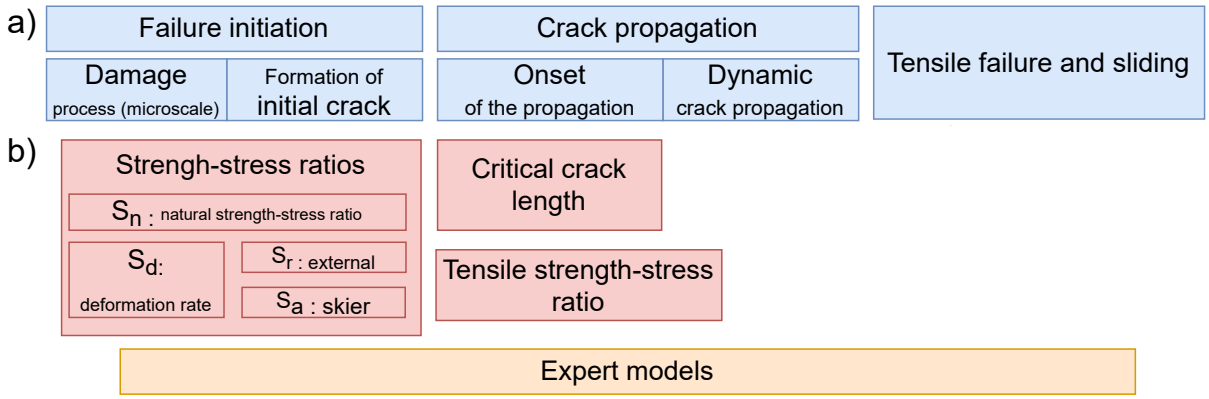

Figure 4.3: (a) Processes involved in avalanche formation according to Schweizer et al. [2021] and (b) classification of stability models according to the processes they represent. Unpublished.

in practice, tested on the output of detailed snow cover models. The stability models all relied on relatively simple mechanics and were generally associated with a specific process of avalanche release (Fig. 4.3). Within a strength-of-material approach, failure occurs when stress is higher than strength [e.g., Timoshenko, 1940]. Stability models thus describe failure initiation propensity with strength over stress ratios [Roch, 1966; Föhn, 1987b; Giraud, 1992; Lehning et al., 2004; Habermann et al., 2008; Reuter et al., 2015; Gaume and Reuter, 2017]. Within linear elastic fracture mechanics, a crack propagates when the stress intensity factor exceeds its critical value [e.g., Perez, 2004]. The critical crack length in a specific standard geometry quantifies the crack propagation propensity in slab modeling [Sigrist et al., 2006; Heierli et al., 2008; Schweizer et al., 2011; van Herwijnen et al., 2016; Reuter and Schweizer, 2018]. However, we identified many subtle differences between models behind this apparent homogeneity: additional expert rules and diverse implementations. We listed this diversity in large tables (publication under revision, not detailed here). In addition, we illustrated the stability models on typical snow profiles and highlighted their sensitivity to the mechanical properties of the layers. Consequently, we also documented the numerous parameterizations relating snow characteristics (e.g., density, grain shape type) to mechanical properties.

Based on this snapshot, we drew some scientific challenges concerning snowpack stability assessment based on snowpack modeling:

- Even the most accurate and resolved model is useless to derive snow stability from simulated profiles if its input cannot be related to the snowpack model output. This point implies balanced research efforts between slab scale modeling and snow material characterization. Moreover, the most advanced models were firstly intended to gain knowledge of the mechanism at work and applied only to simplified cases: a homogeneous slab over a weak layer. The simulated snowpack is generally stratified with an unknown position of the weak layer. It remains unclear how these models could account for detailed and generic layering in a computing efficient manner. Slab-averaged properties might also be irrelevant in some cases [e.g., Monti et al., 2016].

- All stability models assume snow behaves as an elastic brittle material. Snow is known to exhibit a visco-plastic behavior which is a permanent source of energy dissipation and becomes dominant at low strain rates [e.g., Narita, 1984]. To date, all crack propagation

models assume that at the onset of crack propagation, the energy required for crack extension in the weak layer equals the elastic strain energy of the slab and the change of its potential gravitational energy [Heierli et al., 2008]. With this hypothesis, van Herwijnen et al. [2016] reproduced experimental data for elastic modulus ranging between 0.08 and 34 MPa and weak layer fracture energy between 0.08 and 2.7 J m^{-2}, close to the typical values for ice. In contrast, Gerling et al. [2017] estimated the elastic modulus of similar snow between 10 and 300 MPa from measurements of sound propagation. Lebaron and Miller [2014] estimated the weak layer fracture energy between 0.005 and 0.05 J m^{-2} by measuring the minimal ice surface required to separate the sample into two blocks [Hagenmuller et al., 2014a]. The elastic modulus and fracture energy used for stability models are thus "effective" (i.e., adjusted) values instead of intrinsic material characteristics. The developed stability models succeeded in reproducing the observed macroscale mechanical behavior. However, the use of effective values limits the evaluation of the slab and weak layer properties from independent mechanical tests (e.g., Chap. 2). Considering other sources of dissipation in the slab, such as viscosity, or in the weak layer, such as plastic normal deformation induced by shear failure, may bridge the gap between stability models and mechanical testing of snow as a material.

- The stability models are based on fracture mechanics and mainly assess whether a fracture can initiate and propagate. In theory, they are deterministic: a crack initiates or propagates above a certain threshold on stress or crack length. In practice, we somehow adopt a probabilistic approach due to uncertainties in snow characterization and spatial variability. Implicitly, we assume that the distance to the critical threshold translates into a probability of occurrence of the process. First, it is unclear how the variability or uncertainty of the driving parameters translates into probabilities. For instance, Schweizer et al. [2008]; Gaume et al. [2013] demonstrated the so-called knock-down effect in slab modeling: the average strength value in a heterogeneous system is larger than the strength value of the equivalent homogeneous system. This knock-down effect is particularly relevant for avalanche release that partially follows the weakest-link theory [Weibull, 1939]. Second, the separated indicators of snow stability must be combined into one relevant indicator. Gaume and Reuter [2017]; Rosendahl and Weißgraeber [2020] recently introduced a coupled criterion for skier-triggered cracks within a deterministic mechanical approach. Within a probabilistic approach, this coupling remains to be done.

4.2 Machine learning of avalanche activity

The uncertainties related to atmospheric forcing, snowpack and mechanical modeling propagate to the estimated probability of avalanche release [e.g., Vernay et al., 2015; Lafaysse et al., 2017]. Moreover, avalanche release is a highly non-linear non-Lipschitzian phenomenon. A tiny deviation of the meteorological conditions, e.g., wind variations during snowfall, may lead to the formation of a thin weak layer which may cause the release of tons of snow. Without this weak layer, nothing would have probably happened. A pure physically-based approach to avalanche hazard assessment (Sect. 4.1.2) is interesting because it benefits from many developments from other research fields, and its results can be deciphered straightforwardly. However, this approach cannot correct systematic errors in the driving input. For instance, the absence of wind-drifted snow in snowpack modeling inevitably leads to a biased estimation of this avalanche problem by stability models relying solely on fracture mechanics and the simulated snow profiles. A

way to overcome this limitation is to use statistical tools or machine learning to identify critical situations rather than only snow physics and mechanics. An "extreme" strategy would be to learn the relation between avalanche activity (natural or potentially triggered) and time-series of meteorological conditions. This deep learning approach would somehow recover snow physics and mechanics. However, high-quality data do not exist in sufficient quantity to train this kind of model. Here we adopted an intermediate machine learning strategy. We learned the relation between avalanche activity and variables related to meteorological conditions, snow conditions, and snowpack stability.

4.2.1 Prediction of natural avalanche activity

Machine learning methods were already used to capture the complex link between snow cover variables and avalanche activity [e.g., Navarre et al., 1987; Gassner and Brabec, 2002; Kronholm et al., 2006; Pozdnoukhov et al., 2011; Hendrikx et al., 2014; Choubin et al., 2019; Mosavi et al., 2020] [Evin et al., 2021; Dkengne Sielenou et al., 2021]. These studies mainly used meteorological variables or bulk and simple snow variables (e.g., snow depth) to feed the machine learning. These variables are only surrogates for the true drivers of the avalanche formation. Our knowledge of avalanche formation and the associated stability models provide complementary non-linear information readily oriented towards avalanche formation. Using more advanced snow physics and mechanics simplifies the relation to be learned. This approach may increase the predictive power of machine learning on limited data. During the Ph.D. of L. Viallon-Galinier, we tried to predict the natural avalanche activity from the weather, snow, and stability conditions with machine learning. This ongoing work is briefly described below.

We first need to define an avalanche activity index. Avalanches can be classified by their release origin [International Commission on Snow - Ice, 1981]. Natural avalanches release spontaneously due to the natural evolution of the snowpack[1]. Triggered avalanches are released by an external trigger either on purpose (e.g., explosives) or accidentally (e.g., a skier). We focused on natural avalanches recorded in the Enquête Permanente sur les Avalanches (EPA). The EPA reports all the avalanches whose runout exceeded a specific threshold in approximately 3,000 pre-defined paths since the 1900s [Bourova et al., 2016]. The EPA inevitably corresponds to a biased sampling of avalanche activity (e.g., large avalanches close to human infrastructures), and human-based observations contain errors. To overcome these limitations, we focused on a smaller region, the upper valley of Haute-Maurienne, and a shorter period, 1958-2021. We considered EPA as the ground truth of avalanche activity in this zone. The binary target variable to be predicted daily was the occurrence of at least one avalanche in the domain subdivided into eight aspects and three elevation bands. We used Random Forests to predict the probability of avalanche occurrence.

The originality of our work was to investigate the added value of snow physics and mechanical analysis for predicting avalanche activity through machine learning. To this end, we tested different input variables to train our model: meteorological variables, bulk variables (mainly snow depth), stability indices and their time-derivatives or all variables. The model was trained and evaluated with a leave-one-year-out approach on these different groups of variables (Fig. 4.4). The model trained only with meteorological variables is as good as a random classifier. The models trained with bulk snow variables, stability indices, and stability indices with their time-derivatives become better and better. Using the stability indices and their derivatives leads to the

[1]Here, we considered avalanches triggered by a natural element (e.g., animal, cornice fall, or earthquake) as natural avalanches.

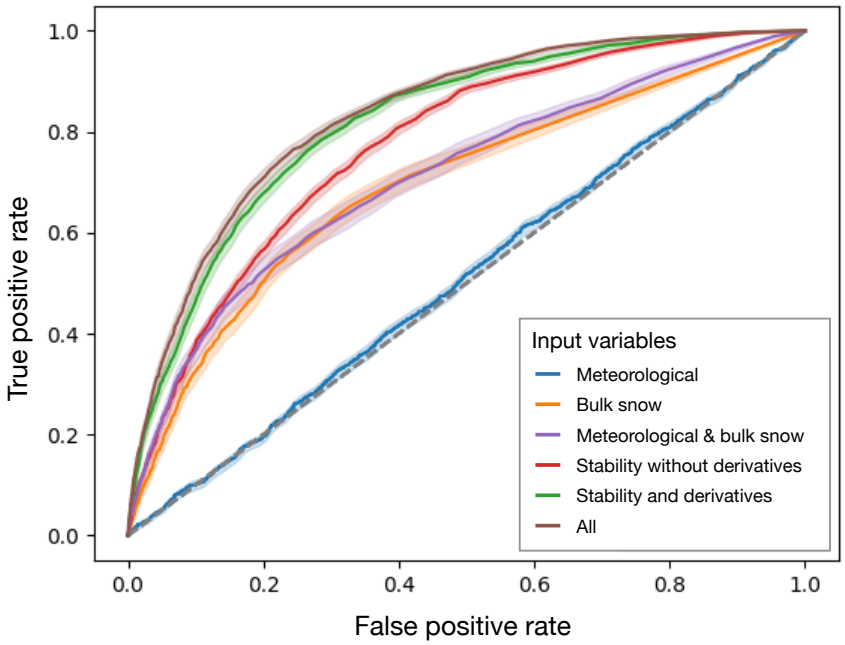

Figure 4.4: Performance of the machine learning model trained with different sets of variables. The Receiving Operating Characteristic (ROC) curve illustrates the diagnostic ability of the binary classifier, as its discrimination threshold on the probability of avalanche occurrence is varied. An optimal classifier would be characterized by a ROC point at (0,1). The ROC curve of a random classifier would be on the first bisector. The area between the first bisector and ROC curve quantifies how good the model is, compared to a random classifier. Shading around the ROC curves represents the uncertainty quantified by bootstrap on test years. Unpublished.

same performance as the one obtained with all variables. Stability indices and their derivatives thus contain all relevant information available in this dataset. These results show that stability indices are relevant for predicting avalanche-prone conditions and summarizing the information produced by meteorological and snow cover models. However, the obtained scores remained rather low[2]: true positive rate of 76.6%, false positive rate of 24.5%. In particular, among the predicted avalanche days, only a few (3.3%) were effectively characterized by an avalanche release. These scores illustrate the pregnant difficulty in predicting avalanche occurrence with high spatio-temporal resolution. Besides, let us recall that EPA is one sampling of avalanche activity and may need to be complemented by other sources of avalanche activity records.

4.2.2 Assessment of avalanche danger

The European Avalanche Warning Services (EAWS) define the avalanche danger as a function of snowpack stability, its spatial distribution, and avalanche size. They describe the danger level on a five-level ordinal scale: low (1), moderate (2), considerable (3), high (4), and very high (5) [EAWS, 2018]. Although snow and avalanche researchers have developed numerous decision aid tools, assessment of avalanche danger remains mainly human-based. To forecast the avalanche danger for the next day, the forecasters examine data of heterogeneous nature, such as diverse field observations and the results of numerical weather prediction models and snowpack models [Coléou and Morin, 2018]. Besides, avalanche danger cannot be measured nor verified. The forecast avalanche danger is sometimes nowcast (prediction of the present state), but formal verification remains impossible [Schweizer and Föhn, 1996; Pérez-Guillén et al., 2022].

The absence of ground truth of the target variable renders machine-learning inapplicable to assess the avalanche danger. Therefore, previous attempts focused on direct observations of the avalanche activity (see Sect. 4.2.1). However, direct learning of the human-predicted avalanche danger remains of interest. Indeed, the trained model will learn to reproduce the biases and errors of the forecasters, but it will do it consistently. Indeed, consistency in applying the avalanche danger scale by individual forecasters is essential to avoid misunderstandings or misinterpretations by users [Murphy, 1993; Techel et al., 2018]. Techel et al. [2018] investigated the spatial consistency and bias in danger level across the European Alps. They observed that forecast danger levels agreed significantly less often when compared across forecast center boundaries (about 60%) than within (about 90%). In France, despite national coordination, the danger level exhibited significant apparent inconsistency across regional forecasting centers [Hagenmuller, 2019b]. This apparent inconsistency is partly due to spatial variability of avalanche climates [e.g., Haegeli and McClung, 2007] but also probably to the forecaster's subjective judgments based on the available but limited data and evidence. A machine-learning model trained on the forecast avalanche danger would somehow provide the "average" choice of all past forecasts and help smooth some inconsistencies.

We trained a random forest on the avalanche danger level forecast on 23 massifs of the French Alps for the period 1994[3] to 2018. This spatio-temporal domain represents about 66 000 data points. The input variables were composed of the snow conditions reanalyzed by the S2M model. We reduced the simulated snow profiles to a few snowpack properties related to the avalanche problems, namely new snow, wind-drifted snow, persistent weak layers, and wet snow [EAWS, 2017]. We selected five meteorological properties:

[2]Scores obtained for the optimal point of the ROC curve trained on all variables, i.e., the point closer to the optimal classifier (0,1).

[3]Avalanche forecasters from Météo-France started using the current five-level avalanche danger scale in 1994.

- Cumulative solid precipitation (kg m^{-2}).
- Cumulative liquid precipitation (kg m^{-2}).
- Average wind speed (m s^{-1}).
- Average wind direction projected along North ().
- Average wind direction projected along East ().

We computed these properties for three periods: the next 24 h, the past 24 h, and the past 72 h, to predict the danger level valid for the next 24 h. We also considered four different elevations (900, 1500, 2100, and 2700 m)[4] on flat terrain. We also selected five snow variables:

- Maximum of total snow height (m).
- Maximum ramsonde penetration[5] (m).
- Maximum of weak layer thickness (m). We define a weak layer as faceted crystals and depth hoar snow not under a melt-freeze crust (thickness > 5 cm) and at least under 10 cm of rounded grains-like snow and 30 cm of snow, but not under more than 150 cm of snow.
- Maximum of mean liquid mass water content (%).
- Maximum thickness of snow that already encountered some wetting (m).

We computed these properties for the next 24 h and their increase compared to the past 24 h and 48 h. We calculated these variables on four different elevations (900, 1500, 2100, and 2700 m) and four different aspects (N, E, S, W) on 40° slopes. Different regions do not react identically to the same snow conditions because of different slope distributions and habits between forecast centers. Thus we also include the number of the massif in the predictive variables. We ended with 301 predictive variables. These definitions might sound like a cuisine recipe, as usual in machine learning. The model was trained on all forecast regions simultaneously and evaluated with a leave-one-year-out strategy.

We did not conduct a detailed analysis of the model sensitivity to this selection of variables. However, we observed that all ten meteorological and snow properties had a non-negligible predictive power[6]. Figure 4.5 shows the distributions of the predicted probability of each danger level for the different observed forecast levels. The level with the highest predicted probability generally corresponds to the observed level. However, there is a substantial overlap between the boxplots. Indeed, if one selects the majority class as the model prediction, the prediction accuracy is only 60%. This accuracy increased with the period considered: higher in recent years compared to the first period when the forecasters started to use the current danger scale without formalized look-up tables. Pérez-Guillén et al. [2022] reached an accuracy of the predicted danger level of about 75% in Switzerland. They used snowpack simulations driven by measurements of meteorological stations. This difference with our simulations may partly explain the higher score but using observed weather data also hampers the application of the methodology of Pérez-Guillén et al. [2022] to predict the future. Indeed, in contrast to station measurement,

[4]Some french massifs are lower than 2700 m, for these, we replaced the value at 2700 m with the values at 2100 m

[5]This quantity corresponds to the height of soft snow at the snowpack surface

[6]The important variables ranked as follows: 1) snow precipitation, 2) height of already wet snow, 3) ram penetration, 4) weak layer thickness, 5) wind properties, etc.

S2M works in reanalysis, re-forecast (forecast conducted in the past), or forecast [Lafaysse et al., 2013]. Our methodology thus applies to real forecasts. With the choice of simple properties related to specific avalanche problems, identifying the key variables that drive the algorithm decision directly provides an indirect estimation of the dominant avalanche problem types (not shown). Overall, our results remain preliminary and need further evaluation. Machine learning did not help us gain any universal knowledge on avalanche formation. However, the finalization of this work may constitute the contribution with the highest short-term impact on the quality (increased consistency) of the avalanche bulletins produced by Météo-France.

4.3 Ongoing and future work

The CNRM strength in research about avalanche formation is the seamless modeling tools, from large-scale meteorological models to indicators of avalanche activity. Our contribution to the fundamental knowledge of avalanche formation at the slope scale remains limited compared to the one on snow mechanics at the snow material scale (e.g., Chaps. 2, 3). The planned future work will mainly exploit this strength.

The mission of the CEN is not only to gain knowledge about snow and avalanche but also to transfer this knowledge to operational services of Météo-France, such as avalanche forecasting services. This transfer can include constantly updating training content and developing new tools to be used in an operational context. This development is rather a engineering work and is not detailed here. However, we will adapt the methodology developed to assess natural avalanche activity and danger from simulated snow profiles for use in avalanche forecasting. Noticeably, the machine-learning-based prediction of the avalanche danger will also require much pedagogy for practical and relevant use of this expert-based indicator.

An essential perspective of my research will be to evaluate the evolution of avalanche activity with climate change. Indeed, the mountain environment and its cryospheric component (snow, glaciers, and permafrost) are particularly sensitive to climate warming. The Intergovernmental Panel on Climate Change (IPCC) states that "mountain hazards are expected to occur in the future at new locations and seasons" [Hock et al., 2019]. Studies on past avalanche activity exhibited various trends with climate change. Eckert et al. [2010, 2013] showed that the avalanche number has decreased, and their runout altitude has retreated upslope since the 1980s in the French Alps. Ballesteros-Cánovas et al. [2018] reported increased avalanche activity in some slopes of the Western Indian Himalayas over the past decades related to increased frequency of wet-snow conditions. Overall, available results remain rare and often inconclusive [Hock et al., 2019], probably because of the altitudinal dependence and confounding factors such as land-cover changes in avalanche terrain. Future projections are even scarcer. Only one study tried to quantify the future evolution of avalanche activity with climate change. Castebrunet et al. [2014] estimated a decrease of the natural avalanche activity by 20-30% in the French Alps for the end of the 21st century compared to the period 1960-1990, with the SRES A1B scenario within the CMIP3 framework. There is a societal need to produce future projections (currently missing) that will contribute to the sustainable development of mountain territories. We will try to produce projections of future avalanche activity in terms of avalanche numbers and avalanche problems. To this end, we will benefit from the modeling tools previously developed (this chapter) and the down-scaling of climatic projections on the French Alps [Verfaillie et al., 2017].

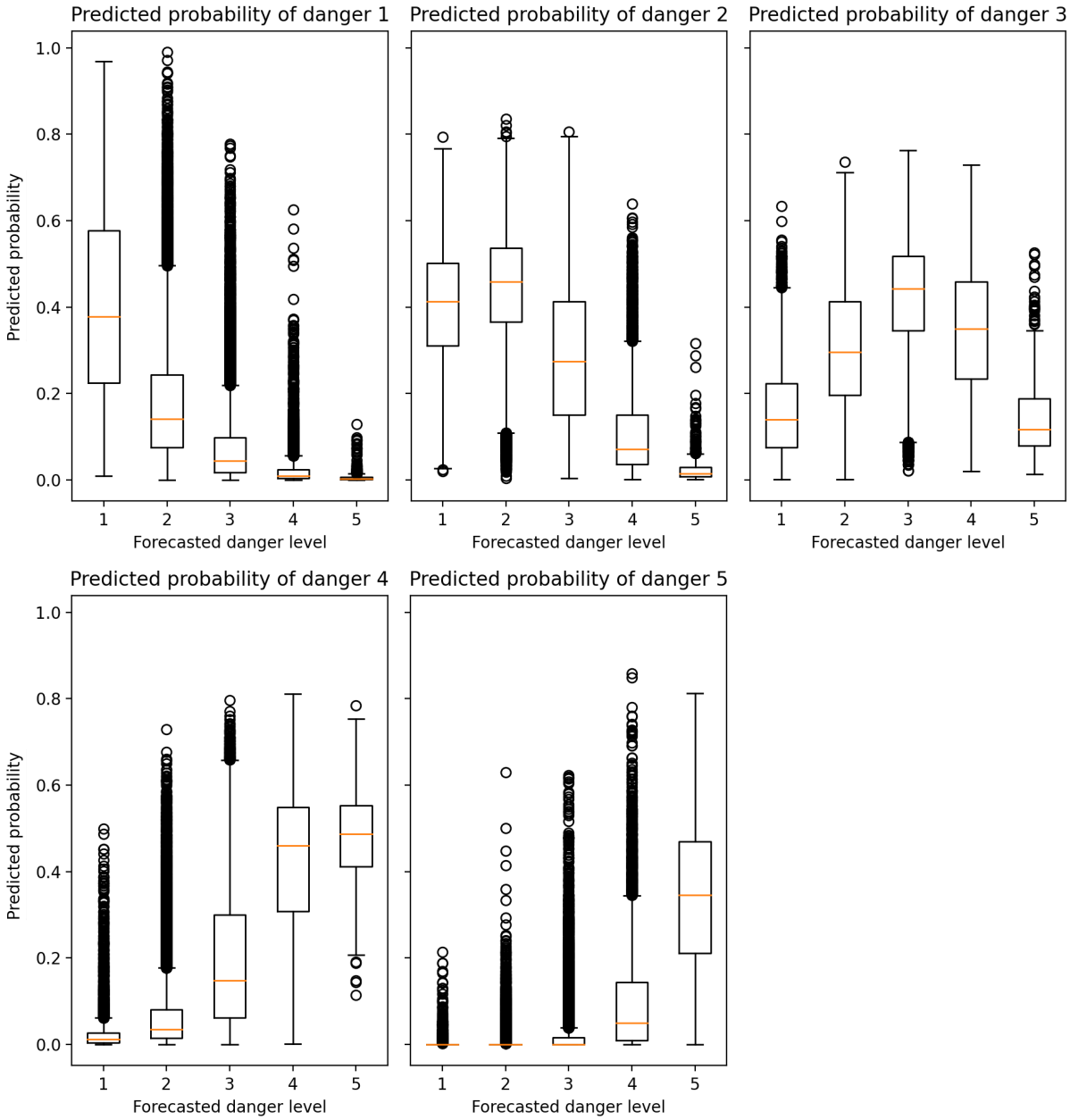

Figure 4.5: Performance of a Random Forest classifier of the forecast avalanche danger. Each subplot shows the predicted probability distribution of a given danger level as a function of the forecast (ground truth) avalanche danger level. The evaluation is performed with a leave-one-year-out strategy. The black boxes span the interquartile range from the first to the third quartile, with the orange horizontal line showing the median. The black whiskers show the range of observed values that fall within 1.5 times the interquartile range, and the black crosses are outliers above or below it. Unpublished.

Chapter 5

Conclusion and perspectives

Preamble

This HDR dissertation synthesizes research on snow mechanics I contributed to during the last eight years: from the underlying physics of processes relevant to snow mechanical behavior to more practical tools for avalanche prediction. My research focused on an object, snow, rather than a discipline but benefited from interactions with material science, mechanics, and statistics. It was pushed forward by the work of motivated students and mutual learning with scientific collaborators.

Even though snow is "just" composed of water, the co-existence of the three water phases in the snow leads to a fascinating and wide variety of microstructural patterns. This diversity and the numerous micromechanisms at play make snow mechanics a rich and open science. Besides, snow is a tangible object of study when enjoying time in the mountains. More broadly, a better understanding of snow directly impacts societal needs such as avalanche prevention, water supply, or climate change estimation, which is a source of motivation. I feel that "the more I learn, the more I realize how much I do not know" (A. Einstein), so in this chapter, I briefly summarize my research with a specific focus on the main directions of future work in the next five years.

Contents

5.1 Snow tomography

Tomography has become a standard tool to characterize snow microstructure. I contributed to this standardization by equipping my lab with a unique tomograph operating down to -30°C at a resolution of 5 microns and developing image processing tools to deal with this kind and quantity of data. The next step is to explore more systematically the diversity of snow microstructure. This step comprises the investigation of snow microstructure evolution under controlled temperature and stress conditions. This data would help us decipher the interactions of microscale processes and how they affect the overall snow microstructure and subsequent properties. Nature is generally more resourceful than lab experiments. We plan to bring tomography to the field to sample the diversity of natural snow microstructure and capture the complete snowpack stratigraphy. Here the goal is not only to capture the evolution of single snow samples under well-controlled conditions but also to understand how a layer evolves in interaction with adjacent layers and complex atmospheric forcing. Bringing tomography to the field (alpine and arctic) will require new equipment, sampling, scanning protocols, and paradigms in image processing.

5.2 Computational microscale modelling

A computational model can predict snow macroscopic properties from its microstructure and the ice-air properties. Thanks to high computing power, this strategy is now convenient to "measure" snow properties on fragile and small homogeneous snow samples, which would have been impossible with direct experiments. We developed computational models describing snow mechanics in the brittle regime. We took advantage of finite and discrete element models to reproduce and understand snow failure under different loading directions. We also investigated and quantified the effective diffusion properties of heat and water vapor in snow. One direction for future work is to exhaustively apply these models to all tomographic data available. These simulations would provide representative relations between microstructural proxies and snow properties, e.g., elastic modulus, failure envelope, and anti-crack failure energy. The second one is to explore regimes where the time dimension matters. In particular, we plan to investigate the visco-plastic behavior of snow within a computational model and include sintering processes in the mechanical models previously developed. These processes are essential to understanding how snow settles. Metamorphism also affects the mechanical evolution of snow microstructure at low strain rates. Microscale computational models of snow metamorphism already exist. We would need to couple them with mechanical ones.

5.3 Detailed snow stratigraphy

Even if we are close to measuring the seasonal snowpack evolution with tomography, this technique is not suited yet (and for a long time) for standard monitoring of the snowpack stratigraphy. The cone penetration test with a high resolution appears promising to capture profiles of snow microstructural characteristics quickly. We contributed a better understanding of the snow-cone interaction with experimental data and proposed statistical models to derive microstructural proxies from the penetration signal. One direction for future work is to use the computational model to provide quantitative relationships between penetration strength and other mechanical properties such as failure envelope or fracture energy or microstructural characteristics such as bond size and number. One may argue that a detailed description of the snowpack is useless given the high variability of the snowpack. First, science progresses by decomposing complex problems into simpler pieces. Second, we showed that a large part of the apparent stratigraphy variability is mainly related to the layer thickness variability (or of some specific layers). Even tiny layers can spread over large areas with little variability in the stratigraphy position. We developed a matching algorithm to track layers in different snowpack profiles. We will not work more on the algorithm. However, we will use it to benefit from high-resolution profiles of snow properties in different applications: registration of scanned snow samples in the stratigraphy, detailed evaluation of current and new snowpack models, synthesis of numerous profiles produced by ensemble gridded simulation of the snow conditions.

5.4 Larger spatial and temporal scales: avalanche and climate change

Knowledge of the processes involved in avalanche formation has increased significantly over the past decades. In particular, various physically-based models were developed to assess the likelihood of avalanche formation given a vertical profile of snow mechanical properties. We implemented these models in the snowpack modeling chain S2M to benefit from the capacity of this

chain to work in reanalysis, short-term forecasting, and long-term projection mode. We used these models to quantify the role of dust-on-snow events on the snowpack stability or to define avalanche climate from avalanche problems distribution. Besides, the approach based on pure mechanical theory cannot correct errors or bias in meteorological inputs or snowpack models. Therefore, we built machine learning models to statistically relate the stability indices to direct observation of avalanche activity or expert-based assessment of the danger. These numerical tools provide a way to produce short-term forecasts and long-term projections of avalanche hazard. One goal will be to provide these tools in an ergonomic manner to avalanche forecasters of Météo-France. An essential perspective of my research will also be to evaluate the evolution of avalanche activity with climate change. Indeed, available results remain rare and often inconclusive, and there is a societal need to produce future projections, currently missing, that will contribute to the sustainable development of mountain territories.

Bibliography

Ai J, Chen JF, Rotter JM and Ooi JY (2011) Assessment of rolling resistance models in discrete element simulations. *Powder Technology*, **206**(3), 269–282 (doi: 10.1016/j.powtec.2010.09.030)

Alvarez RE and Macovski A (1976) Energy-selective reconstructions in X-ray computerised tomography. *Physics in Medicine and Biology*, **21**(5), 002 (doi: 10.1088/0031-9155/21/5/002)

Ancey C (2006) *Dynamique des avalanches*. PPUR presses polytechniques, Lausanne, Suisse, ISBN 2-88074-648-5

Andò E, Hall SA, Viggiani G, Desrues J and Bésuelle P (2012) Grain-scale experimental investigation of localised deformation in sand: A discrete particle tracking approach. *Acta Geotechnica*, **7**(1), 1–13 (doi: 10.1007/s11440-011-0151-6)

Arnaud L, Picard G, Champollion N, Domine F, Gallet JC, Lefebvre E, Fily M and Barnola JM (2011) Measurement of vertical profiles of snow specific surface area with a 1 cm resolution using infrared reflectance: instrument description and validation. *Journal of Glaciology*, **57**(201), 17–29 (doi: 10.3189/002214311795306664)

Auriault Jl (1991) Heterogeneous medium. Is an equivalent macroscopic description possible? *International Journal of Engineering Science*, **29**(7), 785–795 (doi: 10.1016/0020-7225(91)90001-J)

Bader H (1962) The physics and mechanics of snow as a material. Technical report, Cold Regions Research and Engineering Laboratory (US), Hanover, NH, USA

Bader H and Niggli P (1939) *Der Schnee und seine Metamorphose: Erste Ergebnisse und Anwendungen einer systematischen Untersuchung der alpinen Winterschneedecke. Durchgeführt von der Station Weissfluhjoch-Davos der Schweiz. Schnee- und Lawinenforschungskommission 1934-1938*. Kümmerly and Frey

Baker I (2019) Microstructural characterization of snow, firn and ice. *Philosophical Transactions of the Royal Society A: Mathematical, Physical and Engineering Sciences*, **377**(2146) (doi: 10.1098/rsta.2018.0162)

Ballesteros-Cánovas JA, Trappmann D, Madrigal-González J, Eckert N and Stoffel M (2018) Climate warming enhances snow avalanche risk in the Western Himalayas. *Proceedings of the National Academy of Sciences of the United States of America*, **115**(13), 3410–3415 (doi: 10.1073/pnas.1716913115)

Barnola JM, Raynaud D, Korotkevich YS and Lorius C (1987) Vostok ice core provides 160,000-year record of atmospheric CO2. *Nature*, **329**(6138), 408–414 (doi: 10.1038/329408a0)

Bebi P, Seidl R, Motta R, Fuhr M, Firm D, Krumm F, Conedera M, Ginzler C, Wohlgemuth T and Kulakowski D (2017) Changes of forest cover and disturbance regimes in the mountain forests of the Alps. *Forest Ecology and Management*, **388**, 43–56 (doi: 10.1016/j.foreco.2016.10.028)

Blackford JR (2007) Sintering and microstructure of ice: a review. *Journal of Physics D: Applied Physics*, **40**(21), R355–R385 (doi: 10.1088/0022-3727/40/21/R02)

Blackwell JH (1954) A Transient-Flow Method for Determination of Thermal Constants of Insulating Materials in Bulk Part I—Theory. *Journal of Applied Physics*, **25**(2), 137–144 (doi: 10.1063/1.1721592)

Bobillier G, Bergfeld B, Dual J, Gaume J, van Herwijnen A and Schweizer J (2021) Micromechanical insights into the dynamics of crack propagation in snow fracture experiments. *Scientific Reports*, **11**(1), 1–15 (doi: 10.1038/s41598-021-90910-3)

Bourova E, Maldonado E, Leroy JB, Alouani R, Eckert N, Bonnefoy M and Deschatres M (2016) A new web-based system to improve the monitoring of snow avalanche hazard in France. *Natural Hazards and Earth System Sciences*, **16**(5), 1205–1216 (doi: 10.5194/nhess-16-1205-2016)

Boykov Y and Funka-Lea G (2006) Graph cuts and efficient ND image segmentation. *International Journal of Computer Vision*, **70**(2), 109–131 (doi: 10.1007/s11263-006-7934-5)

Boykov Y and Kolmogorov V (2004) An experimental comparison of min-cut/max-flow algorithms for energy minimization in vision. *IEEE Transactions on Pattern Analysis and Machine Intelligence*, **26**(9), 1124–1137 (doi: 10.1109/TPAMI.2004.60)

Brenne EO, Dahl VA and Jørgensen PS (2021) A physical model for microstructural characterization and segmentation of 3D tomography data. *Materials Characterization*, **171** (doi: 10.1016/j.matchar.2020.110796)

Bretin E, Denis R, Flin F, Oudet E and Roussillon T (2015) DigitalSnow - ANR-11-BS02-009 Deliverable 4 Discrete-Continuous approach for deformable partitions. Technical report, ANR-11-BS02-009

Bromiley PA and Thacker NA (2008) Multi-dimensional Medical Image Segmentation with Partial Volume and Gradient Modelling. *Annals of the BMVA*, **2008**(2), 1–23

Brousseau P, Seity Y, Ricard D and Léger J (2016) Improvement of the forecast of convective activity from the AROME-France system. *Quarterly Journal of the Royal Meteorological Society*, **142**(699), 2231–2243 (doi: 10.1002/qj.2822)

Brown RL (1989) Perspective on mechanical properties of snow. In *Proceedings of the 1st International Conference on Snow Engineering*, 502–503, California, USA

Brun E (2006) *Etude et modélisation des interactions neige-climat*. Ph.D. thesis, Université Paul Sabatier

Brun E, Martin E, Simon V, Gendre C and Coléou C (1989) An Energy and Mass Model of Snow Cover Suitable for Operational Avalanche Forecasting. *Journal of Glaciology*, **35**(121), 333–342 (doi: 10.1017/S0022143000009254)

Bruns S, Stipp SL and Sørensen HO (2017) Statistical representative elementary volumes of porous media determined using greyscale analysis of 3D tomograms. *Advances in Water Resources*, **107**, 32–42 (doi: 10.1016/j.advwatres.2017.06.002)

Brzoska JB, Coléou C, Lesaffre B, Borel S, Brissaud O, Lüdwig W, Boller E and Baruchel J (1999) 3D visualization of snow samples by microtomography at low temperature. *ESRF Newsletter*, **32**(22-23), 112

Burr A, Noël W, Trecourt P, Bourcier M, Gillet-Chaulet F, Philip A and Martin CL (2017) The anisotropic contact response of viscoplastic monocrystalline ice particles. *Acta Materialia*, **132**, 576–585 (doi: 10.1016/j.actamat.2017.04.069)

Burr A, Lhuissier P, Martin CL and Philip A (2019) In situ X-ray tomography densification of firn: The role of mechanics and diffusion processes. *Acta Materialia*, **167**, 210–220 (doi: https://doi.org/10.1016/j.actamat.2019.01.053)

Calonne N, Flin F, Morin S, Lesaffre B, Rolland Du Roscoat S, Geindreau C and Rolland du Roscoat S (2011) Numerical and experimental investigations of the effective thermal conductivity of snow. *Geophysical Research Letters*, **38**(23), L23501 (doi: 10.1029/2011GL049234)

Calonne N, Flin F, Geindreau C, Lesaffre B and Rolland du Roscoat S (2014a) Study of a temperature gradient metamorphism of snow from 3-D images: time evolution of microstructures, physical properties and their associated anisotropy. *The Cryosphere*, **8**(6), 2255–2274 (doi: 10.5194/tc-8-2255-2014)

Calonne N, Geindreau C and Flin F (2014b) Macroscopic modeling for heat and water vapor transfer in dry snow by homogenization. *Journal of Physical Chemistry B*, **118**(47), 13393–13403 (doi: 10.1021/jp5052535)

Calonne N, Flin F, Lesaffre B, Dufour A, Roulle J, Pugliese P, Philip A, Lahoucine F, Geindreau C, Panel J, Rolland du Roscoat S and Charrier P (2015) CellDyM : A room temperature operating cryogenic cell for the dynamic monitoring of snow metamorphism by time-lapse X-ray microtomography. *Geophysical Research Letters*, **42**, 3911–3918 (doi: 10.1002/2015GL063541. Received)

Calonne N, Richter B, Löwe H, Cetti C, Ter Schure J, van Herwijnen A, Fierz C, Jaggi M and Schneebeli M (2020) The RHOSSA campaign: Multi-resolution monitoring of the seasonal evolution of the structure and mechanical stability of an alpine snowpack. *The Cryosphere*, **14**(6), 1829–1848 (doi: 10.5194/tc-14-1829-2020)

Capelli A, Reiweger I and Schweizer J (2020) Studying Snow Failure With Fiber Bundle Models. *Frontiers in Physics*, **8**(July), 1–12 (doi: 10.3389/fphy.2020.00236)

Castebrunet H, Eckert N, Giraud G, Durand Y and Morin S (2014) Projected changes of snow conditions and avalanche activity in a warming climate: the French Alps over the 2020–2050 and 2070–2100 periods. *The Cryosphere*, **8**(5), 1673–1697 (doi: 10.5194/tc-8-1673-2014)

Chandel C, Srivastava PK and Mahajan P (2015) Determination of failure envelope for faceted snow through numerical simulations. *Cold Regions Science and Technology*, **116**, 56–64 (doi: 10.1016/j.coldregions.2015.04.009)

Chen S and Baker I (2010a) Evolution of individual snowflakes during metamorphism. *Journal of Geophysical Research*, **115**(D21), 1–9 (doi: 10.1029/2010JD014132)

Chen S and Baker I (2010b) Structural evolution during ice-sphere sintering. *Hydrological Processes*, **24**(14), 2034–2040 (doi: 10.1002/hyp.7787)

Choi H, Haynor D and Kim Y (1991) Partial volume tissue classification of multichannel magnetic resonance images-a mixel model. *IEEE Transactions on Medical Imaging*, **10**(3), 395–407 (doi: 10.1109/42.97590)

Chomette L, Bacardit M, Gavaldà J, Dumont M, Tuzet F and Moner I (2016) Effects of Saharan Dust Outbreaks on the Snow Stability in the Pyrenees. In *Proceedings of the International Snow Science Workshop*, 942–948, Breckenridge, Colorado, USA, 3-7 October 2016

Choubin B, Borji M, Mosavi A, Sajedi-Hosseini F, Singh VP and Shamshirband S (2019) Snow avalanche hazard prediction using machine learning methods. *Journal of Hydrology*, **577**, 123929 (doi: 10.1016/j.jhydrol.2019.123929)

Cluzet B, Revuelto J, Lafaysse M, Tuzet F, Cosme E, Picard G, Arnaud L and Dumont M (2020) Towards the assimilation of satellite reflectance into semi-distributed ensemble snowpack simulations. *Cold Regions Science and Technology*, **170**(October 2019), 102918 (doi: 10.1016/j.coldregions.2019.102918)

Coeurjolly D and Montanvert A (2007) Optimal separable algorithms to compute the reverse euclidean distance transformation and discrete medial axis in arbitrary dimension. *IEEE Transactions on Pattern Analysis and Machine Intelligence*, **29**(3), 437–448 (doi: 10.1109/TPAMI.2007.54)

Colbeck S (1975) Grain and bond growth in wet snow. *International Association of Hydrological Sciences Publication*, **114**(Symposium of Grindelwald 1974 – Snow Mechanics), 51–61

Colbeck S (1982) An overview of seasonal snow metamorphism. *Reviews of Geophysics*, **20**(1), 45 (doi: 10.1029/RG020i001p00045)

Colbeck S (1997) A Review of Sintering in Seasonal Snow. Technical Report December, U.S. Army Cold Regions Research and Engineering Laboratory, Hanover

Coléou C and Morin S (2018) Vingt-cinq ans de prévision du risque d'avalanche à Météo-France. *La Météorologie*, **100**, 79–84 (doi: 10.4267/2042/65147)

Coléou C, Lesaffre B, Brzoska JB, Ludwig W and Boller E (2001) Three-dimensional snow images by X-ray microtomography. *Annals of Glaciology*, **32**(1), 75–81 (doi: 10.3189/172756401781819418)

Comola F, Kok JF, Gaume J, Paterna E and Lehning M (2017) Fragmentation of wind-blown snow crystals. *Geophysical Research Letters*, **44**(9), 4195–4203 (doi: 10.1002/2017GL073039)

Cundall PA and Strack ODL (1979) A discrete numerical model for granular assemblies. *Geotechnique*, **29**(1), 47–65 (doi: 10.1680/geot.1979.29.1.47)

de Montmollin V (1982) Shear Test on Snow Explained by Fast Metamorphism. *Journal of Glaciology*, **28**(98), 187–198 (doi: 10.3189/S0022143000011898)

DeBeer CM and Pomeroy JW (2017) Influence of snowpack and melt energy heterogeneity on snow cover depletion and snowmelt runoff simulation in a cold mountain environment. *Journal of Hydrology*, **553**, 199–213 (doi: 10.1016/j.jhydrol.2017.07.051)

Decharme B, Boone A, Delire C and Noilhan J (2011) Local evaluation of the Interaction between Soil Biosphere Atmosphere soil multilayer diffusion scheme using four pedotransfer functions. *Journal of Geophysical Research*, **116**(D20), D20126 (doi: 10.1029/2011JD016002)

Domine F, Bock J, Morin S and Giraud G (2011) Linking the effective thermal conductivity of snow to its shear strength and density. *Journal of Geophysical Research*, **116**(F4), F04027 (doi: 10.1029/2011JF002000)

Dumont M (2017) *On the colour of snow: measurements, modelling and applications*. Ph.D. thesis, Université de Toulouse

Dumont M, Tuzet F, Gascoin S, Picard G, Kutuzov S, Lafaysse M, Cluzet B, Nheili R and Painter TH (2020) Accelerated Snow Melt in the Russian Caucasus Mountains After the Saharan Dust Outbreak in March 2018. *Journal of Geophysical Research: Earth Surface*, **125**(9), e2020JF005641 (doi: 10.1029/2020JF005641)

Durand Y, Laternser M, Giraud G, Etchevers P, Lesaffre B and Mérindol L (2009) Reanalysis of 44 Yr of Climate in the French Alps (1958–2002): Methodology, Model Validation, Climatology, and Trends for Air Temperature and Precipitation. *Journal of Applied Meteorology and Climatology*, **48**(3), 429–449 (doi: 10.1175/2008JAMC1808.1)

EAWS (2017) EAWS - Avalanche problems

EAWS (2018) EAWS - Avalanche danger scale

Eckert N, Baya H and Deschatres M (2010) Assessing the response of snow avalanche runout altitudes to climate fluctuations using hierarchical modeling: Application to 61 winters of data in France. *Journal of Climate*, **23**(12), 3157–3180 (doi: 10.1175/2010JCLI3312.1)

Eckert N, Keylock CJ, Castebrunet H, Lavigne A and Naaim M (2013) Temporal trends in avalanche activity in the French Alps and subregions: from occurrences and runout altitudes to unsteady return periods. *Journal of Glaciology*, **59**(213), 93–114 (doi: 10.3189/2013JoG12J091)

Fierz C, Durand R, Etchevers Y, Greene P, McClung DM, Nishimura K, Satyawali PK and Sokratov SA (2009) The international classification for seasonal snow on the ground. Technical report, IHP-VII Technical Documents in Hydrology N83, IACS Contribution N1, UNESCO-IHP, Paris

Flin F (2004) *Description physique des métamorphoses de la neige à partir d'images de microstructures 3D naturelles obtenues par microtomographie X*. Ph.D. thesis, Université de Grenoble 1

Flin F and Brzoska JB (2008) The temperature-gradient metamorphism of snow: vapour diffusion model and application to tomographic images. *Annals of Glaciology*, **49**(1), 17–21 (doi: 10.3189/172756408787814834)

Flin F, Brzoska JB, Lesaffre B, Coléou C and Pieritz RA (2003) Full three-dimensional modelling of curvature-dependent snow metamorphism: first results and comparison with experimental tomographic data. *Journal of Physics D: Applied Physics*, **36**(10A), A49–A54 (doi: 10.1088/0022-3727/36/10A/310)

Flin F, Budd WF, Coeurjolly D, Pieritz RA, Lesaffre B, Coléou C, Lamboley P, Teytaud F, Vignoles GL and Delesse JF (2005) Adaptive estimation of normals and surface area for discrete 3-D objects: application to snow binary data from X-ray tomography. *IEEE Transactions on Image Processing*, **14**(5), 585–596 (doi: 10.1109/TIP.2005.846021)

Floyer JA and Jamieson J (2010) Rate-effect experiments on round-tipped penetrometer insertion into uniform snow. *Journal of Glaciology*, **56**(198), 664–672 (doi: 10.3189/002214310793146322)

Föhn PMB (1987a) The Rutschblock as a practical tool for slope stability evaluation. In *Avalanche Formation, Movement, and Effects, Davos Symposium*, 223–228, IAHS Publication 162

Föhn PMB (1987b) The stability index and various triggering mechanisms. *International Association of Hydrological Sciences Publication*, **162**(Symposium at Davos 1986 — Avalanche Formation, Movement and Effects), 195–214

Fourteau K, Gillet-Chaulet F, Martinerie P and Faïn X (2020) A Micro-Mechanical Model for the Transformation of Dry Polar Firn Into Ice Using the Level-Set Method. *Frontiers in Earth Science*, **8**, 101 (doi: 10.3389/feart.2020.00101)

Freitag J, Kipfstuhl S and Laepple T (2013) Core-scale radioscopic imaging: a new method reveals density–calcium link in Antarctic firn. *Journal of Glaciology*, **59**(218), 1009–1014 (doi: 10.3189/2013JoG13J028)

Gassner M and Brabec B (2002) Nearest neighbour models for local and regional avalanche forecasting. *Natural Hazards and Earth System Sciences*, **2**(3/4), 247–253 (doi: 10.5194/nhess-2-247-2002)

Gaume J (2013) *Prédétermination des hauteurs de départ d'avalanches.* Ph.D. thesis, Université de Grenoble

Gaume J and Reuter B (2017) Assessing snow instability in skier-triggered snow slab avalanches by combining failure initiation and crack propagation. *Cold Regions Science and Technology*, **144**(June), 6–15 (doi: 10.1016/j.coldregions.2017.05.011)

Gaume J, Chambon G, Eckert N and Naaim M (2013) Influence of weak-layer heterogeneity on snow slab avalanche release: application to the evaluation of avalanche release depths. *Journal of Glaciology*, **59**(215), 423–437 (doi: 10.3189/2013JoG12J161)

Gaume J, Gast T, Teran J, van Herwijnen A and Jiang C (2018) Dynamic anticrack propagation in snow. *Nature Communications*, **9**(1) (doi: 10.1038/s41467-018-05181-w)

Gauthier D and Jamieson J (2006) Towards a field test for fracture propagation propensity in weak snowpack layers. *Journal of Glaciology*, **52**(176), 164–168 (doi: 10.3189/172756506781828962)

Gélébart L and Dérouillat J (2017) Simulations FFT massivement parallèles en mécanique des matériaux hétérogènes. In *CSMA 2017, 13eme Colloque National en Calcul des Structures*, 1–8

Gerling B, Löwe H and van Herwijnen A (2017) Measuring the Elastic Modulus of Snow. *Geophysical Research Letters*, **44**(21), 088–11 (doi: 10.1002/2017GL075110)

Giraud G (1992) MEPRA an expert system for avalanche risk forecasting. In *Proceedings of the International Snow Science Workshop*, 97–104, Breckenridge, Colorado, USA

Good W (1987) Thin sections, serial cuts and 3D analysis of snow. *International Association of Hydrological Sciences Publication*, **162**(Symposium at Davos 1986 — Avalanche Formation, Movement and Effects), 35–47

Granger R, Flin F, Ludwig W, Hammad I and Geindreau C (2021) Orientation selective grain sublimation–deposition in snow under temperature gradient metamorphism observed with diffraction contrast tomography. *The Cryosphere*, **15**(9), 4381–4398 (doi: 10.5194/tc-15-4381-2021)

Greilinger M and Kasper-Giebl A (2021) Saharan Dust Records and Its Impact in the European Alps (doi: 10.1093/acrefore/9780190228620.013.827)

Gubler H (1978) Determination of the Mean Number of Bonds per snow grain And of the Dependence of the Tensile Strength of Snow on Stereological Parameters. *Journal of Glaciology*, **20**(83), 329–341 (doi: 10.3189/S0022143000013885)

Gubler H and Rychetnik J (1991) Effects of forests near the timberline on avalanche formation. In *International Association of Hydrological Sciences Publication*, 19–38, ISBN 0947571183

Habermann M, Schweizer J and Jamieson J (2008) Influence of snowpack layering on human-triggered snow slab avalanche release. *Cold Regions Science and Technology*, **54**(3), 176–182 (doi: 10.1016/j.coldregions.2008.05.003)

Haegeli P and McClung DM (2007) Expanding the snow-climate classification with avalanche-relevant information: initial description of avalanche winter regimes for southwestern Canada. *Journal of Glaciology*, **53**(181), 266–276 (doi: 10.3189/172756507782202801)

Hansen AC (2019) Revisiting the vapor diffusion coefficient in dry snow. *The Cryosphere Discussions*, **2019**, 1–27 (doi: 10.5194/tc-2019-143)

Hansen AC and Foslien WE (2015) A macroscale mixture theory analysis of deposition and sublimation rates during heat and mass transfer in dry snow. *The Cryosphere*, **9**(5), 1857–1878 (doi: 10.5194/tc-9-1857-2015)

Hasler M, Schindelwig K, Mayr B, Knoflach C, Rohm S, van Putten J and Nachbauer W (2016) A Novel Ski–Snow Tribometer and its Precision. *Tribology Letters*, **63**(3), 33 (doi: 10.1007/s11249-016-0719-2)

Hazanov S (1999) On apparent properties of nonlinear heterogeneous bodies smaller than the representative volume. *Acta Mechanica*, **134**(3-4), 123–134 (doi: 10.1007/BF01312651)

Hazanov S and Huet C (1994) Order relationships for boundary conditions effect in heterogeneous bodies smaller than the representative volume. *Journal of the Mechanics and Physics of Solids*, **42**(12), 1995–2011 (doi: 10.1016/0022-5096(94)90022-1)

Heggli M, Frei E and Schneebeli M (2009) Snow replica method for three-dimensional X-ray microtomographic imaging. *Journal of Glaciology*, **55**(192), 631–639 (doi: 10.3189/002214309789470932)

Heierli J, Gumbsch P and Zaiser M (2008) Anticrack Nucleation as Triggering Mechanism for Snow Slab Avalanches. *Science*, **321**, 240–243 (doi: 10.1126/science.1153948)

Hendrikx J, Murphy M and Onslow T (2014) Classification trees as a tool for operational avalanche forecasting on the Seward Highway, Alaska. *Cold Regions Science and Technology*, **97**, 113–120 (doi: 10.1016/j.coldregions.2013.08.009)

Herla F, Haegeli P and Mair P (2022) A data exploration tool for averaging and accessing large data sets of snow stratigraphy profiles useful for avalanche forecasting. *The Cryosphere*, **16**(8), 3149–3162 (doi: 10.5194/tc-16-3149-2022)

Hill R (1963) Elastic properties of reinforced solids: Some theoretical principles. *Journal of the Mechanics and Physics of Solids*, **11**(5), 357–372 (doi: 10.1016/0022-5096(63)90036-X)

Hobbs PV and Mason BJ (1964) The sintering and adhesion of Ice. *Philosophical Magazine*, **9**(98), 181–197 (doi: 10.1080/14786436408229184)

Hock R, Rasul G, Adler C, Cáceres B, Gruber S, Hirabayashi Y, Jackson M, Kääb A, Kang S, Kutuzov S, Milner A, Molau U, Morin S, Orlove B and Steltzer H (2019) High Mountain Areas. In HO Pörtner, D Roberts, V Masson-Delmotte, P Zhai, M Tignor, E Poloczanska, K Mintenbeck, A Alegría, M Nicolai, A Okem, J Petzold, B Rama and N Weyer (eds.), *IPCC Special Report on the Ocean and Cryosphere in a Changing Climate*, 131–202, Cambridge University Press, Cambridge, UK and New York, NY, USA (doi: 10.1017/9781009157964.004)

Hogue C (1998) Shape representation and contact detection for discrete element simulations of arbitrary geometries. *Engineering Computations*, **15**(3), 374–390 (doi: 10.1108/02644409810208525)

Iassonov P, Gebrenegus T and Tuller M (2009) Segmentation of X-ray computed tomography images of porous materials: A crucial step for characterization and quantitative analysis of pore structures. *Water Resources Research*, **45**(9), W09415 (doi: 10.1029/2009WR008087)

International Commission on Snow - Ice (1981) *Avalanche Atlas: Illustrated International Avalanche*. Unesco, International Institute for Educational Planning

Itakura F (1975) Minimum prediction residual principle applied to speech recognition. *IEEE Transactions on Acoustics, Speech, and Signal Processing*, **23**(1), 67–72 (doi: 10.1109/TASSP.1975.1162641)

Jacobsen A, de Miranda Azevedo R, Juty N, Batista D, Coles S, Cornet R, Courtot M, Crosas M, Dumontier M, Evelo CT, Goble C, Guizzardi G, Hansen KK, Hasnain A, Hettne K, Heringa J, Hooft RW, Imming M, Jeffery KG, Kaliyaperumal R, Kersloot MG, Kirkpatrick CR, Kuhn T, Labastida I, Magagna B, McQuilton P, Meyers N, Montesanti A, van Reisen M, Rocca-Serra P, Pergl R, Sansone SA, da Silva Santos LOB, Schneider J, Strawn G, Thompson M, Waagmeester A, Weigel T, Wilkinson MD, Willighagen EL, Wittenburg P, Roos M, Mons B and Schultes E (2020) FAIR Principles: Interpretations and Implementation Considerations. *Data Intelligence*, **2**(1-2), 10–29 (doi: 10.1162/dint{_}r{_}00024)

Jaeger J (1956) Conduction of Heat in an Infinite Region Bounded Internally by a Circular Cylinder of a Perfect Conductor. *Australian Journal of Physics*, **9**(2), 167 (doi: 10.1071/PH560167)

Jamieson J and Johnston CD (1990) In-Situ Tensile Tests of Snow-Pack Layers. *Journal of Glaciology*, **36**(122), 102–106 (doi: 10.3189/S002214300000561X)

Jamieson J and Johnston CD (1992) A fracture-arrest model for unconfined dry slab avalanches. *Canadian Geotechnical Journal*, **29**(1), 61–66 (doi: 10.1139/t92-007)

Jamriska O, Sykora D and Hornung A (2012) Cache-efficient graph cuts on structured grids. In *2012 IEEE Conference on Computer Vision and Pattern Recognition*, 3673–3680, IEEE, ISBN 978-1-4673-1228-8, ISSN 10636919 (doi: 10.1109/CVPR.2012.6248113)

Johnson JB (2003) A statistical micromechanical theory of cone penetration in granular materials. Technical Report February, Cold Regions Research and Engineering Laboratory (CRREL)

Johnson JB and Schneebeli M (1999) Characterizing the microstructural and micromechanical properties of snow. *Cold Regions Science and Technology*, **30**(1-3), 91–100 (doi: 10.1016/S0165-232X(99)00013-0)

Kaempfer TU and Plapp M (2009) Phase-field modeling of dry snow metamorphism. *Physical Review E*, **79**(3), 031502 (doi: 10.1103/PhysRevE.79.031502)

Kaempfer TU, Schneebeli M and Sokratov SA (2005) A microstructural approach to model heat transfer in snow. *Geophysical Research Letters*, **32**(21), 1–5 (doi: 10.1029/2005GL023873)

Kaempfer TU, Hopkins MA and Perovich DK (2007) A three-dimensional microstructure-based photon-tracking model of radiative transfer in snow. *Journal of Geophysical Research*, **112**(D24), D24113 (doi: 10.1029/2006JD008239)

Keeler CM and Weeks WF (1968) Investigations Into the Mechanical Properties of Alpine Snow-Packs. *Journal of Glaciology*, **7**(50), 253–271 (doi: 10.3189/S0022143000031038)

Kerbrat M, Pinzer BR, Huthwelker T, Gäggeler HW, Ammann M and Schneebeli M (2008) Measuring the specific surface area of snow with X-ray tomography and gas adsorption: comparison and implications for surface smoothness. *Atmospheric Chemistry and Physics*, **8**(5), 1261–1275 (doi: 10.5194/acp-8-1261-2008)

Kingery WD (1960) Regelation, surface diffusion, and ice sintering. *Journal of Applied Physics*, **833**(5), 833–838 (doi: 10.1063/1.1735704)

Köchle B and Schneebeli M (2014) Three-dimensional microstructure and numerical calculation of elastic properties of alpine snow with a focus on weak layers. *Journal of Glaciology*, **60**(222), 705–713 (doi: 10.3189/2014JoG13J220)

Kraft D (1988) A software package for sequential quadratic programming. Technical report, DLR German Aerospace Center - institute for Flight Mechanics, Köln, Germany

Krol QE (2017) *Upscaling the evolution of snow microstructure : From 4D image analysis to rigorous models*. Ph.D. thesis, Ecole Polytechnique Fédérale de Lausanne, Lausanne, Suisse (doi: 10.5075/epfl-thesis-7996)

Krol QE and Löwe H (2016) Analysis of local ice crystal growth in snow. *Journal of Glaciology*, **62**(232), 378–390 (doi: 10.1017/jog.2016.32)

Kronholm K, Schneebeli M and Schweizer J (2004) Spatial variability of micropenetration resistance in snow layers on a small slope. *Annals of Glaciology*, **38**(1), 202–208 (doi: 10.3189/172756404781815257)

Kronholm K, Vikhamar-Schuler D, Jaedicke C, Isaksen K, Sorteberg A and Kristensen K (2006) Forecasting snow avalanche days from meteorological data using classification trees; Grasdalen, Western Norway. In *Proceedings of the International Snow Science Workshop*, 786–795, Citeseer, Telluride, Colorado, USA (doi: 10.1.1.855.5195)

Kruggel-Emden H, Rickelt S, Wirtz S and Scherer V (2008) A study on the validity of the multi-sphere Discrete Element Method. *Powder Technology*, **188**(2), 153–165 (doi: 10.1016/j.powtec.2008.04.037)

Kuroiwa D (1961) A Study of Ice Sintering. *Tellus*, **13**(2), 252–259 (doi: 10.3402/tellusa.v13i2.9450)

LaChapelle ER (1977) Snow Avalanches: A review of Current Research and Applications. *Journal of Glaciology*, **19**(81), 313–324 (doi: 10.3189/S0022143000215633)

Ladyman J, Lambert J and Wiesner K (2013) What is a complex system? *European Journal for Philosophy of Science*, **3**(1), 33–67 (doi: 10.1007/s13194-012-0056-8)

Lafaysse M, Morin S, Coléou C, Vernay M, Serça D, Besson F, Willemet JM, Giraud G and Durand Y (2013) Toward a new chain of models for avalanche hazard forecasting in French mountain ranges, including low altitude mountains. In *Proceedings of the International Snow Science Workshop*, 162–166, Grenoble

Lafaysse M, Cluzet B, Dumont M, Lejeune Y, Vionnet V and Morin S (2017) A multiphysical ensemble system of numerical snow modelling. *The Cryosphere*, **11**(3), 1173–1198 (doi: 10.5194/tc-11-1173-2017)

Landry CC (2014) Desert dust and snow stability. In *Proceedings of the International Snow Science Workshop*, 556–563, Banff, Canada

Le Roux E, Evin G, Eckert N, Blanchet J and Morin S (2020) Non-stationary extreme value analysis of ground snow loads in the French Alps: a comparison with building standards. *Natural Hazards and Earth System Sciences*, **20**(11), 2961–2977 (doi: 10.5194/nhess-20-2961-2020)

Lebaron AM and Miller DA (2014) An Energy-Based Microstructural Constitutive Model for Fracture in Snow. In *Proceedings of the International Snow Science Workshop*, 134–138, Banff, Canada

Lebaron AM, Miller DA and van Herwijnen A (2014) Measurements of the deformation zone around a split-axis snow micropenetrometer tip. *Cold Regions Science and Technology*, **97**(April 2017), 90–96 (doi: 10.1016/j.coldregions.2013.10.008)

Lebensohn RA, Montagnat M, Mansuy P, Duval P, Meyssonnier J and Philip A (2009) Modeling viscoplastic behavior and heterogeneous intracrystalline deformation of columnar ice polycrystals. *Acta Materialia*, **57**(5), 1405–1415 (doi: 10.1016/j.actamat.2008.10.057)

Lehning M, Doorschot J, Raderschall N and Bartelt P (2000) Combining snow drift and SNOWPACK models to estimate snow loading in avalanche slopes. In *Snow Engineering*, 113–122, Balkema, Rotterdam, The Netherlands, ISBN 90-5809-148-1

Lehning M, Bartelt P, Brown B, Fierz C and Satyawali PK (2002) A physical SNOWPACK model for the Swiss avalanche warning. *Cold Regions Science and Technology*, **35**(3), 147–167 (doi: 10.1016/S0165-232X(02)00073-3)

Lehning M, Fierz C, Brown B and Jamieson J (2004) Modeling snow instability with the snow-cover model SNOWPACK. *Annals of Glaciology*, **38**(May 2022), 331–338 (doi: 10.3189/172756404781815220)

Lesaffre B, Brzoska JB, Coléou C, Flin F and Pieritz RA (2003) Images tridimensionnelles de iege: des prélèvements in situ aux fichiers de données volumiques. Technical report, Rapport Technique 22, Centre d'Etudes de la Neige, Centre National de Recherches Météorologiques, Météo-France

Libbrecht KG (2005) The physics of snow crystals. *Reports on Progress in Physics*, **68**(4), 855–895 (doi: 10.1088/0034-4885/68/4/R03)

Libois Q, Picard G, France JL, Arnaud L, Dumont M, Carmagnola CM and King MD (2013) Influence of grain shape on light penetration in snow. *The Cryosphere*, **7**(6), 1803–1818 (doi: 10.5194/tc-7-1803-2013)

Libois Q, Picard G, Dumont M, Arnaud L, Sergent C, Pougatch E, Sudul M and Vial D (2014) Experimental determination of the absorption enhancement parameter of snow. *Journal of Glaciology*, **60**(222), 714–724 (doi: 10.3189/2014JoG14J015)

Löwe H and van Herwijnen A (2012) A Poisson shot noise model for micro-penetration of snow. *Cold Regions Science and Technology*, **70**, 62–70 (doi: 10.1016/j.coldregions.2011.09.001)

Löwe H, Fierz C, Morin S and Dumont M (2016) Splinter meeting: snowpack model revisited. In *European Geoscience Union (EGU) General Assembly*, European Geosciences Union General Assembly, Vienna, Austria

Löwe H, Zaiser M, Mösinger S and Schleef S (2020) Snow Mechanics Near the Ductile-Brittle Transition: Compressive Stick-Slip and Snow Microquakes. *Geophysical Research Letters*, **47**(4) (doi: 10.1029/2019GL085491)

Lutz ER and Marshall HP (2014) Validation study of Avatech's rapid snow penetrometer, SP1. In *Proceedings of the International Snow Science Workshop*, 843–846, Banff, Canada

Maeno N and Ebinuma T (1983) Pressure sintering of ice and its implication to the densification of snow at polar glaciers and ice sheets. *The Journal of Physical Chemistry*, **87**(21), 4103–4110 (doi: 10.1021/j100244a023)

Mallett R (2021) Snow structure with the snow crystal card. *Nature Reviews Earth and Environment*, **2**(3), 165 (doi: 10.1038/s43017-021-00149-9)

Marbouty D (1980) An Experimental Study of Temperature-Gradient Metamorphism. *Journal of Glaciology*, **26**(94), 303–312 (doi: 10.3189/S0022143000010844)

Marshall HP and Johnson JB (2009) Accurate inversion of high-resolution snow penetrometer signals for microstructural and micromechanical properties. *Journal of Geophysical Research*, **114**(F4), F04016 (doi: 10.1029/2009JF001269)

Martin CL, Schneider L, Olmos L and Bouvard D (2006) Discrete element modeling of metallic powder sintering. *Scripta Materialia*, **55**(5), 425–428 (doi: 10.1016/j.scriptamat.2006.05.017)

Martin CL, Yan Z, Jauffres D, Bouvard D and Bordia RK (2016) Sintered ceramics with controlled microstructures: Numerical investigations with the Discrete Element Method. *Journal of the Ceramic Society of Japan*, **124**(4), 340–345 (doi: 10.2109/jcersj2.15269)

Matsushita H, Matsuzawa M and Abe O (2012) The influences of temperature and normal load on the shear strength of snow consisting of precipitation particles. *Annals of Glaciology*, **53**(61), 31–38 (doi: 10.3189/2012AoG61A022)

Mayer S, van Herwijnen A, Techel F and Schweizer J (2022) A random forest model to assess snow instability from simulated snow stratigraphy. *The Cryosphere Discussions*, **Under revi**(March), 1–39 (doi: 10.5194/tc-2022-34)

Mellor M (1975) A review of basic snow mechanics. *International Association of Hydrological Sciences Publication*, **114**(Symposium at Grindelwald 1974 - Snow mechanics), 251–291

Monti F, Gaume J, van Herwijnen A and Schweizer J (2016) Snow instability evaluation: Calculating the skier-induced stress in a multi-layered snowpack. *Natural Hazards and Earth System Sciences*, **16**(3), 775–788 (doi: 10.5194/nhess-16-775-2016)

Morin S, Domine F, Arnaud L and Picard G (2010) In-situ monitoring of the time evolution of the effective thermal conductivity of snow. *Cold Regions Science and Technology*, **64**(2), 73–80 (doi: 10.1016/j.coldregions.2010.02.008)

Mosavi A, Shirzadi A, Choubin B, Taromideh F, Hosseini FS, Borji M, Shahabi H, Salvati A and Dineva AA (2020) Towards an Ensemble Machine Learning Model of Random Subspace Based Functional Tree Classifier for Snow Avalanche Susceptibility Mapping. *IEEE Access*, **8**, 145968–145983 (doi: 10.1109/ACCESS.2020.3014816)

Murphy AH (1993) What Is a Good Forecast? An Essay on the Nature of Goodness in Weather Forecasting. *Weather and Forecasting*, **8**(2), 281–293 (doi: 10.1175/1520-0434(1993)008<0281:WIAGFA>2.0.CO;2)

Nakaya U (1954) *Snow crystals: natural and artificial*. Harvard University Press, 1954

Narita H (1984) An experimental study on tensile fracture of snow. *Contributions from the Institute of Low Temperature Science*, **32**, 1–37

Navarre JP, Guyomar'ch G and Giraud G (1987) Un modèle statistique pour la prévision locale des avalanches. *International Association of Hydrological Sciences Publication*, **162**(Symposium on avalanche formation, movement and effects), 571–580

Pahaut E and Giraud G (1995) La prévision du risque d'avalanche en France. *La Météorologie*, **8**(12), 46–57

Pahr DH and Zysset PK (2008) Influence of boundary conditions on computed apparent elastic properties of cancellous bone. *Biomechanics and Modeling in Mechanobiology*, **7**(6), 463–476 (doi: 10.1007/s10237-007-0109-7)

Perez N (2004) *Fracture Mechanics*. Kluwer Academic Publishers, Boston, ISBN 1-4020-7745-9 (doi: 10.1007/b118073)

Pérez-Guillén C, Techel F, Hendrick M, Volpi M, van Herwijnen A, Olevski T, Obozinski G, Pérez-Cruz F and Schweizer J (2022) Data-driven automated predictions of the avalanche danger level for dry-snow conditions in Switzerland. *Natural Hazards and Earth System Sciences*, **22**(6), 2031–2056 (doi: 10.5194/nhess-22-2031-2022)

Perla R and Beck T (1983) Experience with Shear Frames. *Journal of Glaciology*, **29**(103), 485–491 (doi: 10.3189/S0022143000030380)

Petitjean F, Ketterlin A and Gançarski P (2011) A global averaging method for dynamic time warping, with applications to clustering. *Pattern Recognition*, **44**(3), 678–693 (doi: 10.1016/j.patcog.2010.09.013)

Podolskiy E, Barbero M, Barpi F, Chambon G, Borri-Brunetto M, Pallara O, Frigo B, Chiaia BM and Naaim M (2014) Healing of snow surface-to-surface contacts by isothermal sintering. *The Cryosphere*, **8**(5), 1651–1659 (doi: 10.5194/tc-8-1651-2014)

Pozdnoukhov A, Matasci G, Kanevski M and Purves RS (2011) Spatio-temporal avalanche forecasting with Support Vector Machines. *Natural Hazards and Earth System Sciences*, **11**(2), 367–382 (doi: 10.5194/nhess-11-367-2011)

Proksch M, Löwe H and Schneebeli M (2015) Density, specific surface area and correlation length of snow measured by high-resolution penetrometry. *Journal of Geophysical Research: Earth Surface*, **120**, 346–362 (doi: 10.1002/2014JF003266)

Radjai F and Dubois F (2011) *Discrete Numerical Modeling of Granular Materials*. Wiley-ISTE, ISBN 978-1-84821-260-2

Ramseier RO and Keeler CM (1966) The Sintering Process in Snow. *Journal of Glaciology*, **6**(45), 421–424 (doi: 10.3189/S0022143000019535)

Reiweger I and Schweizer J (2013) Weak layer fracture: facets and depth hoar. *The Cryosphere*, **7**(5), 1447–1453 (doi: 10.5194/tc-7-1447-2013)

Reiweger I, Schweizer J, Dual J and Herrmann HJ (2009) Modelling snow failure with a fibre bundle model. *Journal of Glaciology*, **55**(194), 997–1002 (doi: 10.3189/002214309790794869)

Reiweger I, Gaume J and Schweizer J (2015) A new mixed-mode failure criterion for weak snowpack layers. *Geophysical Research Letters*, **42**(5), 1427–1432 (doi: 10.1002/2014GL062780)

Reuter B and Schweizer J (2018) Describing Snow Instability by Failure Initiation, Crack Propagation, and Slab Tensile Support. *Geophysical Research Letters*, **45**(14), 7019–7027 (doi: 10.1029/2018GL078069)

Reuter B, Schweizer J and van Herwijnen A (2015) A process-based approach to estimate point snow instability. *The Cryosphere*, **9**(3), 837–847 (doi: 10.5194/tc-9-837-2015)

Riche F and Schneebeli M (2010) Microstructural change around a needle probe to measure thermal conductivity of snow. *Journal of Glaciology*, **56**(199), 871–876 (doi: 10.3189/002214310794457164)

Riche F and Schneebeli M (2013) Thermal conductivity of snow measured by three independent methods and anisotropy considerations. *The Cryosphere*, **7**(1), 217–227 (doi: 10.5194/tc-7-217-2013)

Roch A (1966) Les variations de la résistance de la neige. *International Association of Hydrological Sciences Publication*, **69**(Symposium international sur les aspects scientifiques des avalanches de neige), 86–99

Rosendahl PL and Weißgraeber P (2020) Modeling snow slab avalanches caused by weak-layer failure - Part 2: Coupled mixed-mode criterion for skier-triggered anticracks. *The Cryosphere*, **14**(1), 131–145 (doi: 10.5194/tc-14-131-2020)

Sakoe H and Chiba S (1978) Dynamic programming algorithm optimization for spoken word recognition. *IEEE Transactions on Acoustics, Speech, and Signal Processing*, **26**(1), 43–49 (doi: 10.1109/TASSP.1978.1163055)

Satyawali PK and Schneebeli M (2010) Spatial scales of snow texture as indicator for snow class. *Annals of Glaciology*, **51**(54), 55–63 (doi: 10.3189/172756410791386544)

Satyawali PK, Schneebeli M, Pielmeier C, Stucki T and Singh A (2009) Preliminary characterization of Alpine snow using SnowMicroPen. *Cold Regions Science and Technology*, **55**(3), 311–320 (doi: 10.1016/j.coldregions.2008.09.003)

Schaller CF, Freitag J, Kipfstuhl S, Laepple T, Christian Steen-Larsen H and Eisen O (2016) A representative density profile of the North Greenland snowpack. *The Cryosphere*, **10**(5), 1991–2002 (doi: 10.5194/tc-10-1991-2016)

Schleef S and Löwe H (2013) X-ray microtomography analysis of isothermal densification of new snow under external mechanical stress. *Journal of Glaciology*, **59**(214), 233–243 (doi: 10.3189/2013JoG12J076)

Schleef S, Löwe H and Schneebeli M (2014) Hot-pressure sintering of low-density snow analyzed by X-ray microtomography and in situ microcompression. *Acta Materialia*, **71**, 185–194 (doi: 10.1016/j.actamat.2014.03.004)

Schneebeli M (2004) Numerical simulation of elastic stress in the microstructure of snow. *Annals of Glaciology*, **38**, 339–342 (doi: 10.3189/172756404781815284)

Schneebeli M and Bebi P (2004) HYDROLOGY | Snow and Avalanche Control. In Jeffery Burley (ed.), *Encyclopedia of Forest Sciences*, chapter Snow and A, 397–402, Elsevier, Oxford, ISBN 978-0-12-145160-8 (doi: 10.1016/B0-12-145160-7/00271-4)

Schneebeli M and Johnson JB (1998) A constant-speed penetrometer for high-resolution snow stratigraphy. *Annals of Glaciology*, **26**, 107–111 (doi: 10.1017/S0260305500014658)

Schneebeli M and Sokratov SA (2004) Tomography of temperature gradient metamorphism of snow and associated changes in heat conductivity. *Hydrological Processes*, **18**(18), 3655–3665 (doi: 10.1002/hyp.5800)

Schweizer J and Föhn PMB (1996) Avalanche forecasting — an expert system approach. *Journal of Glaciology*, **42**(141), 318–332 (doi: 10.3189/S0022143000004172)

Schweizer J and Wiesinger T (2001) Snow profile interpretation for stability evaluation. *Cold Regions Science and Technology*, **33**(2-3), 179–188 (doi: 10.1016/S0165-232X(01)00036-2)

Schweizer J, Jamieson J and Schneebeli M (2003) Snow avalanche formation. *Reviews of Geophysics*, **41**(4), 1016–1041 (doi: 10.1029/2002RG000123)

Schweizer J, Michot G and Kirchner HO (2004) On the fracture toughness of snow. *Annals of Glaciology*, **38**, 1–8 (doi: 10.3189/172756404781814906)

Schweizer J, Kronholm K, Jamieson J and Birkeland KW (2008) Review of spatial variability of snowpack properties and its importance for avalanche formation. *Cold Regions Science and Technology*, **51**(2-3), 253–272 (doi: 10.1016/j.coldregions.2007.04.009)

Schweizer J, van Herwijnen A and Reuter B (2011) Measurements of weak layer fracture energy. *Cold Regions Science and Technology*, **69**(2-3), 139–144 (doi: 10.1016/j.coldregions.2011.06.004)

Schweizer J, Reuter B, van Herwijnen A and Gaume J (2016) Avalanche Release 101. In *Proceedings of the International Snow Science Workshop*, 1–11, Breckenridge, Colorado, USA, 3-7 October 2016

Schweizer J, Bartelt P and van Herwijnen A (2021) Snow avalanches. In W Haeberli and C Whiteman (eds.), *Snow and Ice-Related Hazards, Risks, and Disasters*, Hazards and Disasters Series, 377–416, Elsevier, second edi edition, ISBN 978-0-12-817129-5 (doi: 10.1016/B978-0-12-817129-5.00001-9)

Seity Y, Brousseau P, Malardel S, Hello G, Bénard P, Bouttier F, Lac C and Masson V (2011) The AROME-France Convective-Scale Operational Model. *Monthly Weather Review*, **139**(3), 976–991 (doi: 10.1175/2010MWR3425.1)

Senin P (2008) Dynamic time warping review. Technical Report December, University of Hawaii, Honolulu, USA

Shapiro LH, Johnson JB, Sturm M and Blaisdell GL (1997) Snow mechanics - Review of the state of knowledge and applications. *CRREL Report*, **97**(3)

Shoop S, Richmond P and Lacombe J (2006) Overview of cold regions mobility modeling at CRREL. *Journal of Terramechanics*, **43**(1), 1–26 (doi: 10.1016/j.jterra.2004.08.004)

Sigrist C, Schweizer J, Schindler HJ and Dual J (2006) The energy release rate of mode II fractures in layered snow samples. *International Journal of Fracture*, **139**(3-4), 461–475 (doi: 10.1007/s10704-006-6580-9)

Simenhois R and Birkeland KW (2009) The Extended Column Test: Test effectiveness, spatial variability, and comparison with the Propagation Saw Test. *Cold Regions Science and Technology*, **59**(2-3), 210–216 (doi: 10.1016/j.coldregions.2009.04.001)

Spandre P, François H, George-Marcelpoil E and Morin S (2016) Panel based assessment of snow management operations in French ski resorts. *Journal of Outdoor Recreation and Tourism*, **16**(September), 24–36 (doi: 10.1016/j.jort.2016.09.002)

Srivastava PK, Chandel C, Mahajan P and Pankaj P (2016) Prediction of anisotropic elastic properties of snow from its microstructure. *Cold Regions Science and Technology*, **125**, 85–100 (doi: 10.1016/j.coldregions.2016.02.002)

Statham G, Haegeli P, Greene EM, Birkeland KW, Israelson C, Tremper B, Stethem C, McMahon B, White B and Kelly J (2018) A conceptual model of avalanche hazard. *Natural Hazards*, **90**(2), 663–691 (doi: 10.1007/s11069-017-3070-5)

Steinbach F, Bons PD, Griera A, Jansen D, Llorens MG, Roessiger J and Weikusat I (2016) Strain localization and dynamic recrystallization in the ice-air aggregate: A numerical study. *The Cryosphere*, **10**(6), 3071–3089 (doi: 10.5194/tc-10-3071-2016)

Sturm M and Benson C (2004) Scales of spatial heterogeneity for perennial and seasonal snow layers. *Annals of Glaciology*, **38**, 253–260 (doi: 10.3189/172756404781815112)

Sturm M and Johnson JB (1992) Thermal conductivity measurements of depth hoar. *Journal of Geophysical Research: Solid Earth*, **97**(B2), 2129–2139 (doi: 10.1029/91JB02685)

Sturm M, Holmgren J, König M and Morris K (1997) The thermal conductivity of seasonal snow. *Journal of Glaciology*, **43**(143), 26–41 (doi: 10.3189/S0022143000002781)

Szabo D and Schneebeli M (2007) Subsecond sintering of ice. *Applied Physics Letters*, **90**(15), 151916 (doi: 10.1063/1.2721391)

Techel F, Mitterer C, Ceaglio E, Coléou C, Morin S, Rastelli F and Purves RS (2018) Spatial consistency and bias in avalanche forecasts – a case study in the European Alps. *Natural Hazards and Earth System Sciences*, **18**(10), 2697–2716 (doi: 10.5194/nhess-18-2697-2018)

Theile TC (2010) *Three-dimensional structural images analysis and micromechanics of snow*. Ph.D. thesis, Technischen Universität Dortmund

Theile TC, Löwe H and Schneebeli M (2011) Simulating creep of snow based on microstructure and the anisotropic deformation of ice. *Acta Materialia*, **59**(18), 7104–7113 (doi: 10.1016/j.actamat.2011.07.065)

Timoshenko S (1940) *Strength of materials: part I*. Lancaster press, New York, NY, USA, 2nd edtion edition

van Herwijnen A (2013) Experimental analysis of snow micropenetrometer (SMP) cone penetration in homogeneous snow layers. *Canadian Geotechnical Journal*, **50**(10), 1044–1054 (doi: 10.1139/cgj-2012-0336)

van Herwijnen A and Jamieson J (2007) Fracture character in compression tests. *Cold Regions Science and Technology*, **47**(1-2), 60–68 (doi: 10.1016/j.coldregions.2006.08.016)

van Herwijnen A, Gaume J, Bair EH, Reuter B, Birkeland KW and Schweizer J (2016) Estimating the effective elastic modulus and specific fracture energy of snowpack layers from field experiments. *Journal of Glaciology*, **62**(236), 997–1007 (doi: 10.1017/jog.2016.90)

Verfaillie D, Déqué M, Morin S and Lafaysse M (2017) The method ADAMONT v1.0 for statistical adjustment of climate projections applicable to energy balance land surface models. *Geoscientific Model Development*, **10**(11), 4257–4283 (doi: 10.5194/gmd-10-4257-2017)

Vernay M, Lafaysse M, Mérindol L, Giraud G and Morin S (2015) Ensemble forecasting of snowpack conditions and avalanche hazard. *Cold Regions Science and Technology*, **120**, 251–262 (doi: 10.1016/j.coldregions.2015.04.010)

Vetter R, Sigg S, Singer HM, Kadau D, Herrmann HJ and Schneebeli M (2010) Simulating isothermal aging of snow. *Europhysics Letters*, **89**(2), 26001 (doi: 10.1209/0295-5075/89/26001)

Vionnet V, Brun E, Morin S, Boone A, Faroux S, Le Moigne P, Martin E and Willemet JM (2012) The detailed snowpack scheme Crocus and its implementation in SURFEX v7 . 2. *Geoscientific Model Development*, **5**, 773–791 (doi: 10.5194/gmd-5-773-2012)

Wang X and Baker I (2013) Observation of the microstructural evolution of snow under uniaxial compression using X-ray computed microtomography. *Journal of Geophysical Research: Atmospheres*, **118**(12), 371–382 (doi: 10.1002/2013JD020352)

Wautier A, Geindreau C and Flin F (2015) Linking snow microstructure to its macroscopic elastic stiffness tensor: A numerical homogenization method and its application to 3-D images from X-ray tomography. *Geophysical Research Letters*, **42**(19), 8031–8041 (doi: 10.1002/2015GL065227)

Wautier A, Geindreau C and Flin F (2017) Numerical homogenization of the viscoplastic behavior of snow based on X-ray tomography images. *The Cryosphere*, **11**(3), 1465–1485 (doi: 10.5194/tc-11-1465-2017)

Weibull W (1939) A statistical theory of the strength of material. *Ingeniors Vetenskapa Acadamiens Handligar*, **151**, 1–45

Willibald C, Löwe H, Theile TC, Dual J and Schneebeli M (2020) Angle of repose experiments with snow: Role of grain shape and cohesion. *Journal of Glaciology*, **66**(258), 658–666 (doi: 10.1017/jog.2020.36)

Wiscombe WJ and Warren SG (1980) A Model for the Spectral Albedo of Snow. I: Pure Snow. *Journal of the Atmospheric Sciences*, **37**(12), 2712–2733 (doi: 10.1175/1520-0469(1980)037<2712:AMFTSA>2.0.CO;2)

Yosida Z (1955) Physical Studies on Deposited Snow 1: Thermal Properties. Technical report, Institute of Low Temperature Science

Yu HS and Carter JP (2002) Rigorous Similarity Solutions for Cavity Expansion in Cohesive-Frictional Soils. *International Journal of Geomechanics*, **2**(2), 233–258 (doi: 10.1061/(ASCE)1532-3641(2002)2:2(233))

Zeidler A and Jamieson J (2006) Refinements of empirical models to forecast the shear strength of persistent weak snow layers PART A: Layers of faceted crystals. *Cold Regions Science and Technology*, **44**(3), 194–205 (doi: 10.1016/j.coldregions.2005.11.005)

Zhang T (2005) Influence of the seasonal snow cover on the ground thermal regime: An overview. *Reviews of Geophysics*, **43**(4) (doi: 10.1029/2004RG000157)

My research production (until April 1, 2022)

All my publications are listed here according to the french nomenclature[1].

[1] https://recherche.uco.fr/aide/459/normes-codifications-utilisees-et-referentiel-acl

Papers in peer-reviewed international journals (ACL)

Dkengne Sielenou P, Viallon-Galinier L, Hagenmuller P, Naveau P, Morin S, Dumont M, Verfaillie D and Eckert N (2021) Combining random forests and class-balancing to discriminate between three classes of avalanche activity in the French Alps. *Cold Regions Science and Technology*, **187**(November 2020), 103276 (doi: 10.1016/j.coldregions.2021.103276)

Dumont M, Flin F, Malinka A, Brissaud O, Hagenmuller P, Lapalus P, Lesaffre B, Dufour A, Calonne N, Rolland du Roscoat S and Andò E (2021) Experimental and model-based investigation of the links between snow bidirectional reflectance and snow microstructure. *The Cryosphere*, **15**(8), 3921–3948 (doi: 10.5194/tc-15-3921-2021)

Evin G, Dkengne Sielenou P, Eckert N, Naveau P, Hagenmuller P and Morin S (2021) Extreme avalanche cycles: Return levels and probability distributions depending on snow and meteorological conditions. *Weather and Climate Extremes*, **33**(June), 100344 (doi: 10.1016/j.wace.2021.100344)

Fourteau K, Domine F and Hagenmuller P (2021a) Impact of water vapor diffusion and latent heat on the effective thermal conductivity of snow. *The Cryosphere*, **15**(6), 2739–2755 (doi: 10.5194/tc-15-2739-2021)

Fourteau K, Domine F and Hagenmuller P (2021b) Macroscopic water vapor diffusion is not enhanced in snow. *The Cryosphere*, **15**(1), 389–406 (doi: 10.5194/tc-15-389-2021)

Fourteau K, Hagenmuller P, Roulle J and Domine F (2022) On the use of heated needle probes for measuring snow thermal conductivity. *Journal of Glaciology*, 1–15 (doi: 10.1017/jog.2021.127)

Georges D, Saletti D, Montagnat M, Forquin P and Hagenmuller P (2021) Influence of Porosity on Ice Dynamic Tensile Behavior as Assessed by Spalling Tests. *Journal of Dynamic Behavior of Materials*, **7**(4), 575–590 (doi: 10.1007/s40870-021-00300-z)

Hagenmuller P and Pilloix T (2016) A New Method for Comparing and Matching Snow Profiles, Application for Profiles Measured by Penetrometers. *Frontiers in Earth Science*, **4**(52) (doi: 10.3389/feart.2016.00052)

Hagenmuller P, Chambon G, Lesaffre B, Flin F and Naaim M (2013) Energy-based binary segmentation of snow microtomographic images. *Journal of Glaciology*, **59**(217), 859–873 (doi: 10.3189/2013JoG13J035)

Hagenmuller P, Calonne N, Chambon G, Flin F, Geindreau C and Naaim M (2014a) Characterization of the snow microstructural bonding system through the minimum cut density. *Cold Regions Science and Technology*, **108**, 72–79 (doi: 10.1016/j.coldregions.2014.09.002)

Hagenmuller P, Chambon G, Flin F, Morin S and Naaim M (2014b) Snow as a granular material: assessment of a new grain segmentation algorithm. *Granular Matter*, **16**(4), 421–432 (doi: 10.1007/s10035-014-0503-7)

Hagenmuller P, Theile TC and Schneebeli M (2014c) Numerical simulation of microstructural damage and tensile strength of snow. *Geophysical Research Letters*, **41**(1), 86–89 (doi: 10.1002/2013GL058078)

Hagenmuller P, Chambon G and Naaim M (2015) Microstructure-based modeling of snow mechanics: a discrete element approach. *The Cryosphere*, **9**(5), 1969–1982 (doi: 10.5194/tc-9-1969-2015)

Hagenmuller P, Matzl M, Chambon G and Schneebeli M (2016) Sensitivity of snow density and specific surface area measured by microtomography to different image processing algorithms. *The Cryosphere*, **10**(3), 1039–1054 (doi: 10.5194/tc-10-1039-2016)

Hagenmuller P, van Herwijnen A, Pielmeier C and Marshall HP (2018) Evaluation of the snow penetrometer Avatech SP2. *Cold Regions Science and Technology*, **149**(February), 83–94 (doi: 10.1016/j.coldregions.2018.02.006)

Hagenmuller P, Flin F, Dumont M, Tuzet F, Peinke I, Lapalus P, Dufour A, Roulle J, Pézard L, Voisin D, Andò E, Rolland du Roscoat S and Charrier P (2019) Motion of dust particles in dry snow under temperature gradient metamorphism. *The Cryosphere*, **13**(9), 2345–2359 (doi: 10.5194/tc-13-2345-2019)

Mede T, Chambon G, Hagenmuller P and Nicot F (2018a) A medial axis based method for irregular grain shape representation in DEM simulations. *Granular Matter*, **20**(1), 16 (doi: 10.1007/s10035-017-0785-7)

Mede T, Chambon G, Hagenmuller P and Nicot F (2018b) Snow Failure Modes Under Mixed Loading. *Geophysical Research Letters*, **45**(24), 95–108 (doi: 10.1029/2018GL080637)

Mede T, Chambon G, Nicot F and Hagenmuller P (2020) Micromechanical investigation of snow failure under mixed-mode loading. *International Journal of Solids and Structures*, **199**, 95–108 (doi: 10.1016/j.ijsolstr.2020.04.020)

Montagnat M, Chambon G, Gaume J, Hagenmuller P and Sandells M (2020) Editorial: About the Relevance of Snow Microstructure Study in Cryospheric Sciences. *Frontiers in Earth Science*, **8**(239) (doi: 10.3389/feart.2020.619509)

Morin S, Horton S, Techel F, Bavay M, Coléou C, Fierz C, Gobiet A, Hagenmuller P, Lafaysse M, Ližar M, Mitterer C, Monti F, Müller K, Olefs M, Snook JS, van Herwijnen A and Vionnet V (2020) Application of physical snowpack models in support of operational avalanche hazard forecasting: A status report on current implementations and prospects for the future. *Cold Regions Science and Technology*, **170**(October 2019), 102910 (doi: 10.1016/j.coldregions.2019.102910)

Peinke I, Hagenmuller P, Chambon G and Roulle J (2019) Investigation of snow sintering at microstructural scale from micro-penetration tests. *Cold Regions Science and Technology*, **162**(March), 43–55 (doi: 10.1016/j.coldregions.2019.03.018)

Peinke I, Hagenmuller P, Andò E, Chambon G, Flin F and Roulle J (2020) Experimental Study of Cone Penetration in Snow Using X-Ray Tomography. *Frontiers in Earth Science*, **8**, 63 (doi: 10.3389/feart.2020.00063)

Reuter B, Viallon-Galinier L, Horton S, van Herwijnen A, Mayer S, Hagenmuller P and Morin S (2022) Characterizing snow instability with avalanche problem types derived from snow cover simulations. *Cold Regions Science and Technology*, **194**(May 2021), 103462 (doi: 10.1016/j.coldregions.2021.103462)

Teich M, Giunta AD, Hagenmuller P, Bebi P, Schneebeli M and Jenkins MJ (2019) Effects of bark beetle attacks on forest snowpack and avalanche formation – Implications for protection forest management. *Forest Ecology and Management*, **438**(February), 186–203 (doi: 10.1016/j.foreco.2019.01.052)

Thibert E, Bellot H, Ravanat X, Ousset F, Pulfer G, Naaim M, Hagenmuller P, Naaim-Bouvet F, Faug T, Nishimura K, Ito Y, Baroudi D, Prokop A, Schön P, Soruco A, Vincent C, Limam A and Héno R (2015) The full-scale avalanche test-site at Lautaret Pass (French Alps). *Cold Regions Science and Technology*, **115**, 30–41 (doi: 10.1016/j.coldregions.2015.03.005)

Vernay M, Lafaysse M, Monteiro D, Hagenmuller P, Nheili R, Samacoïts R, Verfaillie D and Morin S (2022) The S2M meteorological and snow cover reanalysis over the French mountainous areas: description and evaluation (1958–2021). *Earth System Science Data*, **14**(4), 1707–1733 (doi: 10.5194/essd-14-1707-2022)

Viallon-Galinier L, Hagenmuller P and Lafaysse M (2020) Forcing and evaluating detailed snow cover models with stratigraphy observations. *Cold Regions Science and Technology*, **180**(September), 103163 (doi: 10.1016/j.coldregions.2020.103163)

Chapters of scientific books (COS)

Lestel L, Cuif M, Hagenmuller P, Labbas M and Carré C (2013) La transaction comme régulation des déversements industriels en rivière, le cas de la Seine-et-Marne au XXe siècle. In TL Roux and M Letté (eds.), *Débordements industriels, Environnement, territoire et conflit. XVIIIe - XXIe siècle*, 225–247, Presses universitaires de Rennes

Invited talks (C-INV)

Hagenmuller P (2018a) Avalanche hazard forecasting by Météo-France. In *The 22nd Niseko Avalanche Meeting, International Snow and Avalanche Symposium in Niseko*, Niseko, Japan, 30 November - 3 December 2018

Hagenmuller P (2018b) Microstructure-based modeling of snow mechanics. In *The 22nd Niseko Avalanche Meeting, International Snow and Avalanche Symposium in Niseko*, Niseko, Japan, 30 November - 3 December 2018

Hagenmuller P, Morin S, Flin F, Chambon G, Naaim M, Schneebeli M and Theile TC (2015) Microstructure-based modeling of snow mechanics. In *SLab Avalanche Multiscale Mechanical Modelling (SLAM3) workshop*, 1997, 1969–1982, Davos, Switzerland, 3-5 April 2017

Proceedings (C-ACTI)

Hagenmuller P (2016) Matching of vertical snow profiles. In *Proceedings of the International Snow Science Workshop*, 695–, Breckenridge, Colorado, USA, 3-7 October 2016

Hagenmuller P and Pilloix T (2016) Characterizing the snowpack stratigraphy and its mechanical stability with hardness profiles measured by the Avatech SP2. In *8th International Conference on Snow Engineering (ICSE)*, Nantes, France, 14-17 June 2016

Hagenmuller P, Chambon G, Flin F, Wang X, Lesaffre B and Naaim M (2013a) Description of the snow microstructure as a 3D assembly of grains. In *Proceedings of the International Snow Science Workshop*, 87–91, Grenoble - Chamonix Mont-Blanc, France, 7-11 October 2013

Hagenmuller P, Chambon G, Lesaffre B, Flin F, Calonne N and Naaim M (2013b) Energy-based binary segmentation of snow microtomographic images. In *1st International Conference on Tomography of Materials and Structures (ICTMS)*, Ghent, Belgium, 1-5 July 2013

Hagenmuller P, Pilloix T and Lejeune Y (2016) Inter-comparison of snow penetrometers (ramsonde, Avatech SP2 and SnowMicroPen) in the framework of avalanche forecasting. In *Proceedings of the International Snow Science Workshop*, 32–38, Breckenridge, Colorado, USA, 3-7 October 2016

Hagenmuller P, Viallon-Galinier L, Bouchayer C, Teich M, Lafaysse M and Vionnet V (2018) Quantitative Comparison of Snow Profiles. In *Proceedings of the International Snow Science Workshop*, 876–879, Innsbruck, Austria, 7-12 October 2018

Mede T, Chambon G, Hagenmuller P and Nicot F (2017) Mechanical behaviour of weak snow layers: modelling a porous structure of sintered grains. In F Radjai, S Nezamabadi, S Luding and J Delenne (eds.), *Powders and Grains 2017 – 8th International Conference on Micromechanics on Granular Media*, volume 140, 4, Montpellier, France, 3-7 July 2017, ISSN 2100-014X (doi: 10.1051/epjconf/201714006008)

Mede T, Chambon G, Hagenmuller P and Nicot F (2018) Investigation of the interplay between shear failure and normal collapse of weak layers using microstructure-based mechanical simulations. In *Proceedings of the International Snow Science Workshop*, 1021–1024, Innsbruck, Austria, 7-12 October 2018

Morin S, Fierz C, Horton S, Bavay M, Dumont M, Gobiet A, Hagenmuller P, Lafaysse M, Mitterer C, Monti F, Müller K, Olefs M, Snook JS, Techel F, van Herwijnen A and Vionnet V (2018) Application of physical snowpack models in support of operational avalanche hazard forecasting: a status report on current implementations and prospects for the future. In *Proceedings of the International Snow Science Workshop*, 1098–1107, Innsbruck, Austria, 7-12 October 2018

Peinke I, Hagenmuller P, Andò E, Flin F, Chambon G and Roulle J (2018) Microstructure-based analysis of cone penetration tests in snow. In *Proceedings of the International Snow Science Workshop*, 925–929, Innsbruck, Austria, 7-12 October 2018

Talks without proceedings (C-COM)

Bernard A, Hagenmuller P, Chambon G and Montagnat M (2021) Tomography-based investigation of concurrent snow creep and isothermal metamorphism. In *Virtual European Geoscience Union General Assembly (vEGU)*, Copernicus Meetings, Vienna, Austria, 19-30 April 2021

Dick O, Viallon-Galinier L, Hagenmuller P, Fructus M, Lafaysse M and Dumont M (2021) Can Saharan dust deposition impact snow stability in the French Alps? In *Virtual European Geoscience Union General Assembly (vEGU)*, Copernicus Meetings, Vienna, Austria, 19-30 April 2021

Dumont M, Tuzet F, Lafaysse M, Arnaud L, Picard G, Libois Q, Missiaen A, Hagenmuller P, Lejeune Y and Morin S (2016) Numerical investigation of the effect of light absorbing impurities in snow. In *AGU Fall Meeting Abstracts*, volume 2, C12A–04, San Francisco, California, USA

Dumont M, Flin F, Malinka A, Brissaud O, Hagenmuller P, Dufour A, Lapalus P, Lesaffre B, Calonne N, Rolland du Roscoat S and Andò E (2017) Experimental and model based investigation of the links between snow bidirectional reflectance and snow microstructure. In *AGU Fall Meeting Abstracts*, volume 2017, C13C–0980, New Orleans, USA

Flin F, Wang X, Hagenmuller P, Calonne N, Lesaffre B, Dufour A, Coeurjolly D, Chambon G and Rolland Du Roscoat S (2013) Computation of grain sizes from microtomographic images of snow. In *Proceedings of the International Snow Science Workshop*, Grenoble - Chamonix Mont-Blanc, France, 7-11 October 2013

Flin F, Denis R, Mehu C, Calonne N, Lesaffre B, Dufour A, Lapalus P, Hagenmuller P, Roulle J, Rolland du Roscoat S, Bretin E and Geindreau C (2017) Snow isothermal metamorphism : in situ experiment, measurement of interfacial velocities and phase-field modeling for a better understanding of the involved mechanisms. In *9th International Conference on Porous Media & Annual Meeting (Interpore 2017)*, Rotterdam, The Netherlands, 8 - 11 May 2017

Fourteau K, Domine F and Hagenmuller P (2021) The Influence of Vapor Attachment Kinetics on Snow Effective Properties. In *Virtual European Geoscience Union General Assembly (vEGU)*, Copernicus Meetings, Vienna, Austria, 19-30 April 2021

Granger R, Flin F, Ludwig W, Hammad I, Geindreau C, Rolland Du Roscoat S, Philip A, Lahoucine F, Lapalus P, Pezard L, Roulle J, Burr A, Dufour A, Hagenmuller P, Peinke I and Tafforeau P (2019a) Time-lapse Diffraction Contrast Tomography of snow temperature gradient metamorphism. In *International Conference on Tomography of Materials & Structure (ICTMS)*, Cairns, Australia, 22-26 July 2019

Granger R, Geindreau C, Flin F, Calonne N, Dufour A, Lesaffre B, Philip A, Hagenmuller P, Roulle J, Pezard L and Rolland du Roscoat S (2019b) Air bubble migration and faceting in ice : X-ray tomography observations vs phase field modeling. In *International Conference on Tomography of Materials & Structure (ICTMS)*, 3–4, Cairns, Australia, 22-26 July 2019

Hagenmuller P (2013) Etude du comportement mécanique de la neige à partir d'images micro-tomographiques. In *Atelier Neige de l'OSUG*, Grenoble, France, 15 November 2013

Hagenmuller P (2017) Méthode pour aligner des profils verticaux de neige simulés et observés. In *Atelier Neige de l'OSUG*, Grenoble, France, 20 April 2017

Hagenmuller P (2019) TomoCold: tomographie par rayons X en chambre froide. In *Atelier Neige de l'OSUG*, Grenoble, France, 8 March 2019

Hagenmuller P and Eckert N (2018) Projet QUAAACC : QUalification de l'Aléa Avalancheux dans les Alpes en Climat Changeant. In *Journée annuelle GIRN & SDA du PARN*, Gap, France, 27 November 2018

Hagenmuller P and Pilloix T (2016) Méthode pour combiner plusieurs profils stratigraphiques du manteau neigeux, application aux profils de résistance à l'enfoncement. In *Journées nivologie et glaciologie de la Société Hydrotechnique de France (SHF)*, Grenoble, France, April 2016

Hagenmuller P, Chambon G, Lesaffre B, Flin F, Calonne N and Naaim M (2013a) Specific surface area computed with X-ray micro-tomography: Impact of the segmentation technique and the effective resolution. In *Snow Grain Size Workshop (SGSW)*, Grenoble, France, 2 April 2013

Hagenmuller P, Schneebeli M, Theile TC, Naaim M and Chambon G (2013b) Microstructure-based simulation of the brittle tensile failure of snow. In *Journées nivologie et glaciologie de la Société Hydrotechnique de France (SHF)*, Grenoble, France, 15 February 2013

Hagenmuller P, Wang X, Flin F, Chambon G and Naaim M (2013c) Segmentation of snow grains from microtomographic data to derive the specific grain contact area as a mechanical indicator. In *Davos Atmosphere and Cryosphere Assembly (DACA)*, Davos, Switzerland, 8-12 July 2013

Hagenmuller P, Chambon G and Naaim M (2015) Modeling snow as a granular material with a microstructure-based discrete element approach. In *International Union of Geodesy and Geophysics (IUGG)*, Prague, Czech Republic, 22 June - 2 July 2015

Hagenmuller P, Chambon G, Mede T, Peinke I and Nicot F (2019) Microstructure-based Discrete Element Modelling of Snow Mechanics. In *Particles*, Barcelona, Spain, 28-30 October 2019

Hagenmuller P, Morin S, Viallon-galinier L, Reuter B, Gouttevin I, Lafaysse M, Eckert N, Soubeyroux Jm and Samacoïts R (2020) Neige et avalanches dans un climat changeant. In *Journée I-RISK : Evolution des avalanches et vulnérabilité des ouvrages*, Online. Saint-François-Longchamp, France, 20 November 2020

Lafaysse M, Dumont M, Nheili R, Viallon-Galinier L, Carmagnola CM, Cluzet B, Fructus M, Hagenmuller P, Morin S, Spandre P, Tuzet F and Vionnet V (2020) Latest scientific and technical evolutions in the Crocus snowpack model. In *Virtual European Geoscience Union General Assembly (vEGU)*, Vienna, Austria, 4-8 May 2020 (doi: 10.5194/egusphere-egu2020-10217)

Peinke I, Hagenmuller P, Andò E, Flin F, Chambon G and Roulle J (2018) Analysis of cone penetration tests in snow with X-ray tomography. In *4th International Congress on 3D Materials Science (3DMS 2018)*, Helsingor (Elsinore), Denmark, 10-13 June 2018

Reuter B, Viallon-Galinier L, Mayer S, Hagenmuller P and Morin S (2021) A tracking algorithm to identify slab and weak layer combinations for assessing snow instability and avalanche problem type. In *Virtual European Geoscience Union General Assembly (vEGU)*, Copernicus Meetings, Vienna, Austria, 19-30 April 2021

Teich M, Bebi P, Schneebeli M, Hagenmuller P, Giunta AD and Jenkins MJ (2017a) Does bark beetle disturbance alter forests' protective effects against snow avalanches? In *Restoring the West Conference*, Logan, Utah, USA, 16-17 October 2017

Teich M, Hagenmuller P, Bebi P, Jenkins MJ, Giunta AD and Schneebeli M (2017b) Quantifying small-scale spatio-temporal variability of snow stratigraphy in forests based on high-resolution snow penetrometry. In *AGU Fall Meeting Abstracts*, volume 2017, C51E–03, New Orleans, USA

Teich M, Giunta AD, Hagenmuller P, Bebi P, Schneebeli M and Jenkins MJ (2019) Effects of bark beetle attacks on forest snowpack and avalanche formation - implications for protection forest management. In *International Mountain Conference*, Innsbruck, Austria, 8-12 September 2019

Viallon-Galinier L, Hagenmuller P, Eckert N and Reuter B (2021) Mechanical stability indicators derived from detailed snow cover simulations. In *Virtual European Geoscience Union General Assembly (vEGU)*, Copernicus Meetings, Vienna, Austria, 19-30 April 2021

Posters (C-AFF)

Dumont M, Flin F, Malinka A, Brissaud O, Hagenmuller P, Lesaffre B, Dufour A, Calonne N, Rolland du Roscoat S and Andò E (2017) Experimental and model-based investigation of the links between snow bidirectional reflectance and snow microstructure. In *European Geoscience Union (EGU) General Assembly*, Poster. Vienna, Austria, 23-28 April 2017

Dumont M, Flin F, Malinka A, Brissaud O, Lapalus P, Hagenmuller P, Lesaffre B, Dufour A, Calonne N, Rolland du Roscoat S and Andò E (2018) Experimental and model based investigation of the links between snow bidirectional reflectance and snow microstructure. In *Physics and Chemistry of Ice*, Zuerich, Switzerland, 8-12 January 2018

Flin F, Denis R, Mehu C, Calonne N, Lesaffre B, Dufour A, Granger R, Lapalus P, Hagenmuller P, Roulle J, Rolland du Roscoat S, Bretin E and Geindreau C (2018) Isothermal metamorphism of snow : measurement of interface velocities and phase-field modeling for a better understanding of the involved mechanisms. In *Physics and Chemistry of Ice*, Zuerich, Switzerland, 8-12 January 2018

Haffar I, Flin F, Geindreau C, Petillon N, Gervais PC, Edery V, Hagenmuller P, Roulle J, Dufour A, Pezard L, Calonne N, Lapalus P, Münch B, Charrier P and Andò E (2019) µCT for 3D size and shape analysis of ice particles in jet A-1 fuel. In *Energy Materials workshop : Emerging synchrotron techniques for characterization of energy materials and devices*, Grenoble, France, 23-25 September 2019

Hagenmuller P (2017) Microstructure-based finite element modeling of snow failure envelope. In *European Geoscience Union (EGU) General Assembly*, Poster. Vienna, Austria, 23-28 April 2017

Hagenmuller P (2018) TomoCold. In *Colloque LEFE*, Clermont-Ferrand, France, 28-30 March 2018

Hagenmuller P (2019) Avalanche danger forecasting by Météo-France. In *European Avalanche Warning Services (EAWS) General Assembly*, Oslo, Norway, 12-14 June 2019

Hagenmuller P (2020) Numerical homogenization of snow elastic properties. In *Virtual Snow Science Workshop (vSSW)*, Fernie, British Columbia, Canada,4-6 October 2020

Hagenmuller P, Theile TC and Schneebeli M (2011) Measurements and microstructure-based simulations of the tensile strength of snow. In *Micro-DICE 2011 Conference*, Poster. Grenoble, France, 7-9 November 2011

Hagenmuller P, Theile TC and Schneebeli M (2012) Microstructure-based simulations of the tensile strength of snow. In *European Geoscience Union (EGU) General Assembly*, Poster. Vienna, Austria, 22-27 April 2012

Hagenmuller P, Dumont M, Flin F, Tuzet F, Peinke I, Lapalus P, Dufour A, Roulle J, Pezard L and Rolland du Roscoat S (2018a) Snow microstructure evolution in presence of mineral dust. In *Polar 2018*, Davos, Switzerland, 15-26 June 2018

Hagenmuller P, Flin F, Dumont M, Tuzet F, Peinke I, Lapalus P, Dufour A, Roulle J, Pezard L and Andò E (2018b) Time series of the snow microstructure metamorphism in presence of mineral dust. In *European Geoscience Union (EGU) General Assembly*, PICO. Vienna, Austria, 8-13 April 2018

Hagenmuller P, Viallon-Galinier L, Bouchayer C, Teich M, Lafaysse M and Vionnet V (2018c) A new metric between vertical snow profiles using dynamic time warping. In *European Geoscience Union (EGU) General Assembly*, PICO. Vienna, Austria, 8-13 April 2018

Herny C, Hagenmuller P, Chambon G, Roulle J and Peinke I (2021) Microstructure-based modelling of snow mechanics: experimental evaluation on the cone penetration test. In *ALERT Geomaterial Workshop*, Aussois, France, 27-29 September 2021

Mede T, Chambon G, Hagenmuller P and Nicot F (2017a) Modelling the deformation and collapse of a weak snow layer. In *European Geoscience Union (EGU) General Assembly*, PICO. Vienna, Austria, 23-28 April 2017

Mede T, Hagenmuller P, Chambon G and Nicot F (2017b) Multiscale approach to modelling weak snow layers. In *SLab Avalanche Multiscale Mechanical Modelling (SLAM3) workshop*, Davos, Switzerland, 3-5 April 2017

Morin S, Hagenmuller P, Dumont M and Lafaysse M (2016) Evaluation strategies for vertical profiles of physical properties simulated by multilayer snowpack models. In *European Geoscience Union (EGU) General Assembly*, Poster. Vienna, Austria, 17-22 April 2017

Peinke I, Hagenmuller P, Chambon G, Roulle J and Morin S (2017a) Investigation of the sintering rate of snow with high-resolution penetration tests. In *European Geoscience Union (EGU) General Assembly*, Poster. Vienna, Austria, 23-28 April 2017

Peinke I, Hagenmuller P, Flin F, Chambon G, Roulle J, Andò E and Morin S (2017b) Investigation of high-resolution penetration tests in snow by X-Ray tomography. In *SLab Avalanche Multiscale Mechanical Modelling (SLAM3) workshop*, Davos, Switzerland, 3-5 April 2017

Peinke I, Hagenmuller P, Andò E, Flin F, Chambon G and Roulle J (2018) Three-dimensional measurements of the deformation of snow induced by a cone penetration test. In *European Geoscience Union (EGU) General Assembly*, PICO. Vienna, Austria, 8-13 April 2018

Tuzet F, Dumont M, Lafaysse M, Hagenmuller P, Arnaud L, Picard G and Morin S (2017a) Implementation of a physically-based scheme representing light-absorbing impurities deposition, evolution and radiative impacts in the SURFEX/Crocus model. In *AGU Fall Meeting Abstracts*, volume 2017, C13B–0962, New Orleans, USA

Tuzet F, Dumont M, Lafaysse M, Missiaen A and Hagenmuller P (2017b) On the impact of Saharan dust deposition on the evolution of an alpine snowpack. In *European Geoscience Union (EGU) General Assembly*, Poster. Vienna, Austria, 23-28 April 2017

Vernay M, Lafaysse M, Merindol L, Hagenmuller P, Verfaillie D and Morin S (2019) A 60-Years Meteorological and Snow Conditions Re-Analysis over the French Mountainous Areas (1958 - 2018). In *International Union of Geodesy and Geophysics (IUGG)*, Montréal, Québec, Canada, 8-18 July 2019, ISSN 1078-0475 (doi: 10.1289/isee.2011.01727)

Viallon-Galinier L, Hagenmuller P and Eckert N (2019) Combining physical modelling and machine learning to improve avalanche risk forecasting. In *30th ALERT Workshop*, Aussois, France, 30 September - 2 October 2019, ISBN 9782954251714

Viallon-Galinier L, Hagenmuller P and Lafaysse M (2020) Forcing and evaluating detailed snow cover models with stratigraphy observations. In *Virtual Snow Science Workshop (vSSW)*, Fernie, British Columbia, Canada,4-6 October 2020

Outreach documents (PV)

Dick O, Hagenmuller P, Viallon-Galinier L, Tuzet F and Dumont M (2021) Impact du dépôt de poussières minérales sur le manteau neigeux et sa stabilité. *Revue Neige et Avalanches*, n°171

Hagenmuller P (2014) Les mécanismes de cohésion de la neige révélés par la microtomographie. *Revue Neige et Avalanches*, **n°145**

Hagenmuller P (2017a) Influence des croûtes de regel sur la formation de couches fragiles persistantes. *Revue Neige et Avalanches*, **n°159**

Hagenmuller P (2017b) Le déclenchement des avalanches de plaque. *Revue Neige et Avalanches*, **n°157**

Hagenmuller P (2019a) Le déclenchement des avalanches de plaque. *Montagnes Magasine*, **461**

Hagenmuller P (2019b) Variabilité spatiale de l'indice de risque d'avalanche prévu dans l'arc alpin. *Revue Neige et Avalanches*, **n°164**

Pilloix T and Hagenmuller P (2015) Comparaisons préliminaires de profils de résistance à l'enfoncement obtenus par différentes sondes (sonde de battage, SnowMicroPen, Avatech SP1). *Revue Neige et Avalanches*, **n°151**, 6–8

PhD thesis (TH)

Hagenmuller P (2014) *Modélisation du comportement mécanique de la neige à partir d'images microtomographiques*. Ph.D. thesis, Université Grenoble Alpes (doi: 10.13140/2.1.2519.3764)

Mede T (2019) *Numerical investigation of snow mechanical behaviour: a microstructural perspective*. Ph.D. thesis, Université Grenoble Alpes

Peinke I (2019) *Étude à micro-échelle du test de pénétration du cône dans la neige*. Ph.D. thesis, Université de Toulouse

Other (AP)

Hagenmuller P, Flin F, Dumont M, Tuzet F, Peinke I, Lapalus P, Dufour A, Roulle J, Pezard L, Voisin D, Andò E, Rolland du Roscoat S and Charrier P (2019) Dust motion in snow microstructure (doi: 10.1594/PANGAEA.904568)

Réveillet M, Tuzet F, Dumont M, Gascoin S, Arnaud L, Bonnefoy M, Carmagnola CM, Deguine A, Evrard O, Flin F, Fontaine F, Gandois L, Hagenmuller P, Herbin H, Josse B, Lafaysse M, Le Roux G, Morin S, Nabat P, Petitprez D, Picard G, Robledano A, Schneebeli M, Six D, Thibert E, Vernay M, Viallon-Galinier L, Voiron C and Voisin D (2021) Dépôts massifs de poussières sahariennes sur le manteau neigeux dans les Alpes et les Pyrénées du 5 au 7 février 2021 : Contexte, enjeux et résultats préliminaires. Version du 3 mai 2021. Technical report, CNRM, Université de Toulouse, Météo-France, CNRS

Vernay M, Lafaysse M, Hagenmuller P, Nheili R, Verfaillie D and Morin S (2019) The S2M meteorological and snow cover reanalysis in the French mountainous areas (1958 - present) (doi: 10.25326/37)

List of acronyms

3D	three-dimensional
3SR	Laboratoire Sols, Solides, Structures, Risques
ANENA	Association Nationale de l'Etude de la Neige et des Avalanches
ANR	Agence Nationale de la Recherche
CEA	Commissariat à l'énergie atomique et aux énergies
CEN	Centre d'Etudes de la Neige
CNRM	Centre National de Recherche Metéorologique
CNRS	Centre National de la Recherche Scientifique
DBA	DTW Barycenter Averaging
DTW	Dynamic Time Warping
EAWS	European Avalanche Warning Services
EPA	Enquête Permanente sur les Avalanches
ENS	Ecole Normale Supérieure
ENGREF	Ecole Nationale du Génie Rural des Eaux et des Forêts
ERC	European Research Council
HDR	*Habilitation à Diriger des Recherches* - habilitation to supervise research
HPP	Homogeneous Poisson Process
IGE	Institut des Géosciences de l'Environnement
Inrae	Institut national de recherche pour l'agriculture, l'alimentation et l'environnement
IPCC	Intergovernmental Panel on Climate Change
KUBC	Kinetic Uniform Boundary Conditions
MEPRA	*Modèle Expert d'aide à la Prévision du Risque d'Avalanche*
MUBC	Mixed Uniform Boundary Conditions
NHPP	Non Homogeneous Poisson Process
OSUG	Observatoire des Sciences de l'Univers de Grenoble
PARN	Pole Alpin pour la prévention des Risques Naturels
ROC	Receiving Operating Characteristic
S2M	SAFRAN – SURFEX/ISBA–Crocus – MEPRA
SAFRAN	*Système d'Analyse Fournissant des Renseignements Adaptés à la Nivologie*
SMP	Snow Micro-Penetrometer
SP2	Avatech Snow Probe 2
SUBC	Stress Uniform Boundary Conditions
WSL-SLF	WSL Institute for Snow and Avalanche Research